Distribution Agreement

In presenting this thesis or dissertation as a partial fulfillment of the requirements for an advanced degree from Emory University, I hereby grant to Emory University and its agents the non-exclusive license to archive, make accessible, and display my thesis or dissertation in whole or in part in all forms of media, now or hereafter known, including display on the world wide web. I understand that I may select some access restrictions as part of the online submission of this thesis or dissertation. I retain all ownership rights to the copyright of the thesis or dissertation. I also retain the right to use in future works (such as articles or books) all or part of this thesis or dissertation.

Signature: Signed by: Daniel Thomas McManus 986F057EA914453...

Daniel Thomas McManus
Name

12/6/2024 | 3:16 PM EST
Date

Title CD8 T cell Differentiation during Acute and Chronic Viral Infection

Author Daniel Thomas McManus

Degree Doctor of Philosophy

Program Biological and Biomedical Sciences
Immunology and Molecular Pathogenesis

Approved by the Committee

DocuSigned by:
Rafi Ahmed
9F71F7B4C6E9493...

Rafi Ahmed
Advisor

DocuSigned by:
John Altman
FE0039663474443...

John Altman
Committee Member

DocuSigned by:
Eliver Ghosn
951ECA803CA446E...

Eliver Ghosn
Committee Member

Signed by:
Heather D. Hickman
0A7A0F72EE3A42A...

Heather D. Hickman
Committee Member

Signed by:
Jacob E. Kohlmeier
410B4921BF064BB...

Jacob E. Kohlmeier
Committee Member

Committee Member

Accepted by the Laney Graduate School:

_____
Kimberly Jacob Arriola, Ph.D, MPH
Dean, James T. Laney Graduate School

_____
Date

CD8 T cell Differentiation during Acute and Chronic Viral Infection

By

Daniel Thomas McManus

Graduate Division of Biological and Biomedical Sciences

Immunology and Molecular Pathogenesis

Rafi Ahmed, Ph.D.
Advisor

John D. Altman, Ph.D.
Committee Member

Eliver E.B. Ghosn, Ph.D.
Committee Member

Heather D. Hickman, Ph.D.
Committee Member

Jacob E. Kohlmeier, Ph.D.
Committee Member

CD8 T cell Differentiation during Acute and Chronic Viral Infection

By

Daniel Thomas McManus
B.S., University of Massachusetts Boston, 2015

Advisor: Rafi Ahmed
Ph.D., Harvard University

An abstract submitted to the Faculty of the
James T. Laney School of Graduate Studies of Emory University
in partial fulfillment of the requirements for the degree of Doctor of Philosophy in
Immunology and Molecular Pathogenesis
2024

Abstract

How CD8 T cells develop during acute versus chronic antigen exposure is central to understanding immunity during viral infections, cancer, and autoimmunity. Stem-like CD8 T cells are specialized progenitor cells that maintain the CD8 T cell response in these contexts. Here, we examined the generation, fate, and plasticity of these cells during acute and chronic viral infection. We find that nearly identical populations of stem-like CD8 T cells arise early after acute and chronic infection. This indicates that the generation of stem-like CD8 T cells occurs agnostic to infection outcome, ensuring that the host is prepared in advance for a potential long-term infection. In both acute and chronic infection, the transcription factor TOX was required for the generation of stem-like CD8 T cells, and continuous antigen exposure was required for their maintenance. We next performed reciprocal adoptive transfer experiments to track the fate of early stem-like CD8 T cells during viral clearance versus persistence, and to examine the impact that infection origin has on their differentiation potential. When transferred into an acute, resolving infection, early stem-like CD8 T cells from chronic infection converted into memory cells, enriched for properties of central memory CD8 T cells. When transferred into mice harboring a life-long infection, early stem-like CD8 T cells from acute infection performed as chronic resource cells. They expanded vigorously, giving rise to stem-like, effector, and terminally differentiated CD8 T cells. For over a month, they maintained the CD8 T cell response in lymphoid and non-lymphoid tissues, becoming quiescent as the infection reached the late/established phase. They even responded to PD-1 blockade, providing a proliferative burst equal to that of the virus-specific endogenous CD8 T cell response. Altogether, we show that stem-like CD8 T cells are generated early during viral infection and can adapt their differentiation trajectory based on infection outcome. They become memory CD8 T cells if the virus is rapidly cleared, or chronic resource cells if the virus persists. These findings raise new questions on the potential importance of stem-like CD8 T cells for immunological memory and re-emphasize the essential role that they play during chronic viral infection. Lastly, this work provides further insight into the early differentiation events that enable the CD8 T cell response to adapt to acute or chronic viral infection.

CD8 T cell Differentiation during Acute and Chronic Viral Infection

By

Daniel Thomas McManus
B.S., University of Massachusetts Boston, 2015

Advisor: Rafi Ahmed
Ph.D., Harvard University

A dissertation submitted to the Faculty of the
James T. Laney School of Graduate Studies of Emory University
in partial fulfillment of the requirements for the degree of Doctor of Philosophy in
Immunology and Molecular Pathogenesis
2024

Acknowledgments

Table of Contents

List of Figures

Chapter 1: Introduction

Preamble

It's estimated that there are more virus particles on earth (~10^{31}) than stars in the universe[1,2]. How the immune system has evolved to deal with viral infections is one of the most intriguing questions in biomedical research and the focus of viral immunology. Furthermore, the pursuit of this question has revealed truths about the immune system that extend beyond viral immunology.

Cytotoxic CD8 T cells are an essential part of the immune system's multilayered defense against viruses. They are generated in the bone marrow but to reach full maturity must endure a crucible in the thymus termed 'thymic selection'. They must avoid death in the thymus by generating a unique T cell receptor (TCR) that walks the fine line between not recognizing self at all and recognizing self all too well. Ultimately what emerges from the thymus are mature CD8 T cells bearing TCRs highly specific for foreign peptides but not self-peptides[3]. This culminates in a hugely diverse array of TCR specificities. For example, the total number of unique TCRs in the human body is estimated to be ~10^{8}; enough to recognize a universe's worth of potential foreign invaders[4,5].

CD8 T cells are uniquely suited for defense against viruses. Unusual for a somatic cell, CD8 T cells are capable of rapid, repeated bursts in proliferation without loss of growth control or malignant transformation[6]. This allows them to keep up with the rapid reproduction rates of viruses. A challenge posed by many viruses is vast cellular and tissue tropism. CD8 T cells can both migrate to and survive in a wide range of tissues/microenvironments, enabling them to access and persist wherever infected cells may be. CD8 T cells employ many tools for viral control. They can act as sentinels by secreting cytokines that alarm or induce anti-viral defenses within neighboring cells. However, they are most known, and were named for, their ability to directly kill virus-infected cells using cytolytic molecules.

Viral infections can be broadly divided into two main types: acute vs chronic. The former is typically cleared by the immune system within 1-2 weeks. The latter can persist for

weeks, months, and in some cases, the life of the host. Following an acute viral infection, a fraction of virus specific CD8 T cells remains as highly functional memory cells, poised to re-proliferate and kill upon re-infection[7]. Chronic viral infections lead to the “persistence of activated CD8 T cells without effector function”, a phenomenon referred to as T cell exhaustion[8,9]. Compared to memory, exhausted CD8 T cells appear functionally impotent; they proliferate poorly, express high levels of inhibitory receptors, and as infection progresses, gradually lose the ability to secrete cytokines[10]. In addition to functionality, memory and exhausted CD8 T cells have very different transcriptional and epigenetic programs and are considered distinct lineages[11–19]. The former evolved for surveillance and swift protection against reinfection. The latter evolved for control over persistent infections without causing excessive damage or death to the host.

The development of memory versus exhausted CD8 T cells is ostensibly decided by infection outcome. However, the host immune system cannot wait for the outcome of a viral infection to be made salient before deciding on which of these programs to deploy—it cannot ‘catch up’. Nor can this decision be pre-arranged, since the host cannot know the outcome of infection in advance. Hence, potential for either developmental pathway must somehow be bestowed to the CD8 T cell response early after viral infection. This thesis makes a small advance in our understanding of how flexibility is built into the CD8 T cell response early during viral infection—in the form of a stem-like or precursor cell—so that it can adapt to either an acute or chronic outcome.

LCMV as a model system for studying CD8 T cells

Structure, genome, and life cycle

Before expanding on what’s known about the anti-viral CD8 T cell response, it is pertinent to introduce one of the viral infection models that was crucial for revealing this knowledge. Lymphocytic choriomeningitis virus (LCMV) was discovered in 1934 by three groups of scientists working independently [20–22]. LCMV is named for the characteristic infiltration of lymphocytes into the brain that it causes after infection (Fig.1a-c) [20–22]. It is a rodent-borne, non-cytopathic virus belonging to the arenavirus family. The virion is enveloped with a round structure from which evenly spaced spikes protrude from a central core (Fig. 2a)[23]. Its genome is comprised of two, ambisense

RNA segments, the S (for short) and L (for long), which encode four genes in total. The S segment encodes the viral nucleoprotein (NP) that facilitates viral transcription, and a glycoprotein (GP) precursor[23]. The L segment encodes an RNA-dependent RNA polymerase (L) and a zinc-binding protein that supports the structure of the virion (Z) (Fig. 2b)[24]. The GP precursor is post-translationally cleaved into a heavily glycosylated head (GP1) and a transmembrane stalk (GP2)[25]. Together these form a tetrameric spike protein that attaches to α-dystroglycan on the surface of a cell to initiate viral entry[26]. What follows is receptor-mediated endocytosis of the virion and transfer to a late, acidified endosome where the viral envelope fuses to the endosomal membrane in a pH-dependent manner. This enables the virion to uncoat, triggering transcription of the nucleoprotein and polymerase in the cytoplasm [23]. Once enough polymerase is translated and template antigenomic RNA produced, the transcription of GP and Z begins. Fully assembled virions are then transported to the plasma membrane where they exit the cell via budding [23].

Acute and chronic LCMV infection in mice

Infection of mice with LCMV is an excellent model for studying anti-viral CD8 T cell immunity. Firstly, CD8 T cells are crucial for controlling LCMV infection and the virus does not readily escape the endogenous CD8 T cell response. In addition, some strains of LCMV are rapidly cleared in mice whereas others persist. This enables one to track CD8 T cells of the same antigen-specificity in an acute vs. chronic viral infection.

LCMV Armstrong causes an acute viral infection in mice that is cleared within a week. Originally derived from Armstrong, clone 13 results in a chronic viral infection in mice that can persist for months depending on the tissue [27]. The chronicity of clone 13 is owed to two amino acid differences compared to its parental strain. The first is a phenylalanine to leucine (F→L) substitution at position 260 of the spike glycoprotein, which increases the binding affinity of the spike to α-dystroglycan. This enables the spike to displace other proteins, like laminin-1, that compete for the same binding site on α-dystroglycan enhancing the ability of the virus to infect cells[28]. The second is a lysine to glutamine (K→Q) change at position 1079 of the polymerase, which dramatically increases the replication rate of the virus[29–31]. Transient depletion of CD4 T

cells prior to clone 13 infection results in a life-long viral infection, enabling for the study of anti-viral immunity under conditions of long-term and stable antigen exposure, such as occurs during human immunodeficiency virus (HIV) infection and certain types of cancers[32] (Fig. 2c).

The use of the LCMV model has led to invaluable insight into viral immunology[33], tolerance[34], and cancer[35,36]. To begin to understand the cellular plasticity that enables the CD8 T cell response to adapt to acute versus chronic infection we have chosen the model of LCMV infection in mice.

The anti-viral CD8 T cell response

Activation

CD8 T cells recognize internal peptides presented on the cell surface by MHC class I molecules; hence, are specialized for intracellular pathogens like viruses. They spend most of their lives as quiescent, metabolically idle “naïve” cells searching the host for possible signs of a virus. The number of naïve CD8 T cells specific for a given viral peptide can be as low as 100-200[37–39]. “Naive T cells do not attempt to scan all 40 trillion cells in the adult human organism directly”[40]. They confine their surveillance to secondary lymphoid tissues like the spleen and lymph nodes. Within these lymphoid hubs, foreign peptides are concentrated and displayed by antigen presenting cells (APCs). This anatomical design maximizes the likelihood that a very rare naïve precursor CD8 T cell will interact with the virus it is specific to.

A virus-specific CD8 T cell becomes activated once it recognizes cognate peptide (signal 1) in the context of costimulation (signal 2) and cytokines (signal 3). CD80 and CD86, often expressed by activated dendritic cells, are examples of ligands that provide costimulation to T cells via the receptor, CD28. Signal 3 can be provided by myeloid cells, T cells, and non-immune cells alike and include cytokines like type I interferon, IL-12, and IFNγ[41]. Once all three signals are received, naïve CD8 T cells transform from relatively inert cells to some of the most active cells in the body. Over the next 24 hours they will grow dramatically in size, becoming factories for macromolecule production[42,43].

Activated CD8 T cells must next become numerically relevant to control a pathogen that can reproduce as fast as a virus can. This is accomplished by a massive burst in cell proliferation that takes place during acute phase of infection[44]. It was once believed that most of these proliferating CD8 T cells (>95%) were not actually specific to the virus but recruited to the response by inflammation, a notion called bystander activation[45,46].The pioneering work of Altman et al. introduced the ability to directly measure antigen-specific CD8 T cells using MHC I molecules containing peptides, a reagent referred to as a tetramer (Fig. 3a)[47]. In mice infected with LCMV, this tool showed that the actual frequency of antigen-specific cells among activated, dividing cells was closer to 50-70%, not <5%[44]. MHC tetramer technology was an enormous advance in immunology and showed conclusively that the virus-specific CD8 T cell response during acute viral infection proceeds in three phases[44] (Fig. 3b).

CD8 T cell response during acute viral infection: expansion, contraction, memory

Just 30-48 hours after initial antigen encounter, virus-specific CD8 T cells in LCMV-infected mice begin to proliferate. They will divide every ~6-8 hours, committing to at least 7-10 cell divisions. By the end of this ~6-day expansion period ("peak expansion"), the few virus-specific CD8 T cells that began the response will have undergone a 10,000-100,000 fold increase in cell number (Fig. 3b)[44,48]. This extensive proliferation is coupled to effector differentiation, whereby virus-specific cells acquire migratory and cytolytic functions so that they can locate and eliminate virus-infected cells[48].
While the overall magnitude of expansion is driven by initial antigen amount, continuous antigen exposure/contact is not required for antigen-specific CD8 T cells to continue dividing. Once a parent cell is sufficiently stimulated by antigen to divide, its daughter cells will continue dividing even if transferred to an antigen-free environment. Programmed proliferation, as it's called, bypasses the need for every daughter cell participating in the response to see antigen[48,49]. This ensures that a large CD8 T cell response can be mounted in a timely manner and that antigen contact within inductive sites doesn't limit the number of CD8 T cells that can be generated against the virus.

After the first week of infection, the contraction/death phase begins whereby 95% of the CD8 T cell response is culled[44]. For the following three to four weeks, millions of virus-

specific cells will die via apoptosis so that the host doesn't incur excessive damage and energy consumption. The number of virus-specific cells does not return to what it was pre-infection, however. 5-10% of the response evades contraction and goes on to become memory cells that will protect the mouse against reinfection for life[12,44] (Fig. 3b). The cardinal properties of memory CD8 T cells include long-term antigen-independent persistence and the ability to rapidly proliferate and express effector molecules upon re-challenge[50,51]. They maintain their numbers during homeostasis via the survival cytokine interleukin 7 (IL-7) and a slow self-renewal, driven in part by IL-15[52–56].

CD8 T cell response during chronic viral infection: Exhaustion

Antigen persistence yields an alternative CD8 T cell lineage, exhaustion[8,9]. Compared to memory, exhausted CD8 T cells kill targets less effectively, proliferate poorly upon restimulation, and progressively lose the ability to make key cytokines[10]. T cell exhaustion is adapted for viral control without cost to the host. However, T cell exhaustion is a huge problem for human diseases epitomized by chronic antigen, like HIV, cancer, and autoimmunity. Exhausted T cells can be rejuvenated with PD-1 blockade, now a frontline treatment for multiple human cancers[57].

CD8 T cell differentiation pathway during chronic viral infection

Exhausted virus-specific CD8 T cells are not a homogenous population. As chronic viral infection progresses, heterogeneity can be observed among virus-specific CD8 T cells based on the expression of CD44 and PD-1[10,58]. This heterogeneity was not just phenotypic, however. Cells that were PD-1^{int} CD44^{hi} were found to have greater proliferative potential and were more responsive to PD-1 blockade compared to PD-1^{hi}, CD44^{int} cells[58]. It was later found that a lineage relationship exists among exhausted CD8 T cells, occurring between a PD-1^{int} T-bet^{hi} progenitor-like cell and it's PD-1^{hi} Eomes^{hi} terminal progeny[59].

Between 2016 and 2020, a flurry of papers further elaborating on the heterogeneity of exhausted CD8 T cells. They showed that the virus-specific CD8 T cell pool during chronic viral infection is comprised of three main subsets existing in a linear relationship: stem-like cell → transitory effector cell → terminally differentiated cell (Fig.

4a)[60–66]. Stem-like CD8 T cells are a long-lived PD-1+ subset that depends on the transcription factors, TCF-1 and TOX[60,67–70]. Conserved across species and diseases[71–75], stem-like CD8 T cells lack cytotoxic molecules but are capable of huge proliferative bursts. During division, stem-like CD8 T cells couple self-renewal with effector differentiation giving rise to a transitory effector cell that is migratory, highly proliferative, and equipped with potent killing potential[63,64]. With prolonged antigen exposure, transitory effector cells further differentiate into a senescent, terminally differentiated/exhausted subset expressing high levels of inhibitory receptors and intermediate levels of effector molecules[63,64] (Fig. 4a).

Multiple factors coordinate the proliferation, self-renewal, and differentiation of stem-like cells including PD-1, transforming growth factor beta (TGF-β) signaling, CD28 costimulation, interleukin 15 (IL-15) and type I interferon[76–79]. Another key feature regulating the activity of stem-like cells is their location. During the late phase of chronic infection, stem-like cells are resident to lymphoid tissues where they're positioned in microanatomical niches like the T cell zone of the splenic white pulp[60,80]. Without stem-like cells, the virus specific CD8 T cell population wanes numerically over time[60]. An additional consequence of their loss is reduced viral control as new transitory effector cells fail to be generated[63]. Hence, stem-like CD8 T cells act as an essential resource/reservoir cell during chronic antigen exposure, replenishing the T cell pool with numerically and functionally relevant effectors.

In addition to their biological role as a resource/reservoir cell, stem-like cells also provide the massive expansion that follows PD-1 blockade[58,60,73]. This dramatically accelerates their self-renewal and effector differentiation, culminating in a large pool of effectors but without expense to stem-like cell numbers[60,81]. Thus, stem-like CD8 T cells not only provide insight into how the mammalian immune system evolved to cope with chronic antigen exposure, but they also represent a novel target for improving immunotherapy.

This thesis began as a study on stem-like CD8 T cell differentiation during chronic viral infection, under the premise that it would provide better insight into the origin and development of T cell exhaustion. We started with several key questions: When are

these cells first generated during chronic viral infection? How does their program change over time? What is the role of antigen in maintaining the stem-like program? How does the differentiation trajectory of these cells change in the presence or absence of antigen?

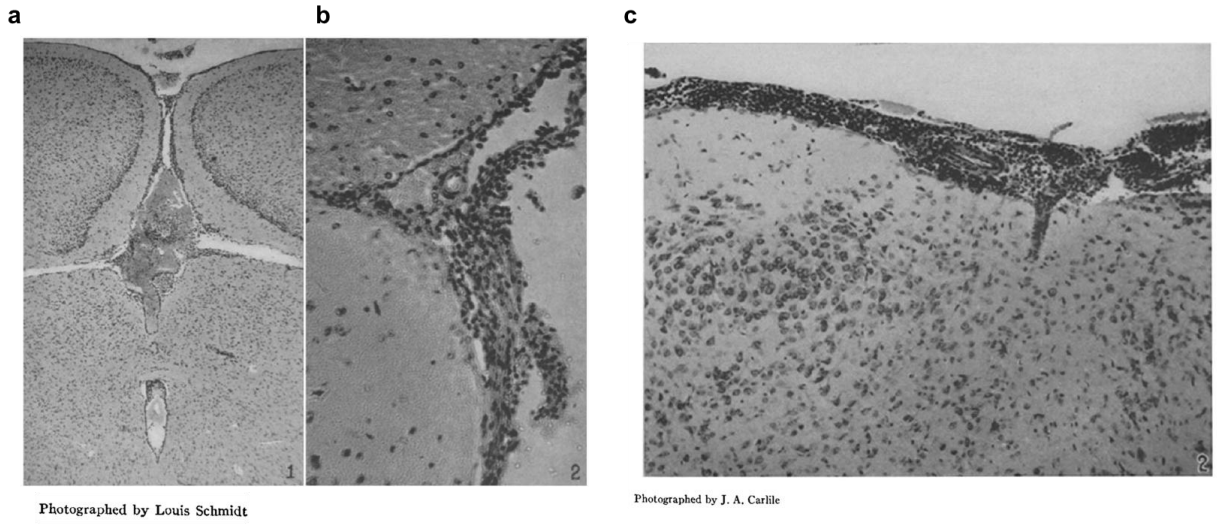

Fig. 1| Lymphocytic infiltrate in the brains of mice infected with a filterable virus. a,b, Hematoxylin and eosin (H & E) staining of brain section from LCMV-infected mouse. Cellular infiltration of meninges, 40x magnification (a). Higher magnification of meninges showing that the exudate most consists of mononuclear cells, 250x (b). **c,** Eosin and methylene blue staining of brain section from mouse infected intracranially with LCMV, 130x. Image highlights substantial meningitis at the base of the brain. Images for a and b adapted from Rivers and Scott, *J. Exp. Med.*, December 14, 1935. Image in c adapted from Traub, *J. Exp. Med*, December 27, 1935.

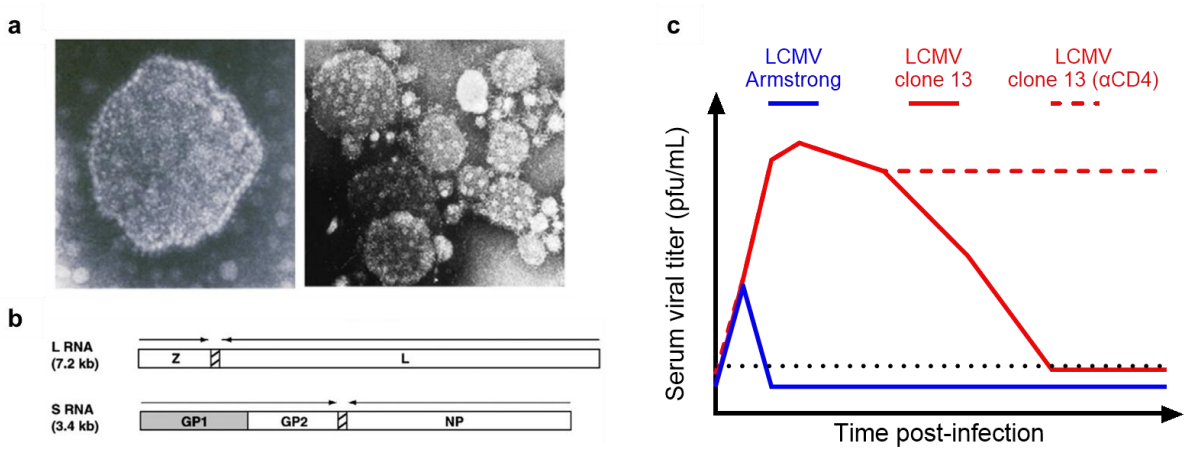

Fig. 2| Structure, genome, and kinetics of LCMV. a, Electron micrographs showing the physical structure of LCMV. Left, zoomed-in image showing entire virion with spike glycoproteins (GP1) extending from virion surface. Right, image showing several virions. **b,** Schematic illustrating arrangement of LCMV genome. There are two segments, L (long) and S (short), encoding four total genes. L encodes a matrix-like protein, Z, and the polymerase, L. The S segment encodes a shared glycoprotein spike/head 1 (GP1) and stalk (GP2) plus the viral nucleoprotein (NP). **c,** Cartoon schematic showing serum viral titer kinetics in mice infected with LCMV Armstrong (acute, blue), clone 13 (chronic, red), and clone 13 with transient CD4 T cell depletion (chronic/life-long, red dashed). Dotted black line roughly depicting limit of detection. Data in a and schematic in b are adapted from Oldstone et al., *Virology,* 2011. Viral titers in c based on data from Ahmed et al., *J. Exp. Med.*, 1984, Matloubian et al., *J. Virol.*, 1993, and Wherry et al., *J. Virol.*, 2003.

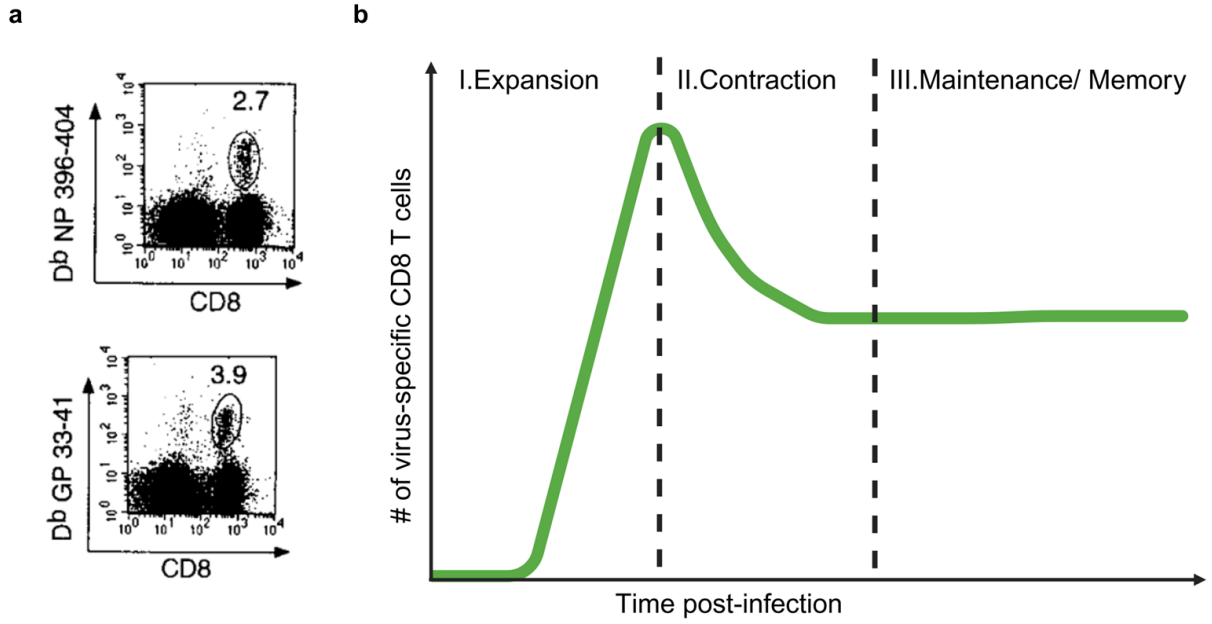

Fig. 3| Phases of the anti-viral CD8 T cell response revealed by MHC class I tetramers. a, Flow cytometry plots showing the frequency of CD8 T cells specific for LCMV-derived epitopes NP396 (top) and GP33 (bottom) as measured by MHC I tetramers. **b,** Cartoon schematic illustrating the three phases of the virus-specific CD8 T cell response: expansion, contraction, and maintenance/memory. Made in BioRender. Flow plots in a adapted from and curve in b based on data from Murali-Krishna et. al., *Immunity*, 1998.

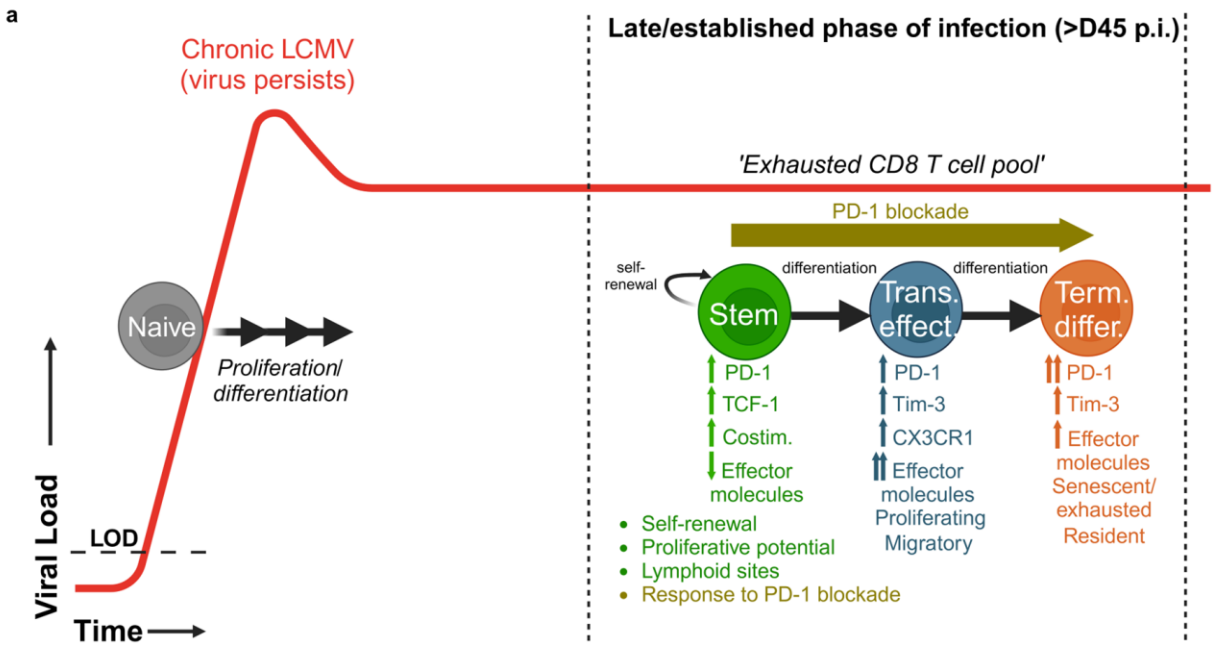

Fig. 4| CD8 T cell differentiation during chronic viral infection.
a, During the established (>D45) phase of chronic LCMV infection, the exhausted CD8 T cell pool can be divided into three phenotypically and functionally distinct subsets existing in a linear relationship: stem-like (stem)→ transitory effector (Trans. Effect.)→ terminally differentiated (Term. differ.). Key properties for each subset are listed. Stem-like CD8 T cells are essential for maintaining CD8 T cell immunity during chronic antigen exposure and also provide the proliferative burst seen following PD-1 blockade.

Chapter 2: Early fate and anatomical commitment of stem-like CD8 T cells

This chapter is reproduced with edits from:

Early generation of a precursor CD8 T cell that can adapt to acute or chronic viral infection

Daniel T. McManus[1,2,11], Rajesh M. Valanparambil[1,2,11], Christopher B. Medina[1,2], Christopher D. Scharer[2], Donald J. McGuire[1,2], Yinghong Hu[1,2], Ewelina Sobierajska[4], Daniel Y. Chang[9], Andreas Wieland[5], Judong Lee[1,2], Tahseen H. Nasti[1,2], Masao Hashimoto[1,2], James L. Ross[1,2], Nataliya Prokhnevska[6], Maria A. Cardenas[4], Amanda L. Gill[1,2], Elisa C. Clark[8], Kathleen Abadie[8], Arjun Kumar[8], Hao Yuan Kueh[8], Jonathan Kaye[7], Byron B. Au-Yeung[10], Haydn T. Kissick[1,2,3,4], and Rafi Ahmed[1,2,3,*]

[1]Emory Vaccine Center, Emory University School of Medicine, Atlanta, GA, USA
[2]Department of Microbiology and Immunology, Emory University School of Medicine, Atlanta, GA, USA
[3]Winship Cancer Institute of Emory University, Atlanta, GA, USA
[4]Department of Urology, Emory University School of Medicine, Atlanta, GA, USA
[5]Department of Otolaryngology, The Ohio State University College of Medicine, Columbus, OH
[6]The Precision Immunology Institute, Icahn School of Medicine at Mount Sinai, New York, NY, USA
[7]Research Division of Immunology, Department of Biomedical Sciences, Cedars-Sinai Medical Center, Los Angeles, CA, USA
[8]Department of Bioengineering, University of Washington, Seattle, WA, USA
[9]Department of Pathology, Mass General Brigham, Harvard Medical School, Boston, MA, USA
[10]Division of Immunology, Lowance Center for Human Immunology, Department of Medicine, Emory University, Atlanta, GA,
[11]These authors contributed equally
*Corresponding author. Email: rahmed@emory.edu

**Under revisions for Nature*

Abstract

Stem-like CD8 T cells (PD-1+ TCF-1+ Tim-3- TOX+) sustain the CD8 T cell response during chronic viral infection and cancer, and residency in lymphoid tissues is a key aspect of their biology. When do these cells first emerge after infection and at what point do they commit to positioning in the splenic white pulp? We used the chronic LCMV strain, clone 13, to address these questions. Phenotypical and transcriptional profiling of virus-specific CD8 T cells indicated that stem-like CD8 T cells emerge as early as day 5 after infection. Intravascular labeling and imaging showed that the spatial commitment of these cells to the white pulp had already started on day 5. This observation is particularly striking as it indicates that the sequestration of these cells to the white pulp has been prioritized even before the outcome of the infection has been determined. RNA sequencing revealed considerable transcriptional overlap between PD-1+ stem-like CD8 T cells from the early (day 5) and established phases (>day 45) of clone 13 infection, indicating that the canonical gene signature of these cells manifests early and is maintained throughout infection. These data show that the fate and anatomical commitment of stem-like cD8 T cells begins as early as day 5.

Introduction

Exhausted CD8 T cells are a distinct immune cell type adapted for chronic illnesses where persistent antigen must be controlled without killing the host. This balance is achieved by stem-like cells that can self-renew but not kill, and effector cells that can kill but have limited proliferative potential[59,60,63,64,67].

The first question we addressed was when are PD-1+ TCF-1+ stem-like CD8+ T cells generated during the course of chronic LCMV infection and how do these cells compare with the stem-like CD8+ T cells present during the later established phases of chronic infection. We have used the LCMV clone 13 strain to study chronic infection. Our previous studies have shown that PD-1+ TCF-1+ Tim-3- virus specific CD8+ T cells are detectable in the spleens of mice during the first week of chronic infection[60]. Other studies have also reported similar observations[70,82]. To extend these observations we did a detailed comparison of LCMV specific stem-like CD8+ T cells present at day 5 versus day 45 post-infection at the phenotypic, transcriptional, and anatomical levels.

Results and Discussion

Early emergence of the stem-like CD8 T cell phenotype during chronic infection

To determine when stem-like CD8 T cells first arise during chronic infection, we used the chronic LCMV infection model in which mice are inflicted with a life-long viremia (Fig. 1a)[27,32]. Based on immunofluorescence imaging, LCMV antigen is continuously present in the spleens of these mice. However, it appears to decline between days 5 and >45, most notably in the splenic white pulp (WP) compared to the red pulp (RP) (Fig. 1b). Protein analysis of CD8 T cells specific to the H-2D^{b}-restricted epitope, GP33-41 revealed a TCF-1+ cell on day 5 expressing PD-1 and TOX, marks associated with both activation and exhaustion (Fig. 1c-g)[68–70,83]. In addition to TCF-1, PD-1, and TOX, these day 5 cells shared other features with *bona fide* stem-like CD8+ T cells from the late phase of chronic infection (>d45); they lacked molecules associated with effector/terminal differentiation like Tim-3, granzyme B, CD101,[60,63] but expressed the costimulatory molecule, CD28, and ectonucleotidase, CD73[60]. A key difference that was observed between day 5 and >45 stem-like CD8 T cells was that the former but not the latter expressed the proliferation marker, Ki67 (Fig. 1b).

Early transcriptional divergence of stem-like and effect./TD CD8 T cells during chronic infection

To further complement our phenotypic analysis above, we performed single cell RNA-sequencing (scRNA-seq) on GP33-specific cells from days 5 and >45 after chronic LCMV infection (Extended Data Fig. 1a). Day 5 cells formed two major clusters, one enriching for the stem-like CD8 T cell gene signature (D5 stem, dark green) and the other enriching for the effector/terminally differentiated CD8 T cell gene signature (D5 effector, orange). Day >45 cells also formed a cluster enriched for the stem-like CD8 T cell gene signature (>D45 stem, light green). Highlighting their transcriptional similarity, day 5 and >45 stem cell clusters were positioned next to each other in the uniform manifold approximation and projection (UMAP) in Fig. 2a. In addition to the stem cluster, day >45 cells formed two additional clusters, effector (>D45 effector, blue) and terminally differentiated (>D45 TD, red) that enriched for the effector/terminally

differentiated gene signature (Fig. 2a-d). As expected for antigen-specific CD8 T cells in an active viral infection, cells in all clusters from days 5 and >45 expressed *Pdcd1* and *Tox*. The stem clusters for days 5 and >45 both expressed high levels of *Tcf7* as well as two transcription factors associated with stem-like CD8+ T cells, *Lef1* and *Id3*. They also contained cells expressing *Xcl1* and *Slamf6*, two additional markers unique to stem-like CD8+ T cells during chronic infection (Fig. 2e-j)[60,82].

Although day 5 and >45 stem clusters were mostly similar, there were notable differences. Cells in the day 5 stem cluster, but not day >45, expressed the proliferation marker, *Mki67* (Fig. 2e-j), consistent with our protein expression data (Fig. 1c). In addition, the day 5 stem cluster exhibited heterogeneity in the expression levels of *Mki67*, *Sell* (encoding CD62L or L-selectin), and *Xcl1* that was not apparent in the day >45 stem cluster. Cells in the day 5 stem cluster could be subdivided into stem clusters (SC) 1 (*Mki67* high, *Sell* high/low, *Xcl1* mid/low), SC2 (*Mki67* high/low, *Sell* high, *Xcl1* mid/low), and SC3 (*Mki67* high, *Sell* low, *Xcl1* high) (Extended Data Fig. 1b and c). This heterogeneity is likely because virus-specific CD8 T cells are proliferating on day 5 whereas most of the day >45 cells are either quiescent or exhausted. In contrast, the co-inhibitory receptor, *Havcr2* , and transcription factors associated with effector differentiation, *Prdm1* and *Id2* and the cytotoxic molecule, *Gzmb*, were almost exclusively expressed by day 5 and >45 cells that fell into the effector and TD clusters. Cells in the >D45 effector cluster could be distinguished from the >D45 TD cluster based on *Mki67* expression and absence of the co-inhibitory receptor, *Cd244* (Fig. 2e-j).

Early anatomical divergence of stem-like and effect./TD CD8 T cells during chronic infection

A key characteristic of stem-like CD8+ T cells in the spleen is their anatomical bias for the white pulp region whereas effect./TD cells are located mainly in the red pulp area[60,80,84]. To determine when this spatial organization begins, we used intravascular labeling[85,86] to compare the intrasplenic locations of GP33-specific TCF-1+ Tim-3- stem-like and TCF-1- Tim-3+ effect./TD cells on days 5 and >45 (Fig. 3a). As early as day 5, a clear discrepancy could be observed with ~50% of stem-like cells locating to the blood-inaccessible white pulp (i.v. staining negative) compared to just 10% of TD cells (Fig. 3b

and c). The anatomical differences between stem-like and effect./TD cells on day 5 were not owed to the absence of CD4 T cell help as mice with virus-specific CD4 T cells showed similar differences (Extended Data Fig. 2a). The frequency of stem-like CD8+ T cells in the white pulp increased to >80% between days 5 and >45, whereas the bias of effect./TD cells for the red pulp (i.v. staining positive) remained throughout infection (Fig. 3b and c). Imaging of PD-1+ stem-like and effect./TD CD8+ T cells confirmed our i.v. labeling results showing a greater percentage (~1.5-2 fold) of stem-like compared to effect./TD CD8+ T cells in the white pulp on day 5 (Fig 3d and e).

Of note, the increase in frequency of white pulp stem-like cells over time was *not* reflected in absolute numbers. White pulp stem-like cell numbers were mostly stable, showing a modest decline between days 5 and >45 (~6-fold drop) whereas numbers in the red pulp declined severely (~32-fold drop) (Extended Data Fig. 2a). Effect./TD cell numbers also declined between days 5 and >45 but not to the extremes of red pulp stem-like cells, nor did the decline appear to be related to location (Extended Data Fig. 2a). The decrease of red pulp stem-like cells over time was matched by a similar drop in the frequency of blood-circulating and liver stem-like cells (Extended Data Fig. 2c and d)[80].

CD69 promotes the retention of lymphocytes in lymphoid tissues[87]. The decline of red pulp stem-like cells over time was coupled with a reduction in CD69- stem-like cells (Extended Data Fig. 2e and f) that may be related to the absence of CD4 T cell help in our model[88]. CD69- stem-like cells could access the blood and red pulp whereas their CD69+ kin were almost exclusively positioned in the white pulp throughout infection (Extended Data Fig. 2e and f). This observation aligns with and expands on previous work relating CD69 expression to the location of stem-like CD8 T cells during chronic LCMV infection[88].

These anatomical data show that the white pulp compartmentalization of stem-like CD8 T cells occurs early during chronic viral infection and is independent of CD4 T cell help. As the infection progresses, stem-like CD8 T cells are preserved in the white pulp but are lost from the blood and blood-accessible compartments, like the red pulp and liver, implicating location as an important factor for the maintenance of stem-like CD8 T cells.

Altogether, these data indicate that virus specific stem-like CD8+ T cells with the canonical phenotype, transcriptional signature, and anatomical features of *bona-fide* stem-like CD8+ T cells can be detected as early as 5 days after infection with LCMV clone 13.

Methods

Mice, viral infections, and virus titration

C57BL/6 and CD45.1 B6 mice were purchased from Jackson laboratory. Chronic viral infections that result in lifelong viremia were performed as follows: mice were transiently depleted of CD4+ T cells via intraperitoneal injection with 300 µg of a rat anti-mouse CD4 antibody (clone GK 1.5 from BioXcell) 2 days before infection and again on the day of infection. Mice were then injected intravenously (i.v.) with $2x10^6$ PFU LCMV clone 13.

Lymphocyte isolation

Lymphocyte isolation from the blood, spleen, liver, and lungs were performed as described previously (Wherry's JV paper). Spleens were dissociated by passing through a 70 uM cell strainer (Corning). Livers were first perfused with cold PBS prior homogenization via mechanical disruption. Lungs chopped prior to shaking at 37C in 1.3 mM EDTA in HBSS for 30 mins. They were then treated with 150 U mL^{-1} of collagenase (Thermo Fisher Scientific) in RPMI 1640 medium containing 5% FBS, 1mM $MgCl_2$ and 1mM $CaCl_2$ for 60 min at 37C with shaking at 200 rpm. Collogenase-treated lungs were then homogenized and filtered through a 70uM cell strainer. A 44-67% Percoll gradient was then used to purify lymphocytes (800g at 20C for 20min).

Reagents and flow cytometry

All antibodies used for flow cytometry were purchased from Biolegend, Thermo Fisher Scientific, Miltenyi Biotec, Cell Signaling Technology, BD Biosciences, and R&D Systems. The following antibody/fluorochrome conjugates were used at the following dilutions: anti-CD8a PerCp-Cy5.5 (1:200), anti-PD-1 Pe-Cy7 (1:200),), anti-CD44 Alexa Fluor 700 (1:200), anti-B220 BV786 (1:200), anti-TCF-1 FITC (1:50), anti-Tim-3 PE

(1:25), anti-Tim-3 FITC (1:25), anti-CD73 APC (1:100), anti-Ki67 BV711 (1:25), anti-TOX PE (1:50), anti-TOX APC (1:50), anti-BCL6 PE (1:50), anti-BCL6 APC (1:50), anti-SLAMF6 APC (1:100), and anti-CD45.1 BV711 (1:200). Endogenous LCMV-specific CD8 T cells were detected using the D^bGP33-41 tetramer (1:200), which was prepared in house. Streptavidin-APC was purchased from (Thermo Fisher Scientific). Dead cells were excluded using the Live/Dead Fixable Near-IR (1:250) or Live/Dead Fixable Aqua (1:250) (Thermo Fisher Scientific). For cell surface staining, antibodies were prepared in PBS supplemented with 2% FBS at indicated concentrations before being added to cells on ice for 30mins. Cells were then washed two times. For detecting intracellular proteins (TCF-1, GzmB, BCL6, and Ki67), the FOXP3 staining buffer set (Thermo Fisher Scientific) was used according to the manufacturer's instructions. Samples were acquired on a Canto, LSR II, the FAC Symphony A3 (BD Biosciences) system, or the Cytek Aurora spectral analyzer. Data were analyzed using FlowJo (v.10.7.1, BD Biosciences).

Cell Sorting

A FACS Aria II (BD Biosciences) was used for cell sorting. For single cell RNA-sequencing of LCMV-specific CD8 T cells, CD8+ PD-1+ GP33+ from chronically infected mice (days 5 and >45 p.i.) were sorted at a purity of greater than 96%.

scRNA-seq

scRNA-seq libraries were generated using the Chromium Single cell 5' Library & Gel Bead Kit (10x Genomics) according to the manufacturer. D^bGP33+ CD8 T cells or naïve CD44lo CD8 T cells were sorted and captured into gel beads-in-emulsion. After being reverse transcribed, gel beads-in-emulsion were disrupted and barcoded cDNA was

isolated, pooled, then amplified by PCR for 13 cycles. Amplified cDNA was then fragmented and processed for end repair and A-tailing before undergoing sample index PCR for 16 cycles. Purified libraries were sequenced to a depth of 50,000 reads per cell on the HiSeq3000 (Illumina) systems with 26 cycles for read 1, 8 cycles for index (i7) and 91 cycles for read 2.

Cell Ranger v.3.1 was used to align, filter, and count barcodes as well as unique molecular identifiers. Further data analyses was performed using Seurat (v.3.0) (Satija, Nature biotech 2015). Cells with greater than 8% mitochondrial genes were excluded from analysis. Cells with more than 2,500-5,000 or less than 100-1,000 detected genes were considered outliers and excluded from downstream analyses. Raw unique molecular identifier counts were then normalized to unique molecular identifier counts per million total counts before being log-transformed. Principle component analysis was performed, and the 10 most statistically significant principal components were used for uniform manifold approximation and projection (UMAP) analysis. Clusters were identified using the nearest neighbor algorithm in Seurat and UMAP plots were generated based on selected PCA dimensions. The Seurat function FindAllMarkers was used to identify marker genes. Log-normalized data are shown. Gene set scoring was performed using the VISION R package v.2.1.0, following the scoring algorithm as described previously (DeTomaso, BMC Bioinformatics 2016). In brief, the expression of signature genes is weighted based on the predicted dropout probability calculated from nearest neighbors, and the normalized expression summed for all genes in the gene set. Gene set used: GSE84105 (Im et al., 2016).

Confocal microscopy of frozen spleen sections

To examine the localization of CD8+ T cell subsets in the spleen, spleens were removed from infected mice at indicated times and fixed overnight in periodate-lysine-paraformaldehyde buffer. Fixed spleens were then placed in 30% sucrose in PBS for 24 hours before embedding in optimal-cutting-temperature medium (Electron Microscopy Sciences) and freezing in dry-ice-cooled isopentane. 18 micron sections were cut on a Leica cryostat (Leica Microsystems). Sections were blocked with 1% bovine serum albumin (BSA), 5% mouse and 5% donkey serum in PBS wash containing 0.01% Tween 20 (Thermo Fisher Scientific) for 45-60mins at room temperature. Slides were then stained for Rat IgG2b anti-CD8β (1:200, Biolegend), Alexa 647 Rat IgG2a anti-PD-1 (clone 29F.1A12, 1:50, Biolegend), biotinylated Rat IgG2a B220 (1:200, Biolegend), and Rabbit IgG anti-TCF-1 (1:100, Cell Signaling) overnight at 4C in the dark. After washing, secondary antibody mix was added for 1 hour at room temperature in the dark containing Alexa 555 anti-Rat IgG2b (1:250, Southern Biotech), streptavidin-Alexa 594 (1:500, Thermo Fisher Scientific) and Alexa 488 anti-rabbit IgG (1:250, Thermo Fisher Scientific). LCMV antigen distribution was visualized on spleen sections, fixed and dehydrated as mentioned above, using guinea pig anti-LCMV sera (1:400) and Rat IgG2a anti-CD169 (1:200, clone 3D6.112, Biolegend). Following a 45-60min blocking step (1% BSA, 5% mouse serum, 5% goat serum, and mouse Fc block (Biolegend, 1:100) in PBS containing 0.01% Tween 20) and washing, sections were incubated with primary antibodies overnight at 4C in the dark. After washing with PBS containing 0.01% Tween 20, goat anti-guinea pig Alexa 555 or Alexa 647 (1:500, Thermo Fisher Scientific) and mouse anti-Rat IgG2A Alexa 488 (1:250, Southern Biotech) were added for 1hr at room temperature in the dark. After final washing steps, slides were mounted

with Prolong Gold mounting medium containing DAPI (Thermo Fisher Scientific) and cover slipped. Images were acquired with a Leica SP8 tiling confocal microscope (Leica Microsystems) equipped with a 40x 1.3NA oil objective.

Intravascular antibody labeling

For intravascular labeling, 3μg of BV421-conjugated anti-CD8α (Biolegend) was injected i.v. into infected mice. Three minutes after injection, splenocytes were isolated and prepared into a single cell suspension before staining *ex vivo*.

Image analysis

Images were analyzed using Imaris software (Bitplane). Stem-like and effector/terminally differentiated CD8 T cells were identified accordingly:

1. The colocalization tool was used to create a new channel for PD-1+ CD8+ T cells.
2. 3D surfaces were then generated for PD-1+ CD8+ T cells to allow for detection of the DAPI nuclear stain, which was then used to distinguish cells from non-cells. A new channel was created for DAPI+ PD-1+ CD8+ T cells.
3. 3D surfaces were generated for DAPI+ PD-1+ CD8+ T cells to enable detection of TCF-1 stain. MFI of the TCF-1 channel was then determined for each surface and cutoff was set for TCF-1 positivity/negativity. Stem-like CD8 T cells = DAPI+ PD-1+ CD8+ TCF-1+. Effector/terminally diff. CD8 T cells = DAPI+ PD-1+ CD8+ TCF-1-. The white pulp and red pulp were manually annotated as discrete regions of interest (ROI) using the B220 and CD8β stains as a guide. Once total stem-like versus effector/terminally diff. 3D surfaces were distinguished from each other, the percentage of each located in the white or red pulp was calculated.

Statistical analysis

GraphPad Prism (v.10.0.3) was used for statistical analysis. The difference between experimental groups was assessed using two-tailed unpaired t-tests or two-tailed unpaired Mann-Whitney *U*-tests or one-tailed paired Wilcoxon matched-pairs signed rank test.

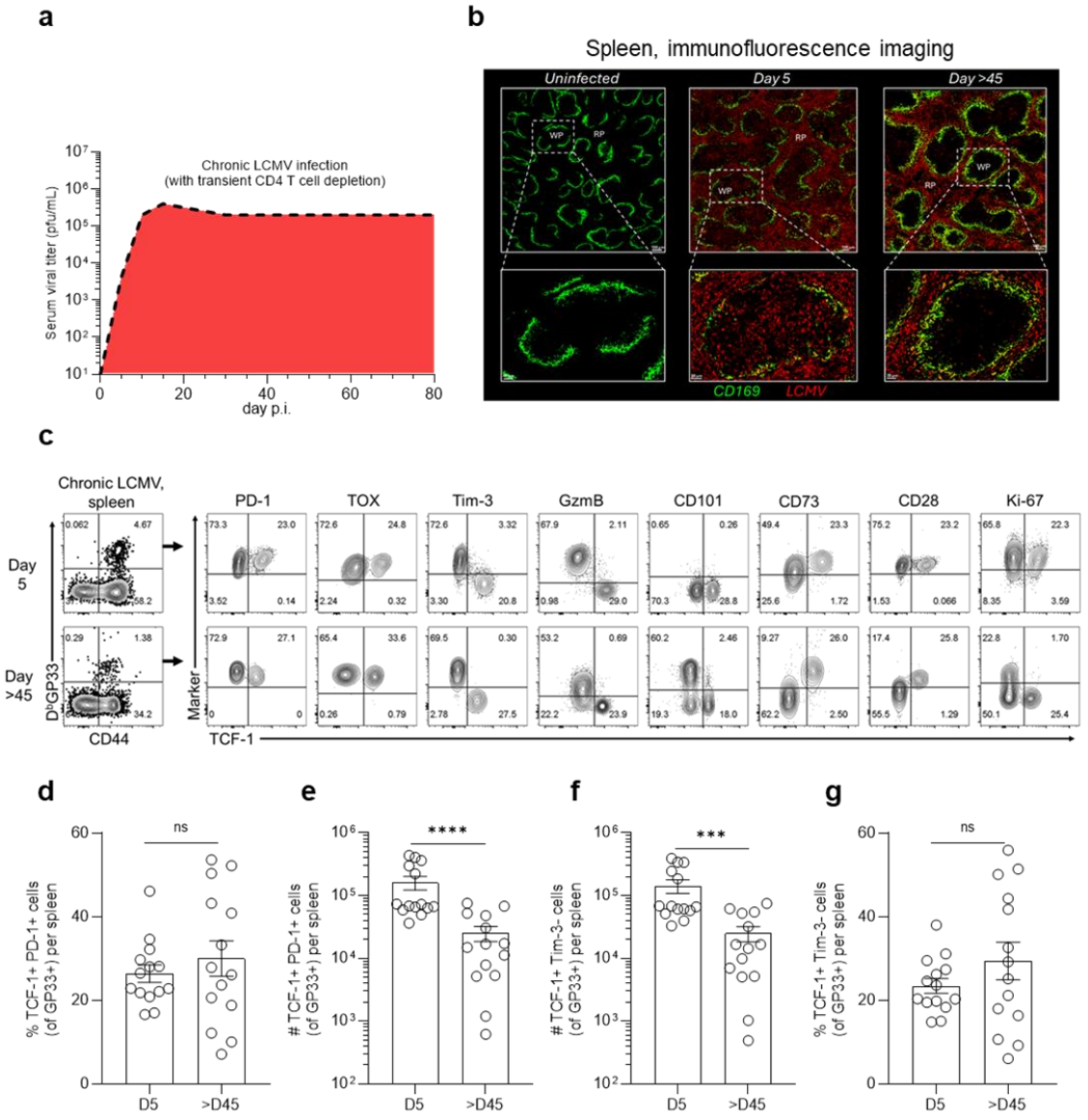

Fig. 1| Early emergence of stem-like CD8+ T cell phenotype.
a, Cartoon illustrating viral titer kinetics in mice were infected with LCMV clone 13 after transient CD4+ T cell depletion. This results in high viral titers and life-long viral infection (Matloubian et al., 1994). **b,** Immunofluorescence imaging showing distribution of LCMV antigen in the spleens of uninfected and chronically mice on days 5 and >45 post-infection. CD169 (green) was used to distinguished between the two major compartments in the spleen, white pulp (WP) and red pulp (RP). LCMV antigen (red) was detected using serum from LCMV immune guinea pigs. Images shown are representative of 1 of 3 independent experiments (n= 5 mice per time point). **c,** Phenotypic analysis of LCMV-specific D^bGP33+ CD8+ T cells in the spleen on days 5 and >45 post-infection (p.i.). **d-g,** Summary graphs showing frequency and numbers of GP33-specific PD-1+ TCF-1+ and TOX+ TCF-1+ stem-like CD8 T cells. Flow plots are representative of 1 of 4 independent experiments (n= 3-5 mice per time point). Summary graphs d-g show mean ± SEM and are pooled from 3 of 4 independent experiments (*n=12-14* mice per time point). P values calculated using Mann-Whitney test. *** and **** indicate p values of less than 0.001, and 0.0001, respectively.

Figure 2

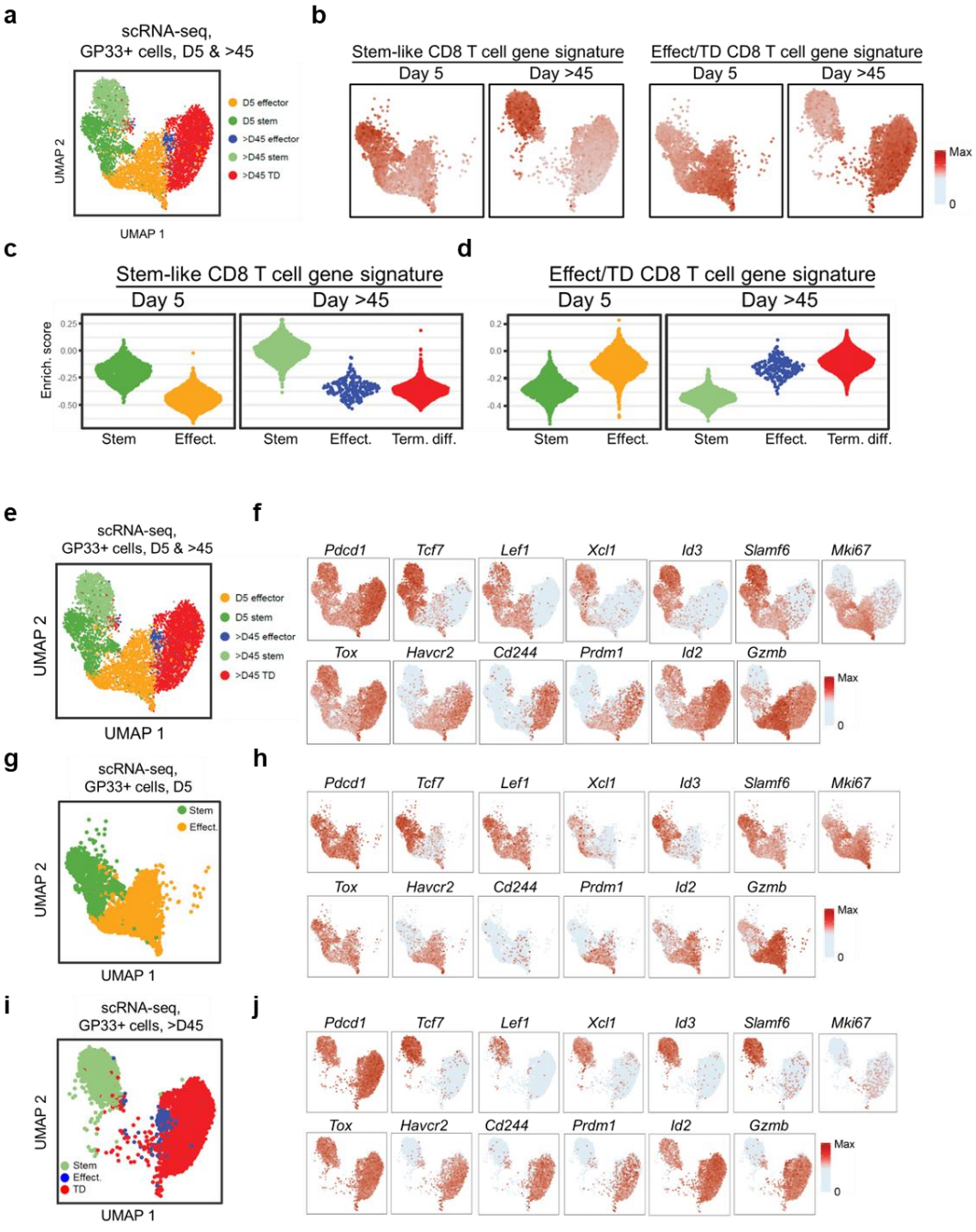

Fig. 2| Early emergence of stem-like CD8+ T cell transcriptional program.
Mice were infected with LCMV clone 13 after transient CD4+ T cell depletion which results in high viral titers and life-long viral infection (Matloubian et al., 1994).**a-j,** scRNA-seq analyses of splenic D^bGP33+ CD8+ T cells on days 5 (60,000 cells) and >45 (40,000 cells) after chronic infection. **a,** Combined data from day 5 and >45 cells projected as a UMAP plot. Day 5 and >45 cells formed two and three distinct clusters, respectively. TD, terminally differentiated. **b,** Enrichment of day 5 and >45 clusters for stem-like and effect/TD gene signatures CD8+ T cell gene signatures (GSE84105, Im et al., 2016). Max = maximum. **c,d,** Enumeration of gene set enrichment analysis in b. **e,** Same UMAP as shown in e. **f,** Expression of selected genes by each cluster. **g, h,** UMAP showing day 5 cell clusters (g) and expression of selected genes by each cluster (h). **i,j,** UMAP showing day >45 cell clusters (i) and expression of selected genes by each cluster (j).

Extended Data Fig. 1

a

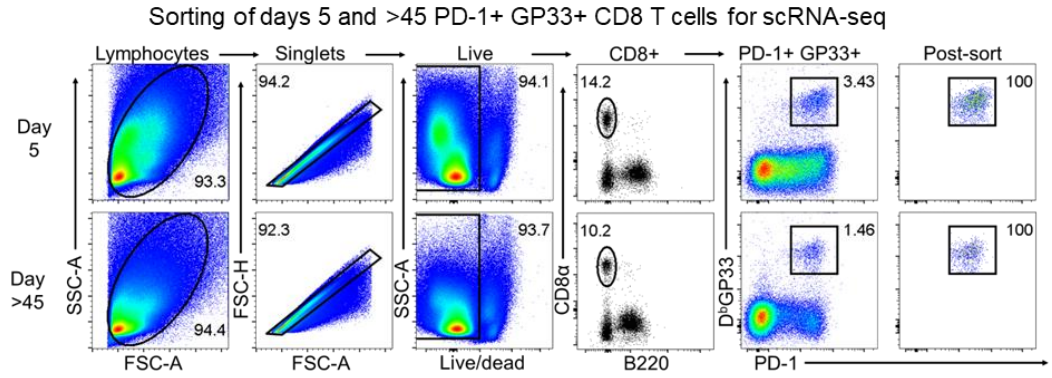

b

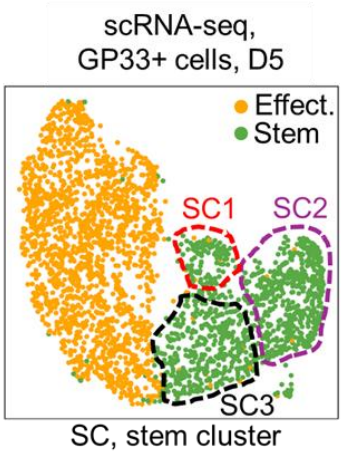

c

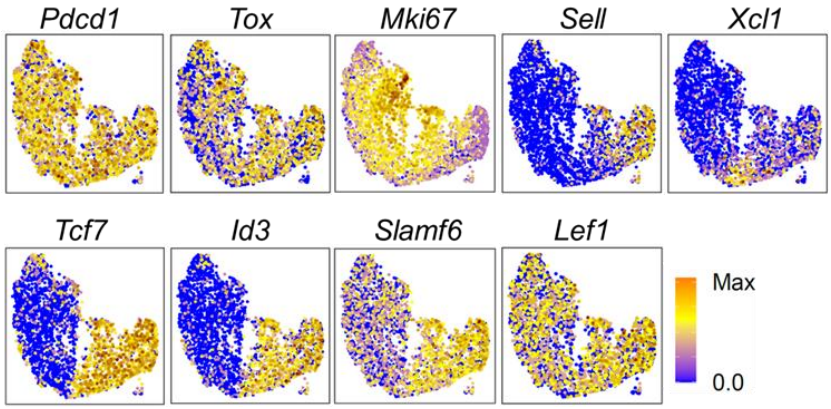

Extended Data Fig. 1| scRNA-seq of LCMV GP33-specific CD8+ T cells on days 5 and >45 after chronic infection. a, Gating strategy for sorting of splenic D^bGP33+ CD8+ T cells on days 5 (60,000 cells) and >45 (40,000 cells) for scRNA-seq. **b,c,** UMAP showing day 5 GP33+ cells (b), with subclusters drawn to highlight heterogeneity in expression of selected genes by stem cluster (c). SC, stem cluster. Max = maximum.

Figure 3

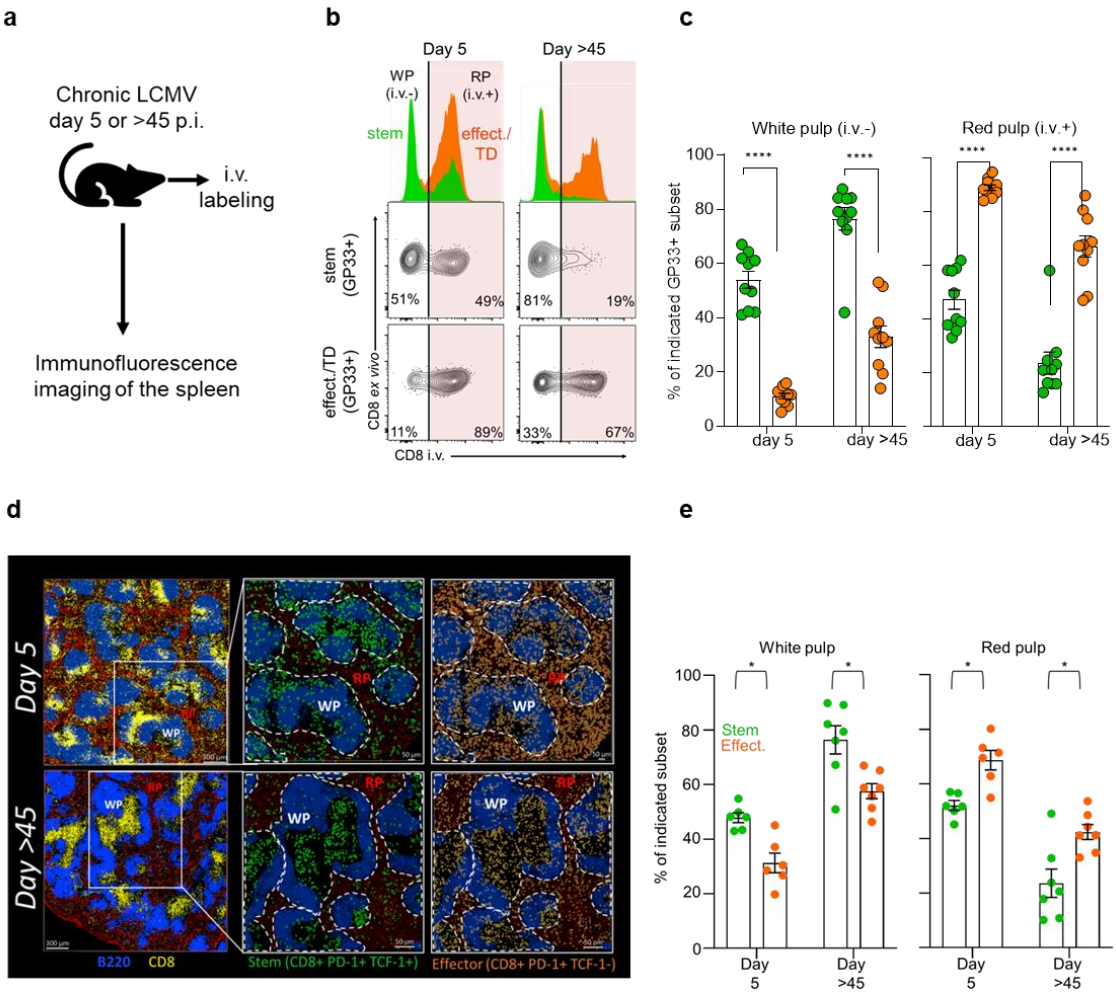

Fig. 3| Early anatomical commitment of stem-like CD8+ T cells to the splenic white pulp. **a,** On days 5 and >45 p.i., chronically infected mice were injected with fluorescently-labeled anti-CD8α (3μg/mouse) and euthanized 3 mins later for flow cytometry analysis. **b,** Representative flow plots/histograms showing frequencies of D^bGP33+ TCF-1+ Tim-3- (stem) and TCF-1- Tim-3+ (effect./TD) CD8+ T cells in the white pulp (CD8α i.v. antibody negative) or the red pulp (CD8α i.v. antibody positive). Numbers on flow plots are frequencies. **c,** Summary graphs showing frequencies of GP33-specific stem-like and effect./TD cells in the white pulp (left) and red pulp (right). **d,** Representative immunofluorescent histology showing the location of stem-like (green) and effector (orange) CD8+ T cells in the spleen on days 5 and >45 after chronic infection. Dashed lines denote border between the white pulp (WP) and red pulp (RP). Stem-like cells were identified as CD8β+ PD-1+ TCF-1+ DAPI+ cells. Effector cells were identified CD8β+ PD-1+ TCF-1- DAPI+ cells). **e,** Frequency of indicated subsets in white pulp (left) and red pulp (right) based on image analysis. Summary graphs in c show mean ± SEM and are data pooled from 2 of 3 independent experiments (*n*= 9-10 mice per time point). P values shown are from Wilcoxon matched-pairs signed rank test. **** indicates p value of less than 0.0001. Images d are representative of 1 of 2 independent experiments (*n*=3-4 mice per experiment). Summary graphs in e show mean ± SEM and are pooled from 2 independent experiments (*n*=6-7 mice per time point). P values shown are from Wilcoxon matched-pairs signed rank test. * indicates p value of less than 0.05.

Extended Data Fig. 2

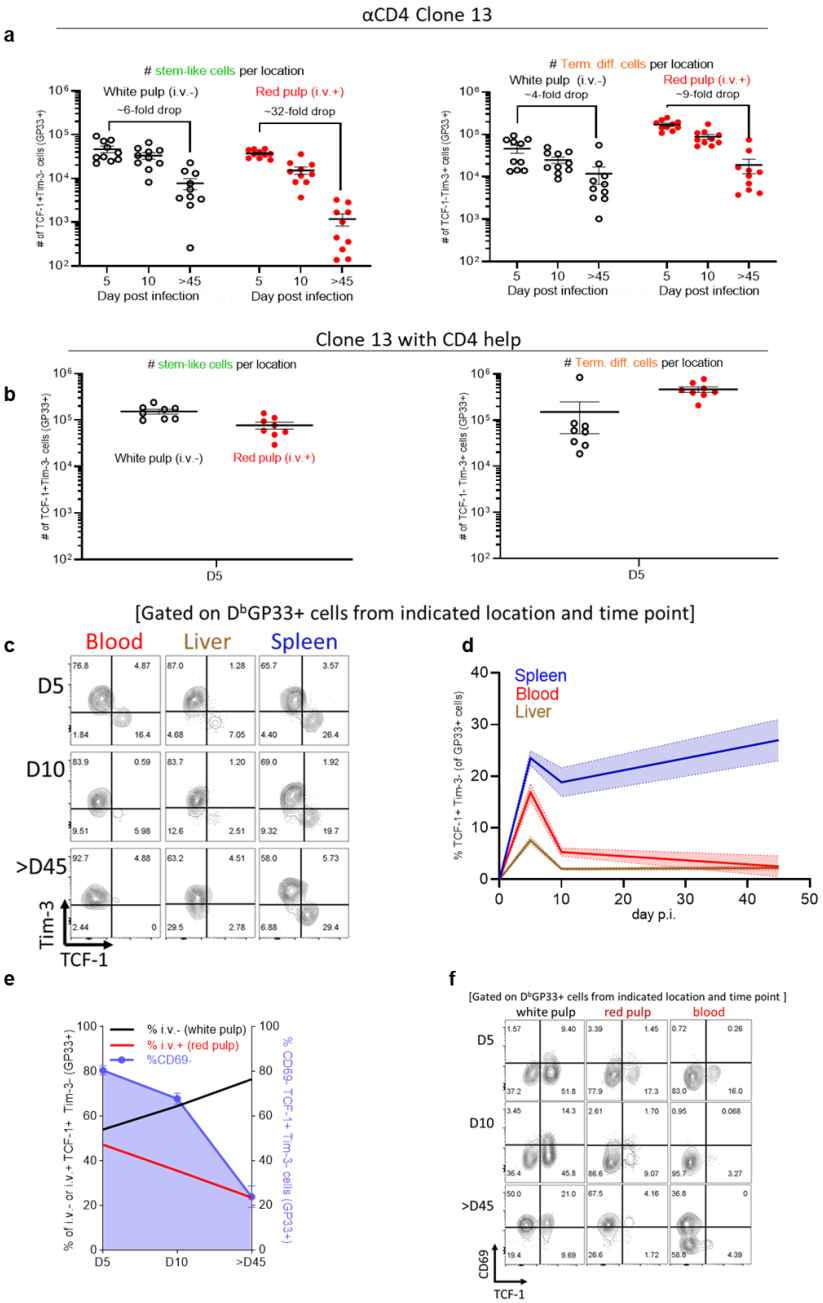

Extended Data Fig. 2| Stem-like CD8 T cell location and CD69 expression as chronic infection progresses. a, Numbers of white pulp or red pulp LCMV-specific (GP33+) stem-like (left) and effect./term. diff. (right) subsets on days 5, 10, >45 after αCD4 clone 13 infection. Graphs show mean±SEM). **b,** Numbers of white pulp or red pulp LCMV-specific (GP33+) stem-like (left) and effect./term. diff. (right) subsets on day 5 after CD4-helped clone 13 infection. Graphs show mean±SEM. **c,** Representative flow plots (c) and summary graph (d) showing frequency of LCMV-specific (GP33+) stem-like in indicated locations over time. Bold lines in (d) represent mean, shading symbolizes ±SEM. **E,** Mean frequency of white pulp (black line) and red pulp (red line) stem-like cells at indicated time points. Purple line represents frequency (mean±SEM) of CD69- stem-like cells at each time point. **f,** Representative flow plots showing LCMV-specific (GP33+) CD69+ and CD69- TCF-1+ cells in the white pulp, red pulp, and blood at indicated time points. Numbers shown are frequencies. Summary graphs are combined data from two of four independent experiments (n = 3-5 mice per time point per experiment). Flow plots are representative of one of four independent experiments (n = 3-5 mice per time point per experiment).

Chapter 3: Development of stem-like CD8+ T cell during chronic infection

This chapter is reproduced with edits from:
Early generation of a precursor CD8 T cell that can adapt to acute or chronic viral infection

Daniel T. McManus[1,2,11], Rajesh M. Valanparambil[1,2,11], Christopher B. Medina[1,2], Christopher D. Scharer[2], Donald J. McGuire[1,2], Yinghong Hu[1,2], Ewelina Sobierajska[4], Daniel Y. Chang[9], Andreas Wieland[5], Judong Lee[1,2], Tahseen H. Nasti[1,2], Masao Hashimoto[1,2], James L. Ross[1,2], Nataliya Prokhnevska[6], Maria A. Cardenas[4], Amanda L. Gill[1,2], Elisa C. Clark[8], Kathleen Abadie[8], Arjun Kumar[8], Hao Yuan Kueh[8], Jonathan Kaye[7], Byron B. Au-Yeung[10], Haydn T. Kissick[1,2,3,4], and Rafi Ahmed[1,2,3,*]

[1]Emory Vaccine Center, Emory University School of Medicine, Atlanta, GA, USA
[2]Department of Microbiology and Immunology, Emory University School of Medicine, Atlanta, GA, USA
[3]Winship Cancer Institute of Emory University, Atlanta, GA, USA
[4]Department of Urology, Emory University School of Medicine, Atlanta, GA, USA
[5]Department of Otolaryngology, The Ohio State University College of Medicine, Columbus, OH
[6]The Precision Immunology Institute, Icahn School of Medicine at Mount Sinai, New York, NY, USA
[7]Research Division of Immunology, Department of Biomedical Sciences, Cedars-Sinai Medical Center, Los Angeles, CA, USA
[8]Department of Bioengineering, University of Washington, Seattle, WA, USA
[9]Department of Pathology, Mass General Brigham, Harvard Medical School, Boston, MA, USA
[10]Division of Immunology, Lowance Center for Human Immunology, Department of Medicine, Emory University, Atlanta, GA,
[11]These authors contributed equally
*Corresponding author. Email: rahmed@emory.edu
**Under revisions for Nature*

Abstract

The canonical phenotypic traits (PD-1+ TOX+ TCF-1+ Tim-3- GzmB-) and anatomical distribution (bias for splenic white pulp) of virus-specific stem-like CD8 T cells arises as early as day 5 after chronic LCMV infection. We next asked when the canonical stem-like CD8 T cell transcriptional and epigenetic program first emerges, and to understand the role of antigen for these cells. We therefore performed additional phenotyping in addition to transcriptional (RNA-seq) and epigenetic (ATAC-seq) profiling of stem-like CD8 T cells from days 5 and >45 after chronic LCMV. Based on RNA- and ATAC-sequencing of sorted CD8 T cell subsets from chronic LCMV, day 5 and >45 stem-like CD8 T cells showed considerable transcriptional and epigenetic overlap. Relative effectors, day 5 and >45 stem-like CD8 T cells had increased expression and chromatin accessibility for costimulatory molecules, transcription factors important for CD8 T cell plasticity and longevity, and molecules related to CD4+ Tfh cells. However, both day 5 and >45 stem-like CD8 T cells lacked expression and accessibility for effector loci. Between days 5 and >45, stem-like CD8 T cells upregulated inhibitory molecules and transitioned from metabolically/mitotically active cells to quiescent cells. Interestingly, the absence of effector molecules by stem-like CD8 T cells was not owed to insufficient TCR signaling as stem-like and effector CD8 T cells showed similar expression levels of *Nur77*-GFP throughout chronic LCMV infection. Discontinuing TCR signaling during chronic LCMV led to the loss of key phenotypic traits of stem-like CD8 T cells, including the transcriptional repressor, Bcl-6. Together these data show that the core stem-like CD8 T cell program emerges early during chronic infection, is preserved throughout, and relies on continuous antigen exposure.

Introduction

In chapter 2 we found that virus-specific CD8 T cells bearing phenotypical properties of virus-specific stem-like CD8 T cells (PD-1+ TOX+ TCF-1+ Tim-3- GzmB-) from day >45 after chronic LCMV infection could be observed as early as day 5. The anatomical bias for lymphoid sites, like the splenic white pulp, is a hallmark feature of stem-like CD8 T cells during chronic LCMV infection. Using intravascular labeling and imaging, we found that the anatomical commitment of virus-specific stem-like CD8 T cells for the splenic white pulp was also evident on day 5 after chronic LCMV.

Stem-like CD8 T cell have a unique transcriptional and epigenetic program combining features both of exhausted and memory CD8 T cells[14,17,19,89,90]. Like exhausted CD8 T cells, they express and show accessibility for the co-inhibitory molecules like *Pdcd1*, *Lag3*, *Ctla4* as well as the transcription factor, *Tox*. Interestingly, stem-like CD8 T cells also express and show accessibility for genes needed for the self-renewal, plasticity, and longevity of memory CD8 T cells including *Tcf7*, *Id3*, and *Lef1*. During chronic LCMV infection, *Tcf7* is crucial for the generation of stem-like CD8 T cells[60,67] while *Id3* is important for the survival of these cells[91]. An additional feature distinguishing stem-like from effector/terminally differeniated CD8 T cells during chronic LCMV infection is the expression of genes typically expressed by CD4+ T follicular helper (Tfh) cells like *Bcl6*, *Plagl1*, and *Izumo1*[60,92]. In a cancer model, the persistence of stem-like CD8 T cells relied on *Bcl6* expression, specifically to antagonize *Prdm1* (encoding BLIMP1)-mediated effector differentiation[93]. Another key difference between stem-like and memory CD8 T cells has to do with granzyme B (*GzmB*) gene. The *Gzmb* locus is first opened by effector cells during the early stages of acute viral infection. After viral clearance, a portion of the effector pool gives rise to memory CD8 T cells, which keep the *GzmB* gene open/accessible enabling for its rapid re-expression upon re-infection.

In stem-like CD8 T cells the *GzmB* locus remains closed and accordingly, untranscribed [94–96].

Here we asked when the stem-like CD8+ T cell transcriptional and epigenetic programs first emerge and how do these programs compare at the early versus established phases of chronic infection. The absence of effector molecules despite being in the middle of an active viral infection is a unique feature of stem-like CD8 T cells. It's unclear whether this is owed to reduced TCR stimulation relative to effector CD8 T cells or some other mechanism. We used *Nur77*-GFP mice[94–97] to examine TCR signaling within virus-specific CD8 T cells. We also examined the important of continuous antigen exposure for stem-like CD8 T cells during chronic LCMV using a clone 13 mutant that fails to elicit a GP33-specific response[97–100].

Results

The core stem-like CD8 T cell transcriptional and epigenetic program arises early and is maintained throughout chronic infection

To further complement the data in chapter 2 we performed transcriptional (RNA-seq) and epigenetic (ATAC-seq) analysis of sorted stem-like (PD-1+ CD73+ Tim-3-) and more differentiated effector/TD (PD-1+ CD73- Tim-3+) subsets at days 5 and >45 post-infection (Fig. 1a and Extended Data Fig. 1a and b). Endogenous GP33-specific stem-like and effect./TD were used for RNA-seq (Extended Data Fig. 1a) whereas monoclonal TCR transgenic GP33-specific CD8 T cell (P14s) subsets were used for ATAC-seq (Extended Data Fig. 2b).
The RNA-seq and ATAC-seq data demonstrated consistent changes between common sample comparisons. For example, a comparison of the accessibility differences between day 5 stem-like to naïve CD8 T cells showed a significant correlation to the corresponding transcriptional differences. The same significant correlation was observed comparing D45 stem-like to naïve, D5 stem-like to day 5 effect./TD, and D45 stem-like to d45 effect./TD (Extended Data Fig. 1c). Importantly, genes upregulated in stem-like cells compared to effect./TD CD8 T cells (*Tcf7*, *Xcl1*) contained regions with increased accessibility in stem-like CD8 T cells whereas genes upregulated in effect./TD (*Gzmb*) more accessible in the corresponding cell type (Extended Data Fig. 1c). In addition, correlation of the accessibility patterns with transcriptional changes pairwise across all sample groups revealed the highest correlation within the same cell type, indicating the ATAC-seq and RNA-seq datasets are highly concordant and that each cell's transcriptional program is underpinned by a matching epigenetic architecture (Extended Data Fig. 1d).

Interestingly, day 5 and >45 stem-like cells were positioned almost identically on PC1 of the PCA plots in Fig. 1b, and c, suggesting considerable transcriptional and epigenetic overlap. Stem-like and effect./TD subsets from both time points shared in the expression and accessibility of multiple inhibitory molecules (*Lag3, Pdcd1, Cd160, Ctla4)* (Fig. 1d-f). Many of the gene expression and chromatin accessibility hallmarks of canonical stem-like CD8+ T cells were in place as early as day 5. These included higher

expression and accessibility for costimulatory molecules like *Tnfsf14*, *Tnfrsf4*, and most notably *Cd28*, which is not only required for the response to PD-1 blockade but is also an important regulator of stem-like CD8+ T cell self-renewal and differentiation[60,77,101]. Gene expression and accessibility for effector genes (*Fasl, Ifng, Prf1, Gzma, Gzmb)* were low for stem-like relative to effect./TD CD8+ T cells, even on day 5 when antigen and inflammation levels are high (Fig. 1d-f). Reciprocally, high expression and accessibility for transcription factors associated with longevity and self-renewal in T cells (*Id3, Tcf7, Prickle1, Kit, Sox4*, *Lef*) and CD4+ Tfh molecules (*Bcl-6, Slamf6*, *Izumo1r*) was also observed in day 5 stem-like CD8 T cells (Fig. 1d-f). Gene set enrichment analysis showed that day 5 stems enriched for the canonical stem-like CD8 T cell gene signature.

In addition, both day 5 and >45 stems shared transcriptional overlap with CD8+ memory precursors and CD4+ Tfh, whereas day 5 and >45 effect./TD cells were more closely related to CD8+ terminal effectors and CD4+ Th1 cells (Fig. 1g). When directly compared to D5 effect./TD, D5 stem-like cells showed increased accessibility and transcription for genes involved in defense response to virus/ response to type I interferon, WNT signaling, negative regulation of leukocyte activation, negative regulation T cell apoptosis, and IL15 signaling. In contrast, D5 effect./TD showed increased accessibility and transcription for genes related T cell and leukocyte activation, effector processes/T cell cytolysis, and type II interferon production (Fig. 2a and b).

Stem-like CD8 T cells become quiescent and upregulate inhibitory molecules as chronic infection progresses

Long-term antigen exposure leads to substantial transcriptional, epigenetic, and metabolic changes to CD8 T cells[14,16,36,42,43,89,102,103]. Consistent with this, day 5 and >45 cells appeared to separate in the PCA plots shown in Fig. 1b and c based on PC2 (y-axis), indicating that the both stem-like and effect./TD subsets acquire time-related transcriptional and epigenetic changes. Interestingly, a comparison of stem-like CD8 T cells between days 5 and 45 revealed increased transcription (719/9999 genes) and accessibility (7945/34594 chromatin regions) at loci involved in activation, cell

proliferation, and inflammatory response pathways on day 5 (Fig. 2a, b). D5 stem-like cells also showed increased transcription for genes related to metabolic pathways important for fueling cell division like the TCA cycle, glycolysis, glutaminolysis, and mammalian target of rapamycin (mTOR) signaling (Fig. 3a and b)[104–106]. In contrast, >D45 stem-like cells showed increased transcription (1026/9999 genes) and accessibility (7945/34594 chromatin regions) for loci involved in cell adhesion, TGFb signaling, and negative regulation of proliferation (Fig. 2a, b). Consistent with these changes, flow cytometry showed that between days 5 to >45, stem-like CD8+ T cells lost expression of the proliferation marker, Ki67, and decreased in cell size (Fig. 3c and d). Moreover, >D45 stem-like cells showed increased mRNA levels for *Cd200r1, Cd200, CD83, Lrig1, Tnfsrf8,* and *Izumo1r*— inhibitory molecules associated with the transforming growth factor β (TGF-β)-mediated quiescence of stem-like CD8 T cells during chronic LCMV[76,107] (Fig. 3e). It's important to note that both stem-like and effect./TD cells on day 5 were enriched for genes involved in and accessory to cell proliferation. Rather than being evidence for two distinct subsets, the key transcriptional and epigenetic differences between day 5 and >45 stem-like cells more likely reflect the changes these cells experience following prolonged antigen exposure and alterations in the environment.

Taken together, these data indicate that virus specific stem-like CD8+ T cells with the canonical transcriptional signature and epigenetic marks of *bona-fide* stem-like CD8+ T cells can be detected as early as 5 days after infection with LCMV clone 13. While there are important time-related differences between day 5 and day >45 stem-like CD8+ T cells (Figs. 2 and 3), the fate decision for generating this cell is made early after infection.

Stem-like CD8 T cells continuously receive TCR signaling during chronic infection

Strong and continuous TCR signaling is thought to be a key driver of effector differentiation[48]. Hence, the absence of transcription factors and molecules associated with effector function in stem-like CD8 T cells suggested that these cells might be receiving less TCR stimulation compared to their effector counter parts during chronic LCMV infection. To examine this, we infected *Nur77*-GFP reporter mice with LCMV clone 13, enabling us to measure *Nur77* expression (as reported by GFP) as a proxy for TCR stimulation[94–96]. As a negative control for TCR signaling, we infected a separate group of *Nur77*-GFP mice with acute LCMV and measured *Nur77*-GFP expression on LCMV-specific memory cells after viral clearance. As expected, GP33+ CD44+ memory CD8 T cells from LCMV immune mice were negative for both PD-1 and *Nur77*-GFP expression (data not shown). Surprisingly, both on days 5 and >45 the percentage of GP33+ stem-like (PD-1+ Tim-3-) and effect./TD (PD-1+ Tim-3+) CD8 T cells positive for *Nur77*-GFP expression was virtually the same, >85% (Fig. 4a, b).

Antigen is required for the maintenance of stem-like CD8 T cells during chronic infection
We next asked how antigen versus the chronic infection environment impacts the maintenance of PD-1+ TCF-1+ stem-like CD8+ T cells during chronic infection. To address this question, we took advantage of a LCMV clone 13 mutant with a mutation in the GP33 epitope (valine to alanine amino acid substitution at position 35) that reduces binding of the peptide to D^b. The set-up for this experiment is described in Fig. 5a; one group of mice were infected with WT LCMV clone 13 as our control group and the other group of mice were infected with a mixture of WT LCMV clone 13 and the GP33 mutant clone 13 (2:1 ratio in favor of the mutant virus). As described previously, under these conditions of mixed infection there is initial presentation of GP33 from the WT virus but over time the GP33 mutant virus becomes dominant since there was a higher ratio of the mutant virus in the inoculum but more importantly because there is less efficient killing of cells infected with the mutant strain. Thus, the WT LCMV clone 13 strain gets outcompeted by the LCMV mutant strain and GP33 presentation decreases over time. This chronic infection setting enables one to track GP33-specific CD8+ T cells as exposure to their cognate antigen disappears over time due to the dominance of the

GP33 mutant virus but the viral burden remains high along with the chronic infection environment[97–100]. LCMV GP33-specific P14 CD8+ T cells were used in this experiment to track their differentiation under these two different conditions of chronic infection where there was either continuous antigen stimulation (group 1) or gradual loss of antigen stimulation (group 2). Similar frequencies of P14 stem-like (TCF-1+ Tim-3-) and effector (TCF-1 Tim-3+) CD8+ T cells were observed in WT Cl13 and WT/Mut Cl13 infections on days 5 and 8. Also, mixed infection with WT/Mut Cl13 resulted in high expression of PD-1 and TOX on both stem-like and effector-like CD8+ T cells at these early time points (Fig. 5b-d). This is important as it indicates that sufficient levels of GP33 were present for the initial priming, differentiation, and expansion of P14 CD8+ T cells in WT/Mut Cl13-infected mice. The expression of Slamf6 and Bcl-6 was also similar in both groups of mice (Fig. 5e-g). However, by day 30 there was a striking loss of the GP33 (P14) stem-like CD8+ T cells in the mixed WT/Mut Cl13-infected mice, and the expression of PD-1, TOX, Slamf6, and Bcl-6 declined markedly relative to WT Cl13-infected mice (Fig. 5b-g). A critical control in this experiment is that the loss of stem-like CD8+ T cells in the WT/Mut Cl13-infected mice was selective for the GP33 epitope and that LCMV GP276-specific stem-like CD8+ T cells were maintained equally well in WT Cl13-infected mice and the mixed WT/Mut Cl13-infected mice (Extended Data Fig. 2a and b). These results show unequivocally that antigen is essential to maintain the stem-like CD8+ T cell program during chronic infection and that the chronic environment alone cannot do it.

Discussion

Stem-like CD8 T cells can be distinguished from other CD8 T cell subsets based on their unique transcriptomic and chromatin accessibility profiles, the latter now accepted as a more stable indicator of cell fate. Here we asked when the stem-like CD8 T cell transcriptional and epigenetic program first arises and evaluated the importance of antigen for these cells.

A direct comparison of sorted day 5 and >45 stem-like CD8 T cells using RNA- and ATAC-seq revealed that Per individual gene, day 5 'stems' harbored many of the gene expression and chromatin accessibility hallmarks of canonical stem-like CD8 T cells. Relative to their effector counterparts, stems showed higher expression and accessibility for costimulatory molecules like *Tnfsf14* (LIGHT), *Tnfrsf4* (OX-40), and *Icos* but not effector molecules like *Prf1* and *Gzma/b* (perforin, granzyme A/B). Transcription factors associated with longevity and self-renewal —*Id3, Tcf7, Prickle1, Kit, Sox4*, *Lef1*— as well as marks of CD4 Tfh cells like *Bcl6, Slamf6*, and *Izumo1r* were also more highly expressed and accessible by stems compared to effector/TD cells. Thus, the defining properties of stem-like CD8 T cells—self-renewing capacity, sensitivity to costimulatory signals, proliferative potential, longevity, and the absence of effector molecules — are transcriptionally and epigenetically imprinted as early as day 5 post infection and are supported throughout.

We next used our day 5 and day >45 comparison to understand how stem-like CD8 T cells differ in the early and late phases of chronic viral infection. Early during infection, stem-like CD8 T cells exhibited hallmarks of rapidly dividing cells: uniform Ki67 expression, large cell size, an enriched mTOR gene signature, and the co-expression of genes involved in glucose and amino acid metabolism. Remarkably, these cells retained transcriptional and epigenetic support for self-renewal, longevity, and proliferative capacity even after months of enduring an active viral infection but upregulated multiple inhibitory molecules driven by TGFβ signaling and stop proliferating. Thus, quiescence and elevated inhibitory molecules are not core features of stem-like CD8 T cells but are the effects of long-term antigen exposure. This is an important insight for two main reasons: firstly, it dissociates identifying traits of stem-like CD8 T cells—self-renewal,

longevity, and proliferative fitness—from the functional impairment classically described by exhaustion. Secondly, it highlights the importance of using basic animal models, like the LCMV infection system, for distinguishing between traits that are fundamental to a T cell subset's identity versus circumstantial.

The absence of effector molecules by stem-like CD8 T cells could be owed to reduced TCR signaling within these cells compared to effector cells during chronic LCMV. Interestingly, virus-specific day 5 and >45 stem-like and effector CD8 T cells showed comparable levels of TCR signaling, based on the expression of *Nur77*-GFP. Coupled with our transcriptional and epigenetic data, this observation indicates that the absence of an effector program within stem-like CD8 T cells is not owed to a passive process, such as inadequate TCR stimulation. Rather, it highlights a crucial feature of stem-like CD8 T cells that protects against terminal differentiation and is shared with CD4+ Tfh cells: active repression at key effector loci regardless of an effector-favored environment.
Using a mixed chronic viral infection containing wild type LCMV clone 13 and a clone 13 mutant that fails to elicit a GP33-specific response, we found that antigen was crucial for maintaining key phenotypic traits of stem-like CD8 T cells, including PD-1, TOX, and Bcl-6.

Thus, the stem-like CD8 T cell fate decision is made early during chronic infection and is preserved throughout. As chronic infection progresses, stem-like CD8 T cells become quiescent. These data also suggest that the active resistance to effector differentiation epitomized by stem-like CD8 T cells is paradoxically driven by continuous antigen exposure.

Methods

Mice, viral infections, and virus titration

C57BL/6 and CD45.1 B6 mice were purchased from Jackson laboratory. CD45.1/45.1 or CD45.1/45.2 P14 TCR transgenic mice were bred and maintained in house. 6-8 week old mice were used for infections. *Nur77*-GFP transgenic mice were provided as a gift from the Au-Yeung laboratory at Emory University. Chronic viral infections that result in lifelong viremia were performed as follows: mice were transiently depleted of CD4+ T cells via intraperitoneal injection with 300 µg of a rat anti-mouse CD4 antibody (clone GK 1.5 from BioXcell) 2 days before infection and again on the day of infection. Mice were then injected intravenously (i.v.) with $2x10^6$ PFU LCMV clone 13. For experiments examining the importance of antigen for stem-like CD8 T cells, a LCMV clone 13 mutant was mixed with wildtype clone 13 at a ratio of 2:1 prior to infection. The mutant clone 13 has a valine to alanine amino acid substitution at position 35 of the GP33 epitope. This reduces binding of the peptide to the MHC class I molecule, D^b, preventing recognition by GP33-specific GP33-specific TCR transgenic P14 cells. For acute viral infection, mice were injected i.p. with $2x10^5$ PFU of LCMV Armstrong.

Lymphocyte isolation

Lymphocyte isolation from the spleen was performed as described previously (Wherry's JV paper). Spleens were dissociated by passing through a 70 uM cell strainer (Corning).

Reagents and flow cytometry

All antibodies used for flow cytometry were purchased from Biolegend, Thermo Fisher Scientific, Miltenyi Biotec, Cell Signaling Technology, BD Biosciences, and R&D Systems. The following antibody/fluorochrome conjugates were used at the following dilutions: anti-CD8a PerCp-Cy5.5 (1:200), anti-PD-1 Pe-Cy7 (1:200),), anti-CD44 Alexa Fluor 700 (1:200), anti-B220 BV786 (1:200), anti-TCF-1 FITC (1:50), anti-Tim-3 PE (1:25), anti-Tim-3 FITC (1:25), anti-CD73 APC (1:100), anti-Ki67 BV711 (1:25), anti-TOX PE (1:50), anti-TOX APC (1:50), anti-BCL6 PE (1:50), anti-BCL6 APC (1:50), anti-

SLAMF6 APC (1:100), and anti-CD45.1 BV711 (1:200). Endogenous LCMV-specific CD8 T cells were detected using the D^{b}GP33-41 tetramer (1:200), which was prepared in house. Streptavidin-APC was purchased from (Thermo Fisher Scientific). Dead cells were excluded using the Live/Dead Fixable Near-IR (1:250) or Live/Dead Fixable Aqua (1:250) (Thermo Fisher Scientific). For cell surface staining, antibodies were prepared in PBS supplemented with 2% FBS at indicated concentrations before being added to cells on ice for 30mins. Cells were then washed two times. For detecting intracellular proteins (TCF-1, GzmB, BCL6, and Ki67), the FOXP3 staining buffer set (Thermo Fisher Scientific) was used according to the manufacturer's instructions. Samples were acquired on a Canto, LSR II, the FAC Symphony A3 (BD Biosciences) system, or the Cytek Aurora spectral analyzer. Data were analyzed using FlowJo (v.10.7.1, BD Biosciences).

Cell Sorting

A FACS Aria II (BD Biosciences) was used for cell sorting. For experiments involving bulk RNA or ATAC sequencing, PD-1+ CD73+ Tim-3-, PD-1+ CD73- Tim-3+, PD-1+ CD44+ CD73+ Tim-3- P14s, PD-1+ CD44+ CD73- Tim-3+ P14s CD8 T cells from chronically infected (days 5 and >45 p.i.) were also sorted at a purity of greater than 96%. Naïve (CD44lo PD-1-) CD8 T cells were isolated from the spleens of uninfected mice.

RNA seq

For experiments comparing CD8 T cell subsets on days 5 or >day 45 after chronic LCMV infection, RNA was isolated from samples using the Qiagen RNA/DNA micro kit

per the manufacturer's instructions. Extracted RNA was sent to Emory Yerkes Nonhuman Primate Genomics core for mRNA library preparation and sequencing using the clontech SMART-Seq V4 and HiSeq1000. Data were normalized and differentially expressed genes were determined using DeSeq. A gene was considered differentially expressed with a normalized count >100, $\log_2$ fold-change >1 or <1 and adjusted P value <0.05. Data was analyzed using custom R scripts and visualized using ggplot2 R package, GraphPad Prism (v9.2), and excel. For Gene Set Enrichment Analysis (GSEA) each subset was analyzed using the pre-ranked list mode with 1,000 permutations. All gene sets used were from the MSigDB Molecule Signature Database unless otherwise noted. Enrichment scores were considered significant with an FDR <0.05 and was visualized using ggplot2 R package and GraphPad Prism (v9.2).

ATAC seq

For experiments comparing CD8 T cell subsets on days 5 or >day 45 after chronic LCMV infection, 2-4x10^3 cells were sorted into PBS containing 2% FBS and transposition was performed as previously described (Guo, JI 2018 paper). Briefly, cells were resuspended in 12.5 µl 2x TD Buffer, 2.5 µl Tn5, 2.5 µl 1% Tween-20, 2.5 µl 0.2% Digitonin, and 5 µl H_2O and incubated at 37C for 1 hr. Following transposition, cells were lysed with 2 µl 10 mg/ml Proteinase-K, 23 µl Tagmentation Clean-up buffer (326 mM NaCl, 109 mM EDTA, 0.63% SDS), and incubated at 40°C for 30 min. DNA was extracted and size-selected for small fragments using AMPureXP beads (Beckman Coulter, A63881) and PCR amplified into a sequencing library using NexteraXT indexing primers (Illumina, FC-131-2004) and KAPA HiFi HotStart Ready Mix (Roche, KK2602). Post-PCR final libraries underwent a second size selection using AMPureXP beads.

Final ATAC-seq libraries were quantitated by qPCR and size distributions determined by bioanalyzer. Each sample was pooled at equimolar ratios and sequenced at the Emory Non-human Primate Genomics Core on a NovaSeq6000 using a PE100 run. Raw fastq reads were processed by removing adapter contamination with Skewer [2] and mapped to the mm10 genome using Bowtie2 v2.4.2. Accessible chromatin regions identified using MACS2 2.2.7.1 and differential accessibility between groups was determined using DESeq2 with a FDR < 0.05 and absolute $\log_2$ fold-change > 1. Transcription factor motif enrichment was assessed using chromVAR. Custom data analysis and data display was performed in R v4.1.0.

Figure 1

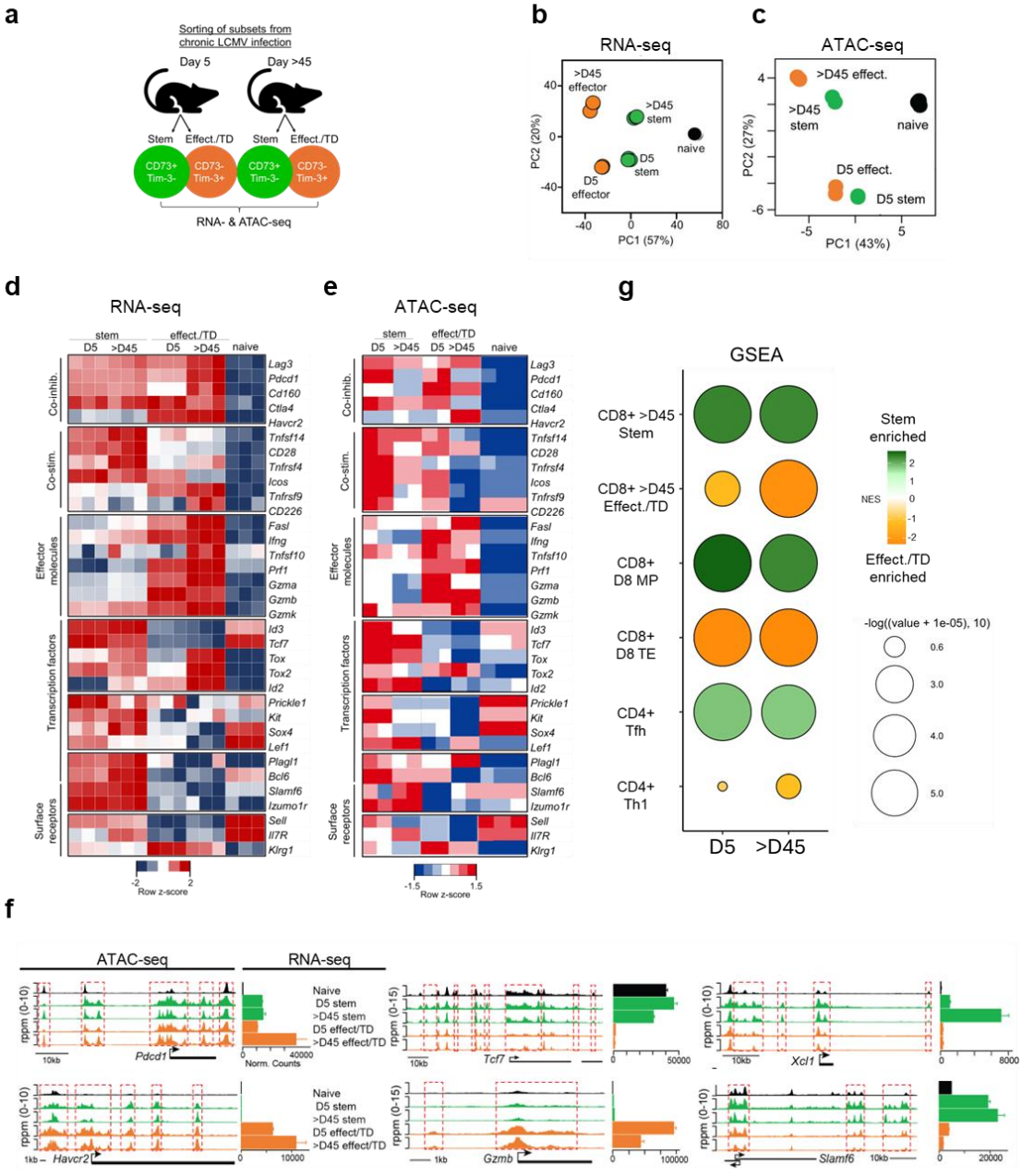

Fig. 1| Core stem-like CD8+ T cell transcriptional and epigenetic program emerges early and is preserved throughout chronic viral infection .

a, Stem-like (CD73+ Tim-3-) and effect./TD (CD73- Tim-3+) CD8+ T cells were sorted from day 5 and >45 spleens for RNA- and ATAC-seq analysis. Bulk PD-1+ cells were used for RNA-seq whereas LCMV GP33-specific P14 cells were used for ATAC-seq. **b,c,** PCA plots showing RNA- (b) and ATAC-seq (c) profiles of indicated subsets. **d,e,** Heatmaps showing relative gene expression (d) and accessibility (e) of selected genes. **f,** Accessibility tracks (ATAC-seq), left) and normalized counts (RNA-seq, right) for selected genes and indicated samples. The location of the transcription start site is indicated by an arrow and a bar depicts the location of the gene body. **g,** GSEA showing enrichment of sorted CD8 T cell subsets for indicated gene signatures based on RNA-seq data. ATAC-seq data represents the mean of all biological replicates. The mean and standard deviation of RNA-seq data is indicated.

Extended Data Fig. 1

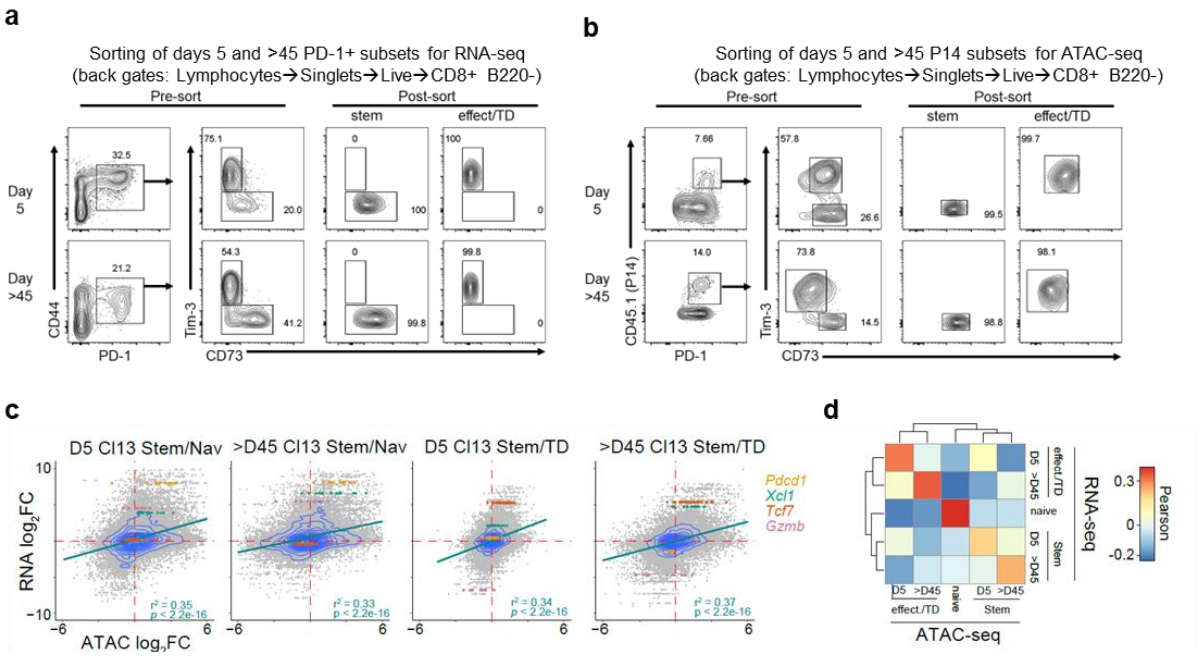

Extended Data Fig. 1| RNA- and ATAC-seq analyses of sorted CD8+ T cell subsets on days 5 and >45 after chronic infection. a, Gating strategy for sorting of day 5 and >45 PD-1+ stem-like (CD73+ Tim-3-) and effector/terminally differentiated (CD73- Tim-3+) CD8+ T cells for RNA-seq. **b,** $2x10^5$ P14 cells were transferred into congenically distinct naïve mice prior to intravenous infection with $2x10^6$ LCMV clone 13. Gating strategy for sorting of day 5 and >45 LCMV GP33-specific P14 stem-like (CD73+ Tim-3-) and effector/terminally differentiated (CD73- Tim-3+) CD8+ T cells for ATAC-seq. Naïve CD8+ T cells (CD44- PD-1-) from uninfected mice were used as a control in each analysis. **c,** Density scatter plot comparing the log2 fold-change in ATAC-seq (x-axis) to the corresponding RNA-seq (y-axis) data for the indicated comparison. Each dot represents accessibility of a single peak and the matching gene expression of the nearest gene. Blue lines indicate data density. Linear correlation trend lines are plotted, and Pearson correlation coefficient and significance of trend are indicated. Colored dots correspond to the data for *Pdcd1*, *Xcl1*, *Tcf7*, and *Gzmb* as indicated. **d,** Heatmap of the Pearson correlation coefficient between ATAC-seq and RNA-seq data for each pairwise comparison between the sample groups.

Figure 2

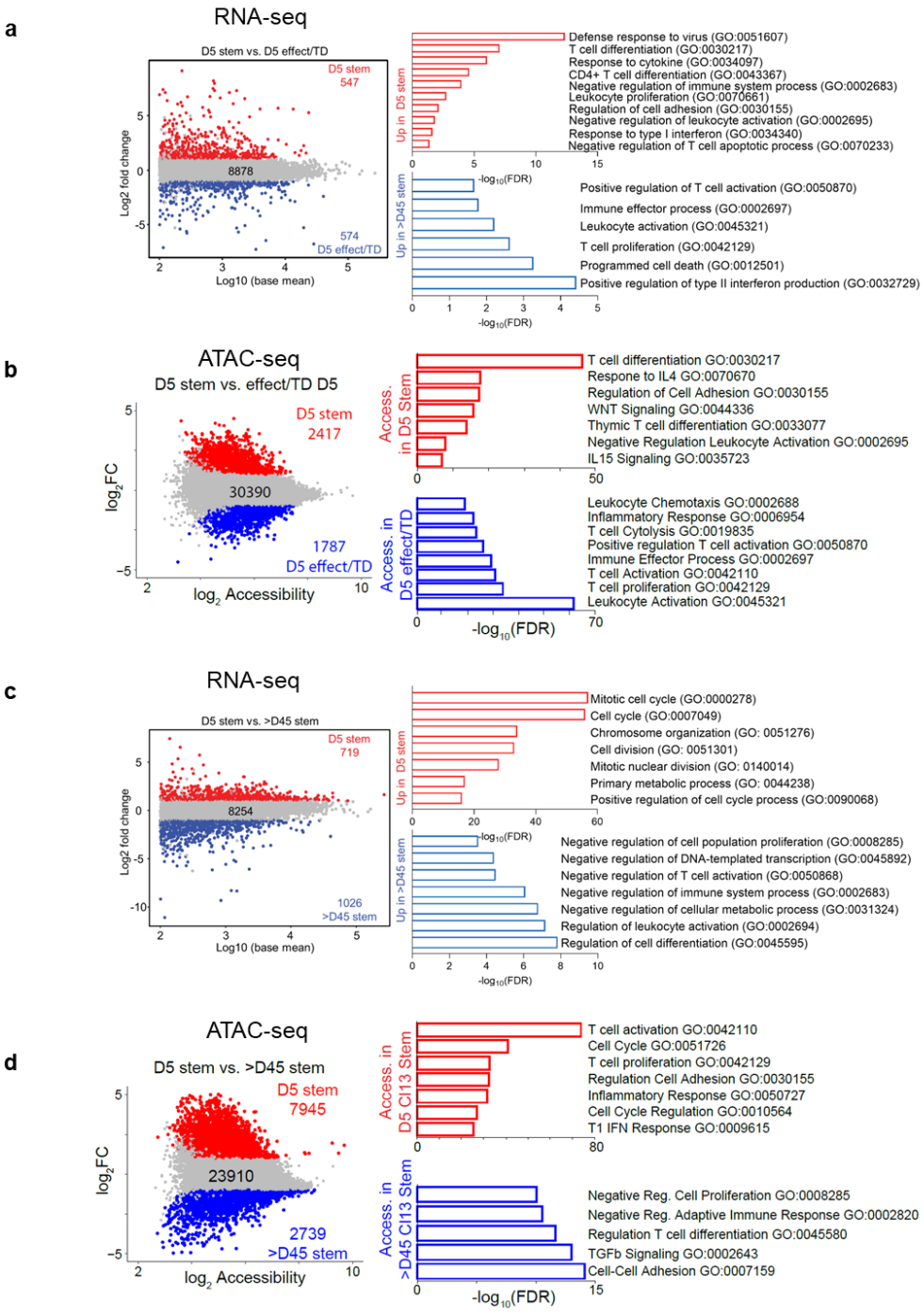

Fig. 2| Transcriptional and epigenetic differences between CD8+ T cell subsets on days 5 and >45 after chronic infection. a,c, (RNA-seq) MA scatter plots of log2 fold-change in RNA expression versus the log10 base mean in RNA expression for indicated comparisons (left). Gene Ontology Biological Process bar plots showing pathways enriched in significantly up (red) or down (blue) differentially expressed genes (right). **b,d,** (ATAC-seq) MA scatter plots of log2 fold-change in accessibility versus the average log2 accessibility for indicated comparisons (left). Gene Ontology Biological Process bar plots showing pathways enriched in significantly up (red) or down (blue) differentially accessible chromatin regions (right).

Figure 3

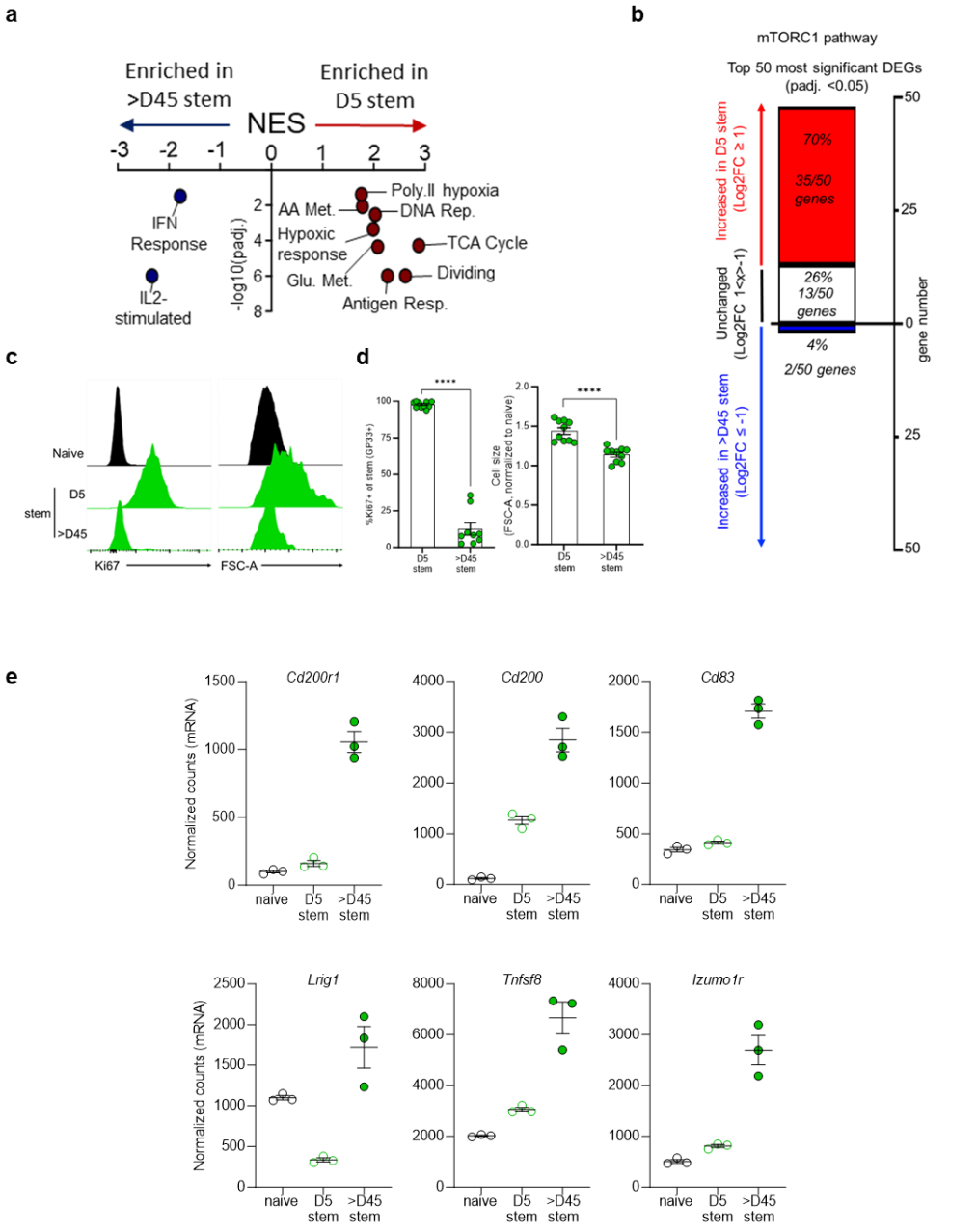

Fig. 3| Changes to stem-like CD8 T cells as chronic infection progresses from days 5 to >45. **a,** Enrichment for indicated gene sets by stem-like CD8+ T cells from day 5 versus >45 (RNA-seq). **b,** Bar graph showing relative expression of top 50 most significant differentially expressed genes (DEGs) from mTORC1 signaling pathway between day 5 and >45 stem-like CD8+ T cells. **c,d,** Flow cytometry analysis of splenic D^bGP33+ TCF-1+ Tim-3- stem-like CD8+ T cells from days 5 and >45. Histograms (c) and summary graphs (d) showing Ki67 expression and cell size based on forward scatter (FSC-A). **e,** Expression of various genes by indicated subsets based on normalized RNA counts. Flow plots/histograms in c,d are representative of 1 of 3 independent experiments (*n*=3-4 mice per time point per experiment). Graphs show mean ± SEM and are pooled data from 3 independent experiments (*n*= 9-10 mice per time point). P values calculated using Mann-Whitney test. **** indicates p value of less than 0.0001.

Figure 4

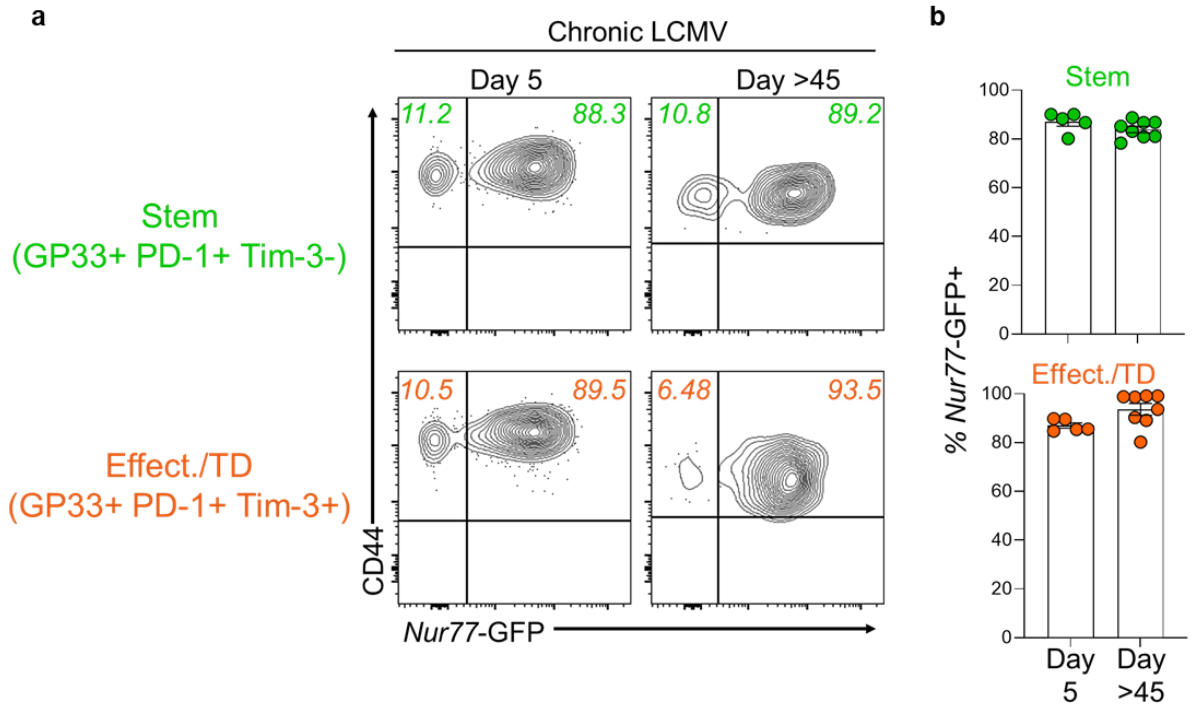

Fig. 4| Stem-like CD8+ T cells continuously receive TCR stimulation during chronic viral infection. *Nur77*-GFP reporter mice were infected intravenously with 2x106 PFU of LCMV clone 13 with transient CD4+ T cell depletion. **a,** CD44 and *Nur77*-GFP expression on GP33-specific stem-like (PD-1+ Tim-3-) and effector/terminally differentiated (PD-1+ Tim-3+) CD8+ T cells on days 5 and >45 post-infection. **b,** Summary graph showing percentage of GP33-specific stem-like versus effector/TD CD8+ T cells that are CD44+ *Nur77*-GFP+. Day 5 flow plots and summary graph are from 1 experiment (n= 5 mice). Day >45 flow plots are representative of 1 of 2 independent experiments. Summary graph for day >45 shows pooled data from 2 independent experiments (*n*= 8).

Figure 5

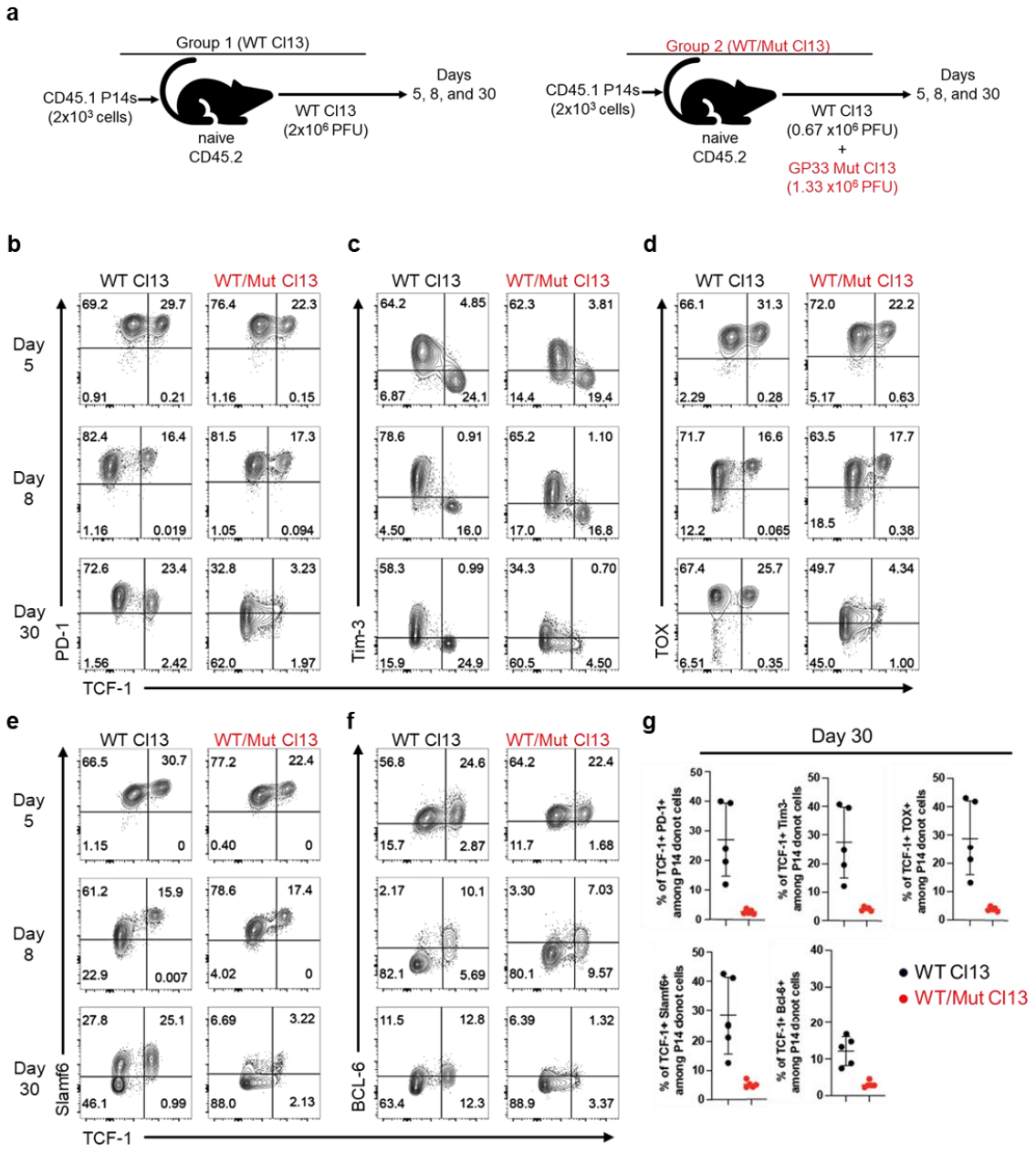

Fig. 5| Continuous TCR signaling is required for the maintenance of stem-like CD8+ T cells during chronic viral infection. a, 2x103 LCMV GP33-specific CD45.1+ P14 CD8+ T cells were transferred into naïve CD45.2+ mice. Recipient mice were then infected with either 2x106 PFU wildtype LCMV clone 13 (WT Cl13) or with a combined dose of 2x106 PFU consisting of 0.66 x106 PFU WT clone 13 plus 1.33 x106 PFU of a mutant GP33-deficient LCMV clone 13 strain (WT/Mut Cl13). **b-f,** Flow plots showing expression of indicated markers on splenic LCMV GP33-specific P14 CD8+ T cells from indicated infection groups at various times post-infection. **g,** Frequencies of indicated splenic TCF-1+ P14 CD8 T cell subsets on day 30 after WT Cl13 or WT/Mut Cl13 infections. Flow plots are representative of 1 of 2 independent experiments (WT Cl13 *n*=5-10, WT/Mut Cl13 *n*= 4-5). Graphs show data from one independent experiment (WT Cl13 *n*=5, WT/Mut Cl13 *n*= 5).

Extended Data Fig. 2

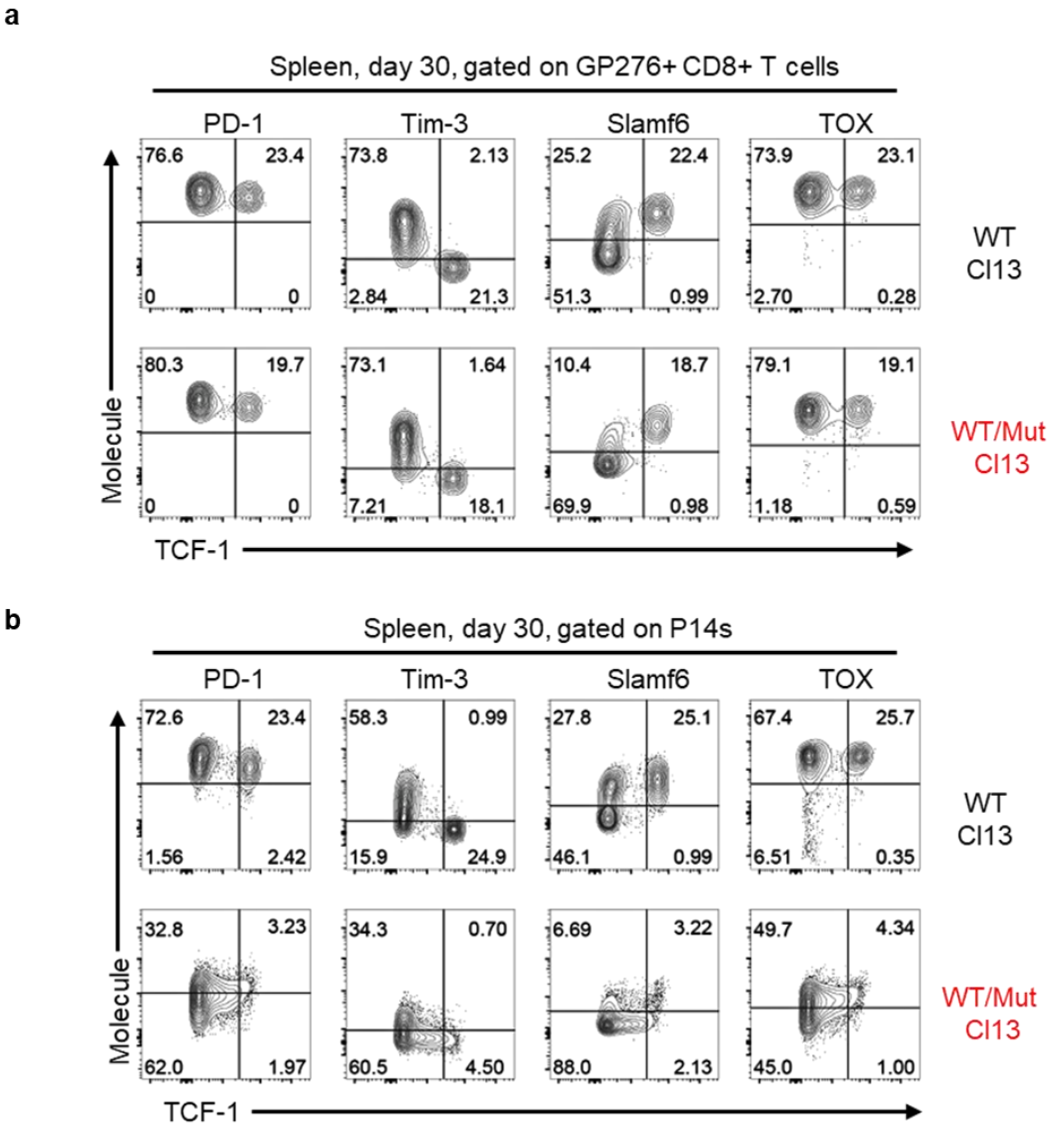

Extended Data Fig. 2| Mixed clone 13 experiment to assess importance of antigen for stem-like CD8+ T cells during chronic infection. As in Figure 8a, 2x103 LCMV GP33-specific CD45.1+ P14 CD8+ T cells were transferred into naïve CD45.2+ mice. Recipient mice were then infected with either 2x106 PFU wildtype LCMV clone 13 (WT Cl13) or with a combined dose of 2x106 PFU consisting of 0.66 x106 PFU WT clone 13 plus 1.33 x106 PFU of a mutant GP33-deficient LCMV clone 13 strain (WT/Mut Cl13). **a,** Frequency of PD-1+ TCF-1+ TOX+ Slamf6+ Tim-3- stem-like CD8+ T cells among LCMV GP276-specific CD8+ T cells in the spleens of mice from indicated infections groups on day 30 post-infection. **b,** Representative flow plots showing expression of indicated markers on splenic, LCMV GP33-specific P14 CD8+ T cells from indicated infections groups on day 30 post-infection. Flow plots are representative of 1 of 2 independent experiments (WT Cl13 *n*=5-10, WT/Mut Cl13 *n*= 4-5).

Chapter 4: The stem-like CD8 T cell fate decision is agnostic to infection outcome

This chapter is reproduced with edits from:
Early generation of a precursor CD8 T cell that can adapt to acute or chronic viral infection

Daniel T. McManus[1,2,11], Rajesh M. Valanparambil[1,2,11], Christopher B. Medina[1,2], Christopher D. Scharer[2], Donald J. McGuire[1,2], Yinghong Hu[1,2], Ewelina Sobierajska[4], Daniel Y. Chang[9], Andreas Wieland[5], Judong Lee[1,2], Tahseen H. Nasti[1,2], Masao Hashimoto[1,2], James L. Ross[1,2], Nataliya Prokhnevska[6], Maria A. Cardenas[4], Amanda L. Gill[1,2], Elisa C. Clark[8], Kathleen Abadie[8], Arjun Kumar[8], Hao Yuan Kueh[8], Jonathan Kaye[7], Byron B. Au-Yeung[10], Haydn T. Kissick[1,2,3,4], and Rafi Ahmed[1,2,3,*]

[1]Emory Vaccine Center, Emory University School of Medicine, Atlanta, GA, USA
[2]Department of Microbiology and Immunology, Emory University School of Medicine, Atlanta, GA, USA
[3]Winship Cancer Institute of Emory University, Atlanta, GA, USA
[4]Department of Urology, Emory University School of Medicine, Atlanta, GA, USA
[5]Department of Otolaryngology, The Ohio State University College of Medicine, Columbus, OH
[6]The Precision Immunology Institute, Icahn School of Medicine at Mount Sinai, New York, NY, USA
[7]Research Division of Immunology, Department of Biomedical Sciences, Cedars-Sinai Medical Center, Los Angeles, CA, USA
[8]Department of Bioengineering, University of Washington, Seattle, WA, USA
[9]Department of Pathology, Mass General Brigham, Harvard Medical School, Boston, MA, USA
[10]Division of Immunology, Lowance Center for Human Immunology, Department of Medicine, Emory University, Atlanta, GA,
[11]These authors contributed equally
*Corresponding author. Email: rahmed@emory.edu
**Under revisions for Nature*

Abstract

The stem-like CD8 T cell fate decision is made as early as day 5 following chronic LCMV, well before the outcome of infection is clearly acute or chronic. This suggests that the generation of stem-like CD8 T cells might not be unique to chronic viral infection. Rather, these cells might represent a general feature of early CD8 T cell differentiation during acute and chronic viral infection, occurring irrespective of infection outcome, perhaps to ensure the host is equipped for antigen persistence before it occurs. To test this hypothesis, we examined virus-specific CD8 T cells early after acute LCMV for the presence of a cell bearing properties of the stem-like CD8 T cells seen during chronic LCMV infection. GP33-specific PD-1+ TOX+ TCF-1+ CD8 T cells lacking effector molecules were present on day 5 after acute and chronic LCMV infection. Day 5 acute and chronic stem-like CD8 T cells were virtually identical in terms of their transcriptional and epigenetic profiles, as well their anatomical distribution (commitment to the splenic white pulp). They were also functionally similar; equally capable of producing cytokines like IFNγ and TNFα and of acting as stem-like CD8 T cells following clone 13 challenge (ie expansion, self-maintenance, and effector differentiation). Akin to chronic LCMV, the optimal generation of stem-like CD8 T cells during acute LCMV was dependent on the transcription factor, TOX. The stem-like CD8 T cell phenotype was lost following resolution of acute LCMV infection owing to loss of antigen, indicating a shared requirement for continuous antigen exposure by acute and chronic stem-like CD8 T cells. Thus, identical populations of stem-like CD8 T cells are generated early after acute and chronic LCMV infection, indicating that this important fate decision represents a typical feature of early CD8 T cell differentiation during LCMV infection.

Introduction

In chapters 2 and 3, we examined when the stem-like CD8 T cell fate commitment first occurs during chronic viral infection. Based on phenotypical, transcriptional, epigenetic, and anatomical profiling of LCMV-specific CD8 T cells, we found that the core stem-like CD8 T cell program is established as early as day 5 and is preserved throughout chronic LCMV infection. This aligns with previous work from our lab and others[60,70,82]. By comparing stem-like CD8 T cells on days 5 and >45, we learned that early during infection they are dividing and metabolically active cells. But as chronic LCMV infection progresses to day >45, they become quiescent in association with the upregulation of inhibitory molecules.

The absence of effector molecule expression by stem-like CD8 T cells is a unique and somewhat peculiar feature for an antigen-specific CD8 (cytotoxic) T cell subset amid an active viral infection. Surprisingly, we found that this property was not owed to insufficient TCR signaling, as comparable frequencies of LCMV-specific stem-like (>80%) and effector CD8 T cells (>85%) expressed *Nur77*-GFP on days 5 and >45 after chronic LCMV infection. This observation suggested that this key feature of stem-like CD8 T cells may be better described as an active repression of effector gene expression, rather than a passive inability to acquire these molecules. Indeed, the high expression of the transcriptional repressor, Bcl6, by stem-like CD8 T cells aligns with this notion. Moreover, in experiments making use of a mutant LCMV clone 13 strain, we found that continuous antigen exposure was required for sustaining key phenotypic properties of stem-like CD8 T cells during chronic LCMV, including Bcl6 expression. Paradoxically, the active resistance to effector differentiation by stem-like CD8 T cells appears to be an antigen-driven phenomenon.

The early generation of stem-like CD8 T cells is a surprising finding since at this early stage of infection the immune system does not know whether this is going to be a persistent infection or an acute infection. It suggests that the stem-like CD8+ T cell fate commitment is agnostic to antigen outcome, that the host prepares *a priori* for long-term antigen exposure. If so, a similar population of antigen-specific stem-like CD8 T cells should also be generated early after acute viral infection. To address this, we compared

LCMV-specific CD8 T cells during the early phases of acute and chronic LCMV using phenotypical, transcriptional, epigenetic, anatomical, and functional analyses.

Results

Phenotypically, transcriptionally, epigenetically, and anatomically identical populations of stem-like CD8 T cells are generated early after acute and chronic infection

To determine whether stem-like CD8 T cells are also generated during acute viral infection, we examined the phenotype of virus specific CD8+ T cells early after acute (LCMV Armstrong) versus chronic (LCMV clone 13) infection. For a fair comparison, acute and chronic LCMV infections were both performed intravenously at a dose of 2 x 10^6 plaque forming units (PFU) (Fig. 1a). Interestingly, GP33-specific CD8+ T cells expressing important phenotypic traits of stem-like CD8 T cells— PD-1, TOX, and TCF-1 — were present on day 5 after acute and chronic LCMV infection. PD-1+ TOX+ TCF-1+ cells from acute infection shared markers with day 5 stem-like cells from chronic infection including the expression of CD73, CD4+ Tfh markers (Bcl-6 and Slamf6), costimulatory molecules (CD27, CD28, and CD226), and the chemokine receptor, CXCR3 (Fig. 1b and Extended Data Fig. 1a). Like stem-like CD8 T cells from chronic infection, PD-1+ TOX+ TCF-1+ cells from acute LCMV also lacked effector markers like Tim-3, GzmB, CX3CR1, KLRG1, and CD25 (Fig. 1b and Extended Data Fig. 1a). Importantly, the presence of these cells was not an artifact of administering a high dose of acute LCMV i.v. as GP33-specific PD-1+ TOX+ TCF-1+ with the stem-like CD8 T cell phenotype (Slamf6+, CD73+, Tim-3-, GzmB-) could also be observed on day 5 post-infection when a lower dose of LCMV Armstrong (2 x 10^5 PFU) given intraperitoneally was used (Extended Data Fig. 1b). Of note, the frequency of GP33-specific PD-1+ TCF-1+ cells was lower in acute infection compared to chronic. Moreover, numbers of PD-1+ TCF-1+ cells declined as infection dose was lowered, suggesting that initial infection dose determines the magnitude of these cells (Extended Data Fig. 1c and d). Thus, antigen-specific CD8+ T cells with the same phenotype as stem-like CD8+ T cells from chronic infection are generated during acute infection.

For a more detailed analysis, we sorted day 5 stem-like (P14 PD-1+ CD73+ Tim-3-) and effector (P14 PD-1+ CD73- Tim-3+) CD8+ T cells from acute and chronic LCMV infection and compared gene expression (RNA-seq) and chromatin accessibility (ATAC-

seq) (Extended Data Fig. 1e). When projected onto principal component analysis (PCA) plots, stem-like CD8+ T cells from acute and chronic infection were positioned in almost the same location for both RNA- and ATAC-seq analyses (Fig. 1c and d). They were remarkably similar, differing in gene expression by less than 1% (DEGs= 93/9634) and displaying no differentially accessible chromatin regions (DARs = 0/65547) (Fig. 1e and f). Irrespective of infection origin, both stem-like and effector CD8 T cells showed expression and accessibility for *Pdcd1* and *Tox*. Consistent with the transcriptional and epigenetic signature originally described for stem-like CD8 T cells during chronic viral infection, costimulatory molecules (*Cd28*, *Tnfrsf4, Icos)* were more highly expressed and accessible in day 5 acute and chronic stem-like relative to effector CD8+ T cells. They also showed low expression/accessibility at effector loci (*Fasl, Ifng, Prf1, Gzma*, *Gzmb*) but higher expression/accessibility for CD4+ Tfh transcription factors (*Plagl1*, *Bcl-6*), long-lived memory cells (*Tcf7*, *Id3*), and chemokines expressed by stem-like CD8+ T cells (*Xcl1, Cxcl10*) (Fig. 1g-l, and Extended Data Fig. 1f).

We next asked if the early anatomical divergence of stem-like and effector CD8+ T cells observed during the early stages of chronic infection (Chapter 2) also occurs during acute infection. Intravascular labeling[85,86] was performed on mice 5 days after acute or chronic LCMV infection to determine the intrasplenic locations of GP33-specific stem-like and effector CD8+ T cells (Fig. 1j). Regardless of infection, greater than 60% of GP33-specific stem-like CD8 T cells were localized to the white pulp compared to less than 20% of effectors (Fig. 1k and l). Thus, the anatomical organization of virus-specific stem-like and effector CD8+ T cells occurs early during both acute and chronic infection.

Consistent with the similar expression of TCR-driven molecules (PD-1 and TOX) (Fig. 1b) and shared anatomical distribution in the spleen (Fig. 1j-l), day 5 GP33-specific stem-like CD8 T cells from acute and chronic LCMV displayed comparable levels of TCR signaling, based on *Nur77*-GFP expression (Extended Data Fig. 1g).

Stem-like CD8 T cells from acute and chronic infection are functionally equivalent

It was important to also do a functional comparison of the early (day 5) stem-like CD8+ T cells from acute and chronic infection. We first examined their ability to produce interferon gamma (IFNγ) and tumor necrosis factor-alpha (TNFα), two cytokines produced by CD8 T cells following antigen encounter to effect viral control[10,48]. Naïve, GP33-specific P14 cells (2.5K) were transferred into uninfected mice prior to infection with either acute or chronic LCMV. On day 5, splenocytes were isolated and stimulated *ex vivo* with GP33 peptide for 5 hours before intracellular cytokines were measured (Fig. 2a). Similar frequencies and numbers of LCMV-specific acute and chronic stem-like CD8 T cells produced IFNγ alone (~50%). Moreover, the frequency and number of 'polyfunctional' (ie IFNγ+ TNFα+) stem-like CD8 T cells was also similar in acute and chronic LCMV (~20%) (Fig. 2b-d). In both acute and chronic LCMV, the percentage and numbers of LCMV-specific effector cells producing IFNγ alone was higher (~65%) compared to stem-like cells (Fig. 2b-d). Although this difference was not as apparent for IFNγ production alone, a greater frequency (~35% vs. ~16%) and number of acute LCMV effectors could make IFNγ and TNFα in tandem compared to chronic LCMV effectors (Fig. 2b-d). Hence, chronic LCMV infection impairs the polyfunctionality of effector CD8 T cells. However, stem-like CD8 T cells from acute and chronic LCMV are equally capable of producing cytokines.

The term 'stem-like CD8 T cell' is a functional definition, describing the ability of these cells to self-renew and effector differentiate, thereby acting as a 'stem cell' for the CD8 T cell response during chronic antigen exposure[60]. We therefore next examined the ability of stem-like CD8+ T cells from acute versus chronic infection to expand, effector differentiate, and maintain themselves in response to LCMV clone 13 challenge. LCMV GP33-specific day 5 P14 stem-like (Slamf6+ Tim-3-) and effector (Slamf6- Tim-3+) CD8+ T cells were isolated from the spleens of acutely or chronically infected mice and then transferred in equal numbers into separate groups of congenically distinct naive mice. Recipients were then challenged with LCMV clone 13 and 7 days later the recovery and phenotype of donor cells were assessed (Fig. 3a and Extended Data Fig. 2a). Higher numbers of donor cells were recovered from the spleens and livers of mice that received stem-like compared to effector CD8+ T cells (Fig. 3b and c). Interestingly,

stem-like cells from acute and chronic LCMV gave rise to similar numbers of progeny in both the spleen and liver (Fig. 3b and c). These were primarily effector CD8+ T cells (PD-1+ TCF-1- TOX+ GzmB+) that were generated in similar numbers by the day 5 stem-like CD8+ T cells from either LCMV Armstrong or clone 13 infection (Fig. 3d and e). The remainder of the cells at day 7 post-challenge consisted of stem-like CD8+ T cells (PD-1+ TCF-1+ TOX+ GzmB-) that were also maintained in equal numbers (Fig. 3d and e). In mice that received the effector subset (Slamf6- Tim-3+), there was less expansion of the donor cells (Fig. 3b and c) and these cells did not show any change in their phenotype (Fig. 3f and g). This experiment shows that stem-like CD8+ T cells from acute and chronic LCMV are equally capable of expansion, maintenance, and effector differentiation in response to clone 13 challenge. Coupled with the analysis of cytokine production, these data indicate that functionally equivalent populations of stem-like CD8+ T cells are generated during the early phase of acute or chronic LCMV infection.

Optimal generation of acute stem-like CD8 T cells depends on TOX

TOX is essential for the generation of stem-like CD8 T cells during chronic antigen exposure[68–70]. Previous work showed no impact of TOX deletion on the generation or preservation of CD8 T cells arising *after* clearance of acute viral infection[68,69] but its importance for cells *during* acute viral infection is unknown. Based on their resemblance to chronic stem-like CD8 T cells, we hypothesized that TOX would also be required for the generation of acute stem-like CD8 T cells. We infected TOX knockout mice[108] with equivalent doses (2E6 PFU i.v.) of either acute or chronic LCMV infection before assessing the the magnitude of virus-specific stem-like CD8 T cells on day 5 (Fig. 4a). Irrespective of infection type, the absence of TOX resulted in reduced frequencies and numbers of stem-like CD8 T cells in the blood, spleen, and liver (Fig. 3b-g). Hence, TOX is required for the optimal generation of stem-like CD8 T cells during acute and chronic viral infection. These results extend the importance of TOX beyond T cell exhaustion, establishing it as a key transcription factor for stem-like CD8 T cell differentiation irrespective of infection outcome.

Continuous antigen exposure is required for maintenance of stem-like CD8 T cells during acute infection

Our results showing that the canonical stem-like CD8+ T cells are also generated during the early stages of acute LCMV infection while antigen is still present raises the obvious question of what happens to these cells as the acute infection is rapidly cleared. To address this, we monitored expression of phenotypic markers that define these LCMV-specific stem-like CD8+ T cells (PD-1+ TOX+ TCF-1+) at days 5, 8 and 14 post-infection with LCMV Armstrong. The data in Fig. 5a-d show that LCMV specific CD8+ T cells of this phenotype are lost as the infection is cleared.

Continuous antigen exposure, but not the infection environment, was required for the maintenance of key phenotypic traits of stem-like CD8 T cells during chronic viral infection (Chapter 3, Fig. 5 and Extended Data Fig. 4). This suggested that the loss of stem-like CD8+ T cells following clearance of acute infection might also be due to the absence of antigen. To test this, we injected acutely infected mice with 200ug of GP33 peptide on days 5, 7, and 10 following infection with the LCMV Armstrong strain (Fig. 5e). This resulted in an increase in the frequency of GP33-specific CD8+ T cells (Fig. 5f and Extended Data Fig. 3a) but more importantly this peptide immunization during acute infection prevented the loss of LCMV GP33-specific stem-like CD8+ T cells (Fig. 5g-i and Extended Data Fig. 3b). Stem-like CD8+ T cells expressing PD-1, TOX, and TCF-1 were maintained at day 14 in numbers equivalent to what was seen at day 5. In contrast, acutely infected mice not injected with peptide showed a significant drop in the number of GP33-specific stem-like CD8+ T cells (Fig. 5g-i). Providing antigen exposure during this interval by peptide also increased the expression of Slamf6 and Bcl-6 (Extended Data Fig.3b). These data highlight the importance of antigen for maintaining the stem-like CD8+ T cell program.

Discussion

The stem-like CD8 T cell fate commitment occurs within the first week of chronic LCMV, before the outcome of infection is clearly acute or chronic. This suggested that the generation of stem-like CD8 T cells might not be unique to chronic viral infections; that these important cells may also arise early during acute viral infection. To determine if stem-like CD8 T cells are generated in acute infection, we began by phenotyping GP33+ CD8 T cells early after acute versus chronic LCMV infection. For a fair comparison of antiviral CD8 T cells under these conditions, acute and chronic infections were administered via the same route (intravenous) at the same dose (2×10^6 PFU). On day 5 after acute LCMV, we found virus-specific CD8 T cells exhibiting key phenotypical traits of stem-like CD8 T cells from chronic LCMV infection (PD-1+ TOX+ TCF-1+ Tim-3-). Day 5 acute and chronic stem-like CD8 T cells shared additional marks including the expression of CD73, Tfh-related markers (BCL6 and SLAMF6), costimulatory molecules (CD28 and CD226) but not effector traits (GzmB, CX3CR1, KLRG1, and CD25) or the memory precursor marker, CD127. These cells could also be detected when a lower dose (2×10^5 PFU) of acute LCMV infection was used but at a lower frequency and number, indicating that the magnitude of stem-like CD8 T cells is related to initial antigen load.

The transcriptional and epigenetic profiles of day 5 acute and chronic stem-like CD8 T cells were virtually identical; they differed in gene expression by less than 1% and had zero differentially accessible chromatin regions. The anatomical distribution of acute and chronic stem-like CD8 T cells was also the same, biased for positioning in the splenic white pulp compared to their effector counterparts. We then compared the functional capacity of these cells. Acute and chronic stem-like CD8 T cells were equally capable of producing IFNγ and TNFα. Interestingly, this was not the case for acute and chronic effector CD8 T cells with the latter showing impaired polyfunctionality (IFNγ+ TNFα+) relative to the former. Acute and chronic stem-like CD8 T cells were also equally capable of functioning as ‘stem cells’ for the CD8 T cell response. Following LCMV clone 13 challenge, they both underwent a large expansion generating similar numbers of effector cells while maintaining a similar number of stem-like cells.

Conversely, effector CD8 T cells from acute LCMV showed superior expansion capacity compared to their chronic LCMV counterparts.

One possibility for why infection type impacted the polyfunctionality and expansion capacity of effector but not stem-like CD8 T cells is related to anatomical location. Effector CD8 T cells are primarily located in the splenic red pulp, in which they would be exposed to a much larger number of virus-infected cells during chronic LCMV infection compared to acute. This difference in antigen exposure between acute and chronic LCMV is not as dramatic in the splenic white pulp on day 5, however, which is where stem-like CD8 T cells are primarily located. In addition to antigen load, the increased diversity and sheer number of infected cells in chronic LCMV likely creates a distinct red pulp environment compared to acute LCMV, differing with respect to the levels of cytokines present like type I interferon, IFNγ, and TGFβ. A final explanation is related to cell-intrinsic differences between stem-like and effector CD8 T cells. Stem-like CD8 T cells withstand weeks of continuous TCR signaling during chronic LCMV infection without being lost to terminal differentiation. This is not the case for effector CD8 T cells, which during the late phase of chronic LCMV are primarily made up of senescent, terminally differentiated cells. Hence, the inherent ability of stem-like CD8 T cells to resist effector differentiation despite continuous TCR signaling likely makes them less prone to differences in antigen load compared to effector CD8 T cells.

Previous reports showed that the transcription factor TOX orchestrates CD8 T cell exhaustion during chronic LCMV infection but has no impact on the CD8 T cell response during acute LCMV infection. More specifically these papers showed that without TOX, stem-like CD8 T cells are not generated during chronic LCMV infection leading to the eventual collapse of the virus-specific CD8 T cell response. They also reported that TOX deletion has no impact on CD8 T cells responding to acute viral infection. By contrast, we show that TOX is required for stem-like CD8 T cell differentiation during both acute and chronic viral infection. This likely went unnoticed by other groups because stem-like CD8 T cells comprise just ~5-10% at the conventional conditions used for acute LCMV infection. Indeed, this may also explain why prior work on CD8 T cell differentiation failed to uncover stem-like CD8 T cells during acute viral

infection. Moreover, the aforesaid reports assessed the impact of TOX deletion beginning on day 8, when the putative stem-like CD8 T cell phenotype is no longer detectable. For a fair comparison to chronic infection, we assessed TOX deletion at a higher dose of acute LCMV where stem-like CD8 T cells make up ~15-20%. Our finding complements the aforesaid reports and further emphasizes the importance of TOX specifically for the generation of stem-like CD8 T cells, whether this occurs in an acute or chronic viral infection.

With clearance of acute viral infection, the putative stem-like cell phenotype was lost. Providing cognate peptide during the resolution of acute viral infection maintained the expression of PD-1 and TOX. Moreover, it also prevented the slight downregulation of TCF-1 that coincides with clearance of acute viral infection. Hence, antigen, but not the acute infection environment, is essential for maintaining key features of stem-like CD8 T cells.

Altogether these data show that stem-like CD8 T cells—although essential during chronic antigen exposure —are not exclusive to this context. Rather, they are a general feature of CD8 T cell differentiation during antigen exposure, produced agnostically of antigen outcome.

Methods

Mice, viral infections, and virus titration

C57BL/6 and CD45.1 B6 mice were purchased from Jackson laboratory. CD45.1/45.1 or CD45.1/45.2 P14 TCR transgenic mice[109] were bred and maintained in house. 6-8 week old mice were used for infections. *Nur77*-GFP transgenic mice were provided as a gift from the Au-Yeung laboratory at Emory University. TOX knockout mice were provided as a gift from Jonathan Kaye at Cedars-Sinai Medical Center. Chronic viral infections were performed by injecting $2x10^6$ PFU LCMV clone 13 i.v. For acute viral infections, mice were injected i.v. with $2x10^6$ PFU of LCMV Armstrong. Quantification of infectious virus was performed via plaque assay on Vero E6 cells as previously described (Rafi/Oldstone, 1984 JEM paper). All mice were used in accordance with the Emory University Institutional Animal Care and Use Committee Guidelines.

Lymphocyte isolation

Lymphocyte isolation from the blood, spleen, liver, and lungs were performed as described previously (Wherry's JV paper). Spleens were dissociated by passing through a 70 uM cell strainer (Corning). Livers were first perfused with cold PBS prior homogenization via mechanical disruption. Lungs chopped prior to shaking at 37C in 1.3 mM EDTA in HBSS for 30 mins. They were then treated with 150 U mL^{-1} of collagenase (Thermo Fisher Scientific) in RPMI 1640 medium containing 5% FBS, 1mM $MgCl_2$ and 1mM $CaCl_2$ for 60 min at 37C with shaking at 200 rpm. Collogenase-treated lungs were then homogenized and filtered through a 70uM cell strainer. A 44-67% Percoll gradient was then used to purify lymphocytes (800g at 20C for 20min).

Reagents and flow cytometry

All antibodies used for flow cytometry were purchased from Biolegend, Thermo Fisher Scientific, Miltenyi Biotec, Cell Signaling Technology, BD Biosciences, and R&D Systems. The following antibody/fluorochrome conjugates were used at the following dilutions: anti-CD8a PerCp-Cy5.5 (1:200), anti-CD8a BUV395 (1:200), anti-CD8b PerCp-Cy5.5 (1:200), anti-PD-1 Pe-Cy7 (1:200), anti-PD-1 BV785 (1:200), anti-CD44 Alexa Fluor 700 (1:200), anti-CD44 BUV737 (1:200), anti-CD4 BUV805 (1:200), anti-CD19 BUV805 (1:200), anti-B220 BV786 (1:200), anti-TCF-1 FITC (1:50), anti-Tim-3 PE (1:25), anti-Tim-3 FITC (1:25), anti-Granzyme B PE-CF594 (1:100), anti-CD73 APC (1:100), anti-CD73 BV421 (1:100), anti-CD28 PE (1:50), anti-CD28 APC (1:50), anti-Ki67 BV711 (1:25), anti-CD45.1 BV711 (1:200), anti-CD45.1 BUV563 (1:200), CD45.2 FITC (1:200), CD45.2 Pe-Cy7 (1:200), anti-TOX PE (1:50), anti-TOX APC (1:50), anti-BCL6 PE (1:50), anti-BCL6 APC (1:50), anti-SLAMF6 APC (1:100), anti-SLAMF6 Pacific blue (1:100), SLAMF6 BUV496 (1:100), anti-CD226 PE-Texas Red (1:100), anti-CX3CR1 PE-Cy7 (1:100), anti-CX3CR1 APC-Fire 810 (1:100), anti-KLRG1 PE/Dazzle 594 (1:100), anti-KLRG1 BV605 (1:100), anti-KLRG1 BV421 (1:100), anti-CD127 PE (1:50), anti-CD127 BV421 (1:50), anti-CD127 BV711 (1:50), anti-CD25 PE (1:100), anti-CXCR3 PE-Cy7 (1:100), anti-CD27 BV785 (1:100), and anti-CD62L BV605 (1:100). Endogenous LCMV-specific CD8 T cells were detected using the D^{b}GP33-41 tetramer (1:100), which was prepared in house. Streptavidin-APC was purchased from (Thermo Fisher Scientific). Dead cells were excluded using the Live/Dead Fixable Near-IR (1:250) or Live/Dead Fixable Aqua (1:250) (Thermo Fisher Scientific). For cell surface staining, antibodies were prepared in PBS supplemented with 2% FBS at indicated

concentrations before being added to cells on ice for 30mins. Cells were then washed two times. For detecting intracellular proteins (TCF-1, GzmB, TOX, and Bcl6), the FOXP3 staining buffer set (Thermo Fisher Scientific) was used according to the manufacturer's instructions. Samples were acquired on a Canto, LSR II, the FAC Symphony A3 (BD Biosciences) system, or the Cytek Aurora spectral analyzer. Data were analyzed using FlowJo (v.10.7.1, BD Biosciences).

Intravascular antibody labeling

For intravascular labeling, 3μg of BV421-conjugated anti-CD8α (Biolegend) was injected i.v. into infected mice. Three minutes after injection, splenocytes were isolated and prepared into a single cell suspension before staining *ex vivo*.

In vivo peptide treatment

200ug of GP33 peptide was administered intravenously on days 5, 7, and 10 after acute LCMV infection (GenScript, RP20257).

Cell Sorting

A FACS Aria II (BD Biosciences) was used for cell sorting. For experiments involving bulk RNA or ATAC sequencing, PD-1+ CD73+ Tim-3-, PD-1+ CD73- Tim-3+, PD-1+ CD44+ CD73+ Tim-3- P14s, PD-1+ CD44+ CD73- Tim-3+ P14s CD8 T cells from chronically infected (days 5 and >45 p.i.) or acutely infected mice (day 5 p.i.) were sorted at a purity of greater than 96%. This was true also for bulk RNA or ATAC sequencing of CD44+ PD-1- CD127+ KLRG1- and CD44+ PD-1- CD127- KLRG1+ P14 CD8 T cells from mice in which acute viral infection had resolved (day 15 p.i.). For experiments involving single cell RNA sequencing, PD-1+ GP33+ CD8 T cells from

chronically infected (days 5 and >45 p.i.) or acutely infected mice (day 5 p.i.) were also sorted with greater than 96% purity. Naïve (CD44lo PD-1-) CD8 T cells were isolated from the spleens of uninfected mice.

Adoptive transfers of stem-like and effector CD8 T cells

TCR transgenic P14 chimeras were generated by transferring splenocytes from naïve P14 mice (containing $2.5x10^3$ P14s) into congenically mismatched hosts one day prior to infection. For adoptive transfers assessing the function of day 5 subsets in response to LCMV clone 13 challenge, Slamf6+ Tim-3- stem-like or Slamf6- Tim-3+ effector P14 cells were FACs sorted from infected spleens of indicated donor mice. $2.5x10^3$ cells of each subset were transferred i.v. into naïve mice before recipients were infected 12 hours later with $2x10^6$ PFU LCMV clone 13 i.v.

RNA seq

For experiments comparing CD8 T cell subsets on days 5 or >day 45 after acute or chronic LCMV infection, RNA was isolated from samples using the Qiagen RNA/DNA micro kit per the manufacturer's instructions. Extracted RNA was sent to Emory Yerkes Nonhuman Primate Genomics core for mRNA library preparation and sequencing using the clontech SMART-Seq V4 and HiSeq1000. Data were normalized and differentially expressed genes were determined using DeSeq. A gene was considered differentially expressed with a normalized count >100, $\log_2$ fold-change >1 or <1 and adjusted P value <0.05. Data was analyzed using custom R scripts and visualized using ggplot2 R package, GraphPad Prism (v9.2), and excel. For Gene Set Enrichment Analysis (GSEA) each subset was analyzed using the pre-ranked list mode with 1,000 permutations. All gene sets used were from the MSigDB Molecule Signature Database unless otherwise

noted. Enrichment scores were considered significant with an FDR <0.05 and was visualized using ggplot2 R package and GraphPad Prism (v9.2).

ATAC seq

For experiments comparing CD8 T cell subsets on days 5 or >day 45 after acute or chronic LCMV infection, 2-4x10^3 cells were sorted into PBS containing 2% FBS and transposition was performed as previously described (Guo, JI 2018 paper). Briefly, cells were resuspended in 12.5 µl 2x TD Buffer, 2.5 µl Tn5, 2.5 µl 1% Tween-20, 2.5 µl 0.2% Digitonin, and 5 µl H_2O and incubated at 37C for 1 hr. Following transposition, cells were lysed with 2 µl 10 mg/ml Proteinase-K, 23 µl Tagmentation Clean-up buffer (326 mM NaCl, 109 mM EDTA, 0.63% SDS), and incubated at 40°C for 30 min. DNA was extracted and size-selected for small fragments using AMPureXP beads (Beckman Coulter, A63881) and PCR amplified into a sequencing library using NexteraXT indexing primers (Illumina, FC-131-2004) and KAPA HiFi HotStart Ready Mix (Roche, KK2602). Post-PCR final libraries underwent a second size selection using AMPureXP beads. Final ATAC-seq libraries were quantitated by qPCR and size distributions determined by bioanalyzer. Each sample was pooled at equimolar ratios and sequenced at the Emory Non-human Primate Genomics Core on a NovaSeq6000 using a PE100 run. Raw fastq reads were processed by removing adapter contamination with Skewer [2] and mapped to the mm10 genome using Bowtie2 v2.4.2. Accessible chromatin regions identified using MACS2 2.2.7.1 and differential accessibility between groups was determined using DESeq2 with a FDR < 0.05 and absolute $\log_2$ fold-change > 1. Transcription factor motif enrichment was assessed using chromVAR. Custom data analysis and data display was performed in R v4.1.0.

Statistical analysis

GraphPad Prism (v.10.0.3) was used for statistical analysis. The difference between experimental groups was assessed using two-tailed unpaired t-tests or two-tailed unpaired Mann-Whitney *U*-tests or one-tailed paired Wilcoxon matched-pairs signed rank test.

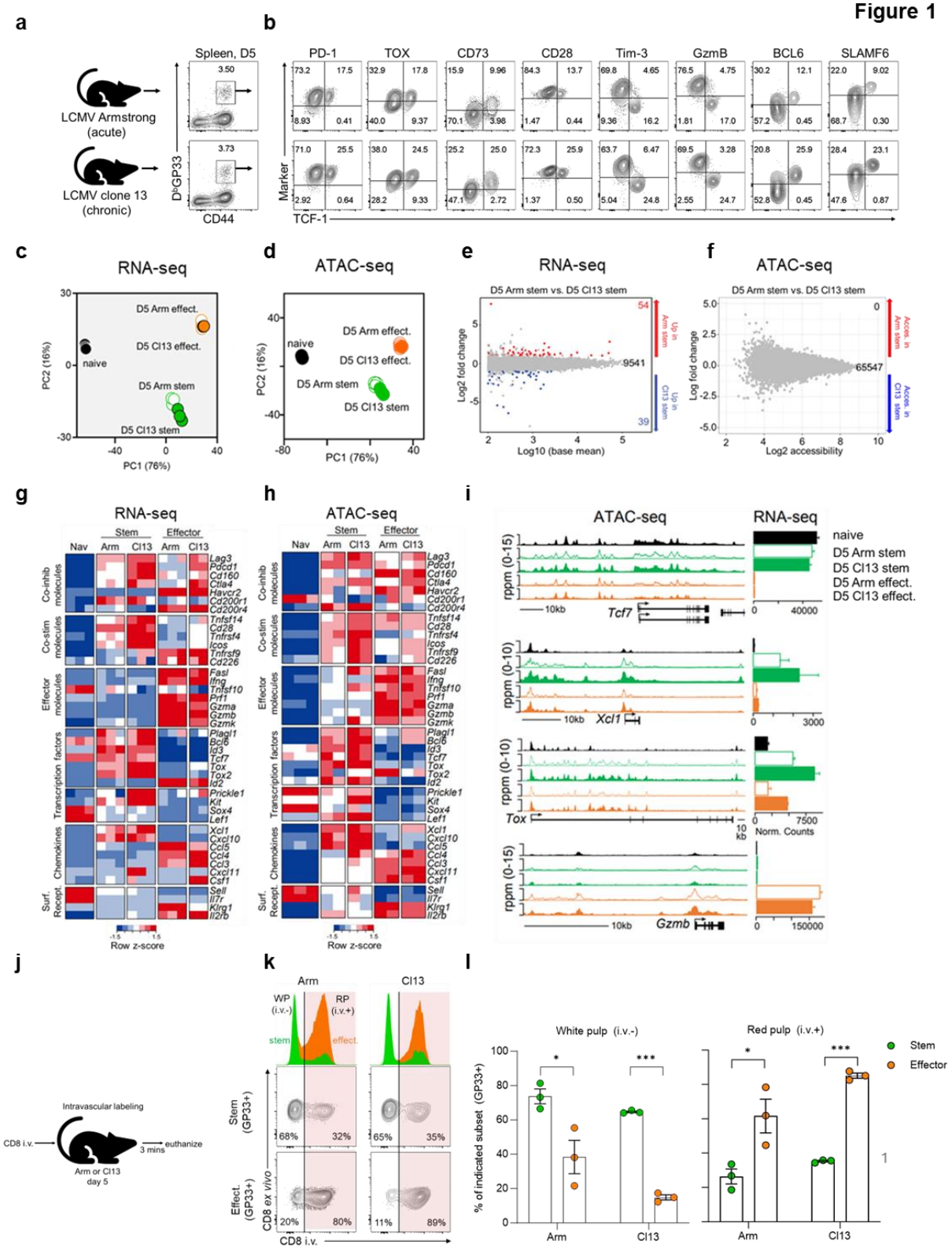
a
b
Spleen, D5
LCMV Armstrong (acute)
LCMV clone 13 (chronic)
DbGP33
CD44
PD-1
TOX
CD73
CD28
Tim-3
GzmB
BCL6
SLAMF6
Marker
TCF-1
c
RNA-seq
D5 Arm effect.
D5 Cl13 effect.
naive
D5 Arm stem
D5 Cl13 stem
PC1 (76%)
PC2 (16%)
d
ATAC-seq
e
RNA-seq
D5 Arm stem vs. D5 Cl13 stem
Log2 fold change
Log10 (base mean)
Up in Arm stem
Up in Cl13 stem
f
ATAC-seq
Log2 accessibility
Acces. in Arm stem
Acces. in Cl13 stem
g
RNA-seq
Stem
Effector
Nav
Arm
Cl13
Co-inhib molecules
Co-stim molecules
Effector molecules
Transcription factors
Chemokines
Surf. Recept.
Row z-score
h
ATAC-seq
i
ATAC-seq
RNA-seq
naive
D5 Arm stem
D5 Cl13 stem
D5 Arm effect.
D5 Cl13 effect.
rppm (0-15)
rppm (0-10)
Norm. Counts
Tcf7
Xcl1
Tox
Gzmb
j
Intravascular labeling
CD8 i.v.
3 mins
euthanize
Arm or Cl13 day 5
k
Arm
Cl13
WP (i.v.-)
RP (i.v.+)
stem
effect.
Stem (GP33+)
Effect. (GP33+)
CD8 ex vivo
CD8 i.v.
l
White pulp (i.v.-)
Red pulp (i.v.+)
% of indicated subset (GP33+)
Stem
Effector

Fig. 1| Identical populations of stem-like CD8+ T cells are generated early after acute and chronic infection. a,b, Phenotypic analysis of D^bGP33+ CD8+ T cells in the spleen on day 5 after LCMV Armstrong (acute) or clone 13 (chronic) infection. Flow plots are representative of 3 independent experiments (*n*= 4-5 recipients per donor per experiment). Both infections were administered intravenously (i.v.) at a dose of $2x10^6$ PFU. **c-i,** $2x10^5$ P14 cells were transferred into congenically distinct naïve mice prior to intravenous infection with LCMV Armstrong or clone 13. LCMV GP33-specific P14 stem-like and effector CD8+ T cells were isolated from the spleens of acute or chronic LCMV mice on day 5 for RNA- and ATAC-seq analysis. **c,d,** PCA plots showing RNA- (c) and ATAC-seq (d) profiles of indicated subsets. **e,f,** MA plots showing differentially expressed genes (e) and differentially accessible regions (f) between indicated subsets. Red dots/number = genes upregulated/more accessible in stem-like cells from acute infection. Blue dots/number = genes upregulated/more accessible in stem-like cells from chronic infection. Grey dots/black number = genes not differentially expressed/accessible. **g,h,** Heatmaps showing relative expression (g) and accessibility (h) of selected genes by indicated subsets. **i,** Accessibility tracks (ATAC-seq, left) and normalized counts (RNA-seq, right) for selected genes. RNA- and ATAC-seq results are each from 1 independent experiment. **j,** On day 5 after acute or chronic infection, mice were injected with fluorescently-labeled anti-CD8α (3µg/mouse) and euthanized 3 mins later for flow cytometry analysis. **k,** Flow plots/histograms showing frequencies of D^bGP33+ TCF-1+ Tim-3- (stem-like) and TCF-1- Tim-3+ (effect./TD) CD8+ T cells in the white pulp (CD8α i.v. antibody negative) or the red pulp (CD8α i.v. antibody positive). Numbers on flow plots are frequencies. **l,** Frequencies of stem-like and effect./TD CD8+ T cells in the white pulp (left) and red pulp (right). Flow plots/histograms are representative of 1 of 2 independent experiments (*n*= 3-5 mice per infection group). Graph shows mean±SEM, data are from 1 of 2 independent experiments (n= 3 per infection group) and p values shown from Wilcoxon matched-pairs signed rank test. * and *** indicate p values of less than 0.05 and 0.001, respectively.

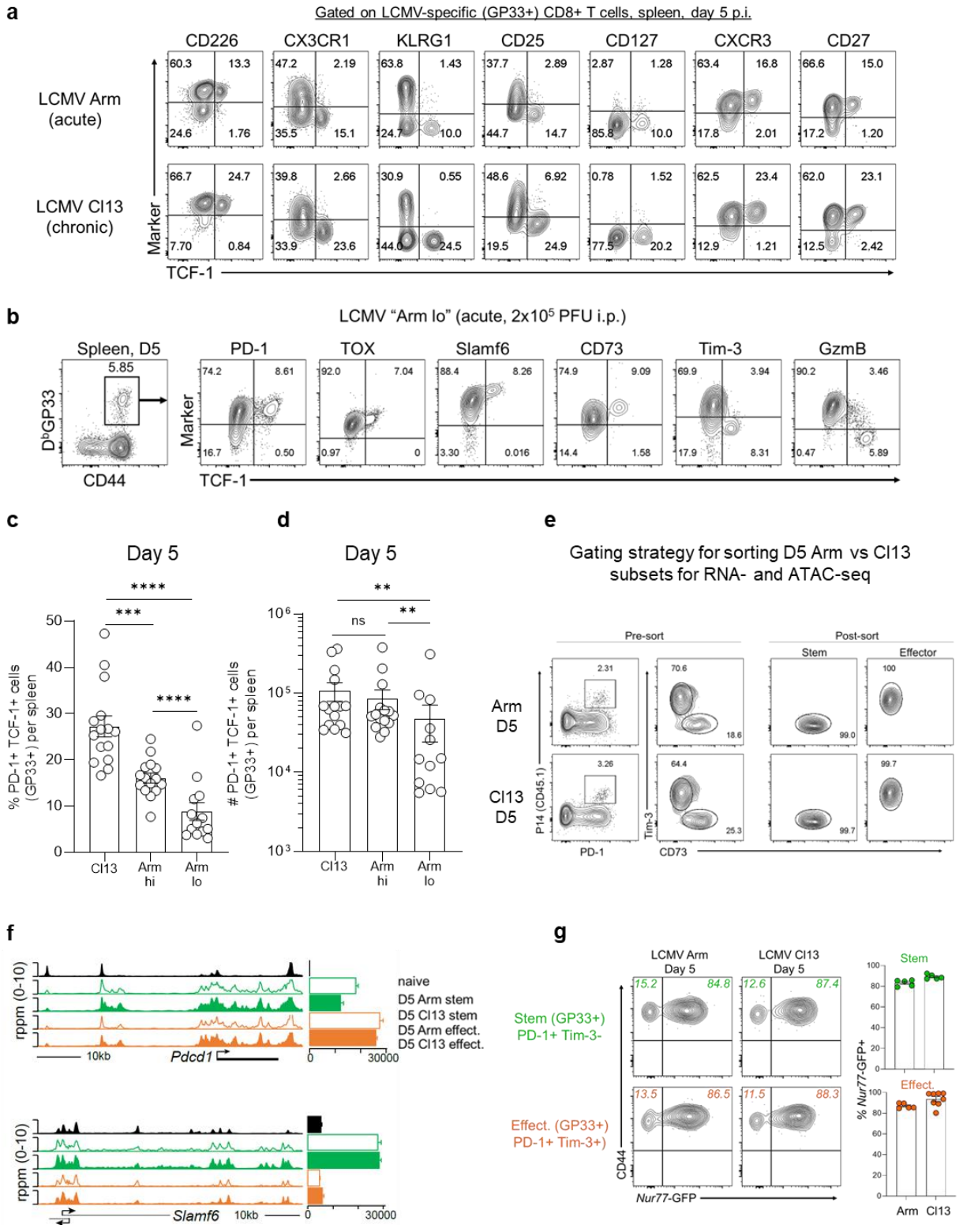
a
Gated on LCMV-specific (GP33+) CD8+ T cells, spleen, day 5 p.i.
CD226
CX3CR1
KLRG1
CD25
CD127
CXCR3
CD27
LCMV Arm (acute)
LCMV Cl13 (chronic)
Marker
TCF-1
b
LCMV "Arm lo" (acute, 2x10^5 PFU i.p.)
Spleen, D5
DbGP33
CD44
PD-1
TOX
Slamf6
CD73
Tim-3
GzmB
c
Day 5
% PD-1+ TCF-1+ cells (GP33+) per spleen
Cl13
Arm hi
Arm lo
d
Day 5
PD-1+ TCF-1+ cells (GP33+) per spleen
ns
e
Gating strategy for sorting D5 Arm vs Cl13 subsets for RNA- and ATAC-seq
Pre-sort
Post-sort
Stem
Effector
Arm D5
Cl13 D5
P14 (CD45.1)
PD-1
Tim-3
CD73
f
rppm (0-10)
naive
D5 Arm stem
D5 Cl13 stem
D5 Arm effect.
D5 Cl13 effect.
10kb
Pdcd1
Slamf6
g
LCMV Arm Day 5
LCMV Cl13 Day 5
Stem (GP33+) PD-1+ Tim-3-
Effect. (GP33+) PD-1+ Tim-3+)
CD44
Nur77-GFP
% Nur77-GFP+
Arm
Cl13

Extended Data Fig. 1| Identical stem-like CD8+ T cells are generated early after acute and chronic infection. a, Phenotypic analysis of D^bGP33+ CD8+ T cells in the spleen on day 5 after LCMV Armstrong (acute, Arm) or LCMV clone 13 (chronic, Cl13) infection. Both infections were administered intravenously (i.v.) at a dose of $2x10^6$ PFU. Flow plots are representative of 3 independent experiments. **b,** Phenotypic analysis of D^bGP33+ CD8+ T cells in the spleen on day 5 after a lower dose of acute LCMV infection administered intraperitoneally (i.p.) at a dose of $2x10^5$ PFU. **c,d,** Frequency (c) and number (d) of LCMV GP33-specific PD-1+ TCF-1+ CD8+ T cells in the spleen on day 5 after acute versus chronic infection. Graphs show mean±SEM and are combined data from 3 independent experiments (*n*= 12-15 mice per infection group). **e,** Gating strategy used for sorting LCMV GP33-specific P14 stem-like (PD-1+ CD73+ Tim-3-) and effector (PD-1+ CD73- Tim-3+) CD8+ T cells from Arm or Cl13-infected spleens on day 5 for RNA- and ATAC-seq. **f,** Accessibility tracks (ATAC-seq, left) and normalized counts (RNA-seq, right) for selected genes. RNA- and ATAC-seq results are each from 1 independent experiment. **g,** *Nur77*-GFP reporter mice were infected intravenously with 2x106 PFU of LCMV Armstrong or clone 13. CD44 and *Nur77*-GFP expression on GP33-specific stem-like (PD-1+ Tim-3-) and effector (PD-1+ Tim-3+) CD8+ T cells on day 5 post-infection (left). Summary graph showing percentage of GP33-specific stem-like versus effector CD8+ T cells that are CD44+ *Nur77*-GFP+. Day 5 flow plots and summary graph are from 1 experiment (n= 5 mice). P values calculated using Mann-Whitney test. **, ***, and **** indicate p value of less than 0.01, 0.001, and 0.0001, respectively.

Figure 2

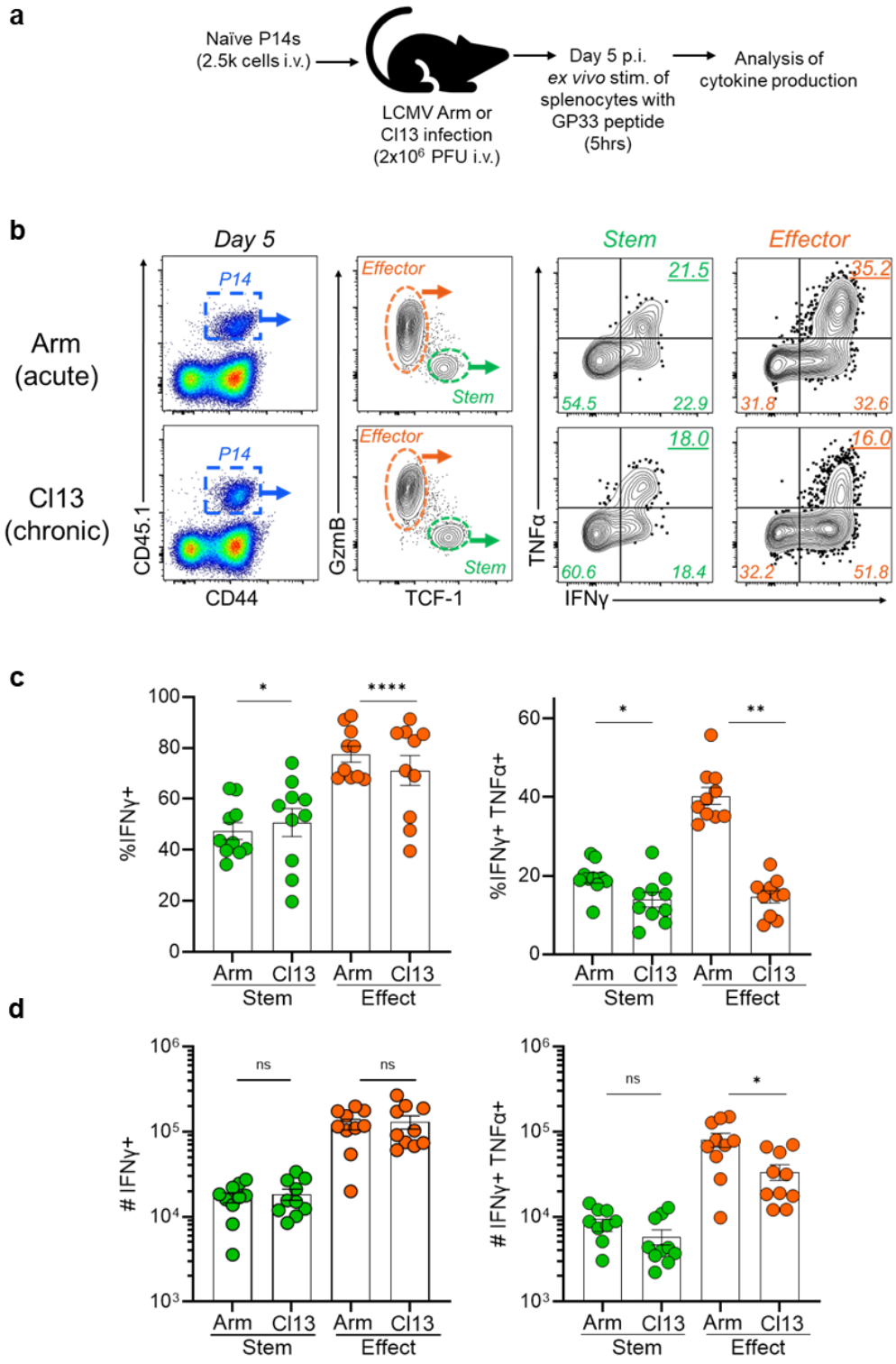
a
Naïve P14s
(2.5k cells i.v.)
LCMV Arm or
Cl13 infection
(2x10^6 PFU i.v.)
Day 5 p.i.
ex vivo stim. of
splenocytes with
GP33 peptide
(5hrs)
Analysis of
cytokine production
b
Day 5
Stem
Effector
Arm
(acute)
Cl13
(chronic)
P14
Effector
Stem
21.5
35.2
54.5
22.9
31.8
32.6
18.0
16.0
60.6
18.4
32.2
51.8
CD45.1
CD44
GzmB
TCF-1
TNFα
IFNγ
c
%IFNγ+
%IFNγ+ TNFα+
Arm
Cl13
Stem
Effect
d
IFNγ+
IFNγ+ TNFα+
ns

Fig. 2| Stem-like CD8 T cells from acute and chronic infection are equally capable of cytokine production. a, 2,500 naïve P14s were transferred intravenously (i.v.) into uninfected mice. Separate groups of P14 chimera mice were then infected with LCMV Armstrong (Arm, acute) or clone 13 (Cl13, chronic) i.v. at a dose of $2x10^6$ PFU. On day 5 post-infection, splenocytes were isolated and cultured *ex vivo* with 0.2 µg/mL of GP33 peptide in the presence of golgi plug and golgi stop for 5 hours at 37ºC. Following surface stain, cells were measured for intracellular cytokine production. **b,** Production of IFNγ and TNFα by P14 stem-like (TCF-1+ GzmB-) and effector (TCF-1- GzmB+) CD8 T cells. **c,d,** Summary graphs showing percentage (c) and number (d) of IFNγ+ (TNFα-) and IFNγ+ TNFα+ cells. Flow plots are representative of 1 of 2 independent experiments. Summary graphs show data pooled from 2 independent experiments (n=10 mice per group). P values calculated using Mann-Whitney test. *, **, and **** indicate p value of less than 0.05, 0.01, and 0.0001, respectively.

Figure 3

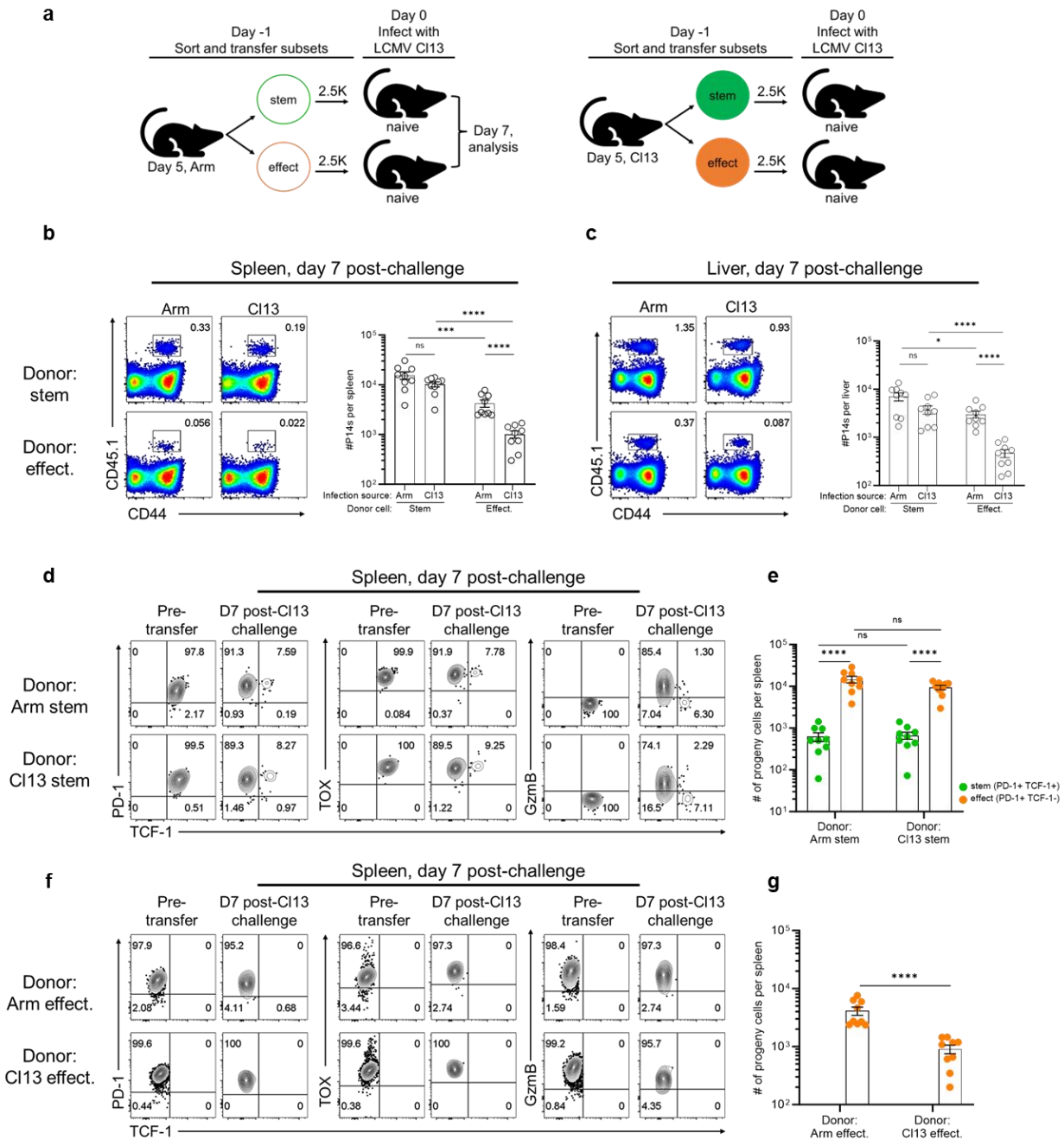
a
Day -1
Sort and transfer subsets
Day 0
Infect with
LCMV Cl13
stem
effect
2.5K
naive
Day 7,
analysis
Day 5, Arm
Day 5, Cl13
b
Spleen, day 7 post-challenge
Arm
Cl13
Donor:
stem
Donor:
effect.
CD45.1
CD44
#P14s per spleen
Infection source:
Donor cell:
Stem
Effect.
c
Liver, day 7 post-challenge
#P14s per liver
d
Spleen, day 7 post-challenge
Pre-
transfer
D7 post-Cl13
challenge
Donor:
Arm stem
Donor:
Cl13 stem
PD-1
TCF-1
TOX
GzmB
e
# of progeny cells per spleen
stem (PD-1+ TCF-1+)
effect (PD-1+ TCF-1-)
f
Donor:
Arm effect.
Donor:
Cl13 effect.
g

Fig. 3| Stem-like CD8+ T cells from acute and chronic infection are equally able to expand, self-renew, and effector differentiate after clone 13 challenge. a, CD45.1+ LCMV GP33-specific P14 stem and effect. CD8+ T cells were isolated from LCMV Arm or Cl13-infected spleens on day 5 and transferred into naïve CD45.2+ mice. Recipients were then challenged i.v. with $2x10^6$ PFU of LCMV Cl13. **b,c,** Frequency and numbers of donor cells recovered from indicated recipient spleens (b) and livers (c) on day 7 after clone 13 challenge. **d,** Expression of indicated markers on stem-like donor cells from acute (top) or chronic (bottom) infection pre- and on day 7 post-clone 13 challenge. **e,** Numbers of splenic stem-like (TCF-1+ GzmB-) and effector (TCF-1- GzmB+) CD8+ T cells derived from indicated donor cells. **f,** Expression of indicated markers on effector donor cells from acute (top) or chronic (bottom) infection pre- and on day 7 post-clone 13 challenge. **g,** Numbers of splenic stem-like (TCF-1+ GzmB-) and effector (TCF-1- GzmB+) CD8+ T cells derived from indicated donor cells. Flow plots represent 2 of 3 independent experiments (*n*= 4-5 recipient mice per group per experiment). Summary graphs show mean ± SEM and data are combined from 2/3 independent experiments (*n*=9 per group). P values calculated using Mann-Whitney test. *, ***, and **** indicate p values of less than 0.05, 0.001, and 0.0001, respectively.

a

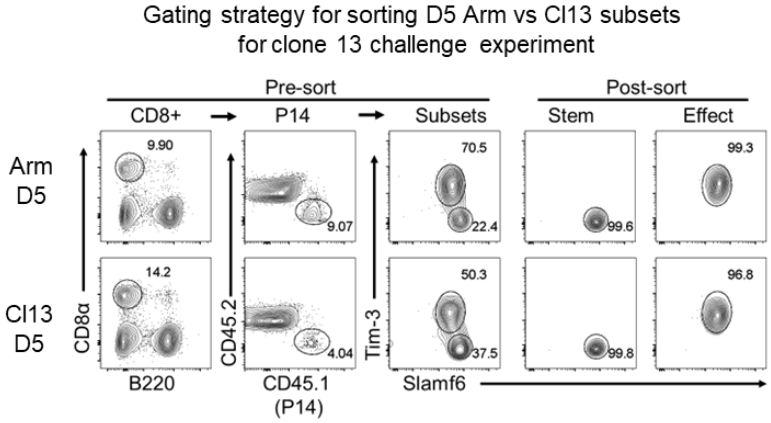

Extended Data Fig. 2| Sorting of stem-like and effector CD8+ T cells from acute versus chronic infection for clone 13 challenge experiment. a, Gating strategy used to isolate stem-like (Slamf6+ Tim-3-) and effector (Slamf6- Tim-3+) P14 CD8 T+ cells from acute versus chronic LCMV infection on day 5 to evaluate their response to clone 13 challenge.

Figure. 4

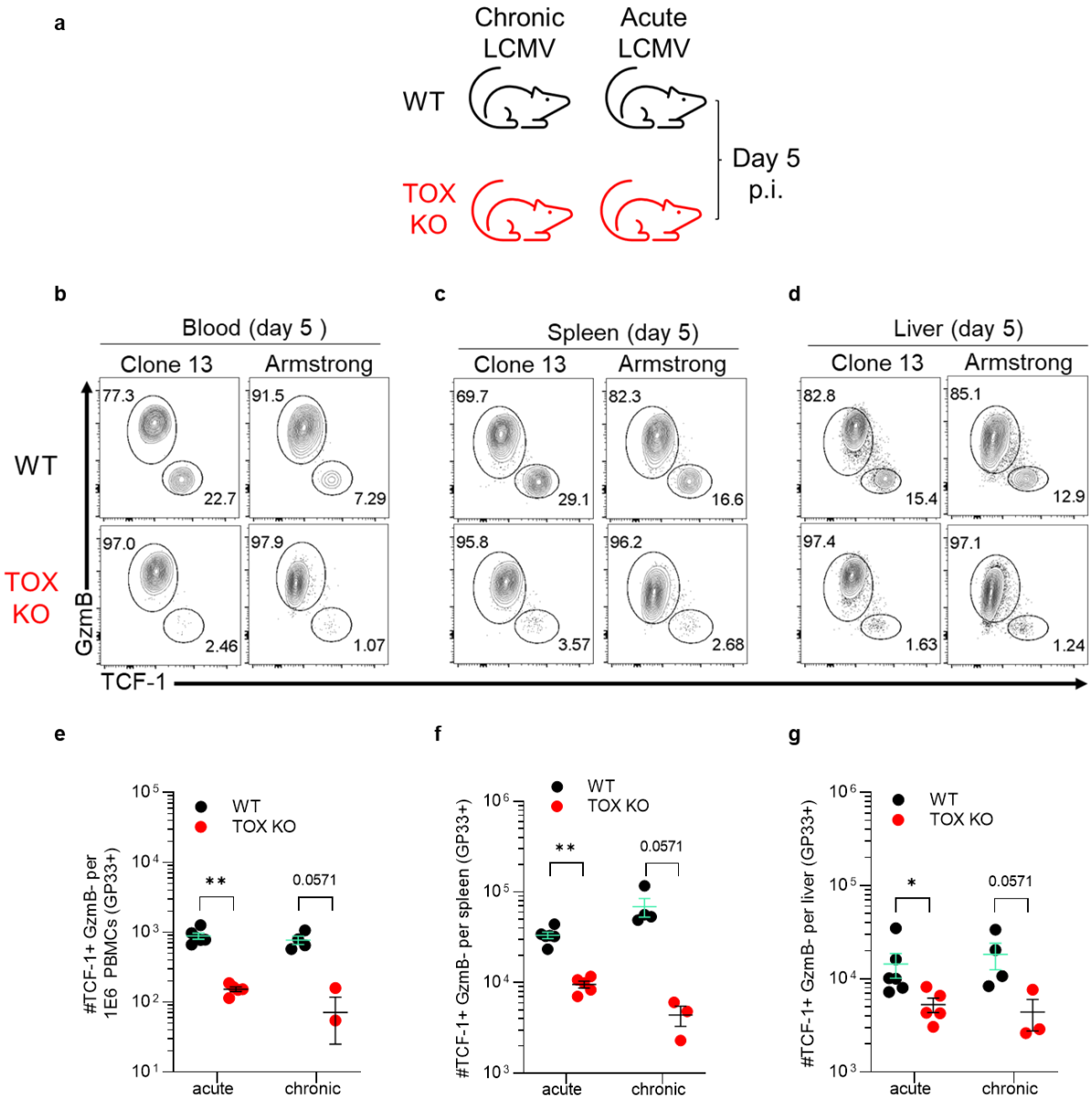

Fig. 4| TOX is required for the optimal generation of stem-like CD8 T cells during acute and chronic infection. a, Separate groups of wildtype (black) and TOX knockout mice (red) were infected with either LCMV Armstrong (Arm, acute) or clone 13 (Cl13, chronic) intravenously at a dose of $2x10^6$ PFU. On day 5 post-infection, phenotypic analysis was performed on LCMV-specific CD8 T cells from the blood, spleen, and liver. **b-d,** Representative flow plots showing TCF-1 and GzmB expression on LCMV-specific GP33+ CD8+ T cells in the blood (b), spleen (c), and liver (d). **e-g,** Summary graphs showing numbers of GP33+ stem-like (TCF-1+ GzmB-) CD8+ T cells in the blood (e), spleen (f), and liver (g). Flow plots shown are representative of 1 of 3 independent experiments (*n*= 1-5 mice per group). Summary graphs e-g show mean ± SEM and are combined data from 2 independent experiments (*n*= 3-6 mice per group). P values calculated using Mann-Whitney test. * and ** indicate p values of less than 0.05 and 0.01, respectively.

Figure. 5

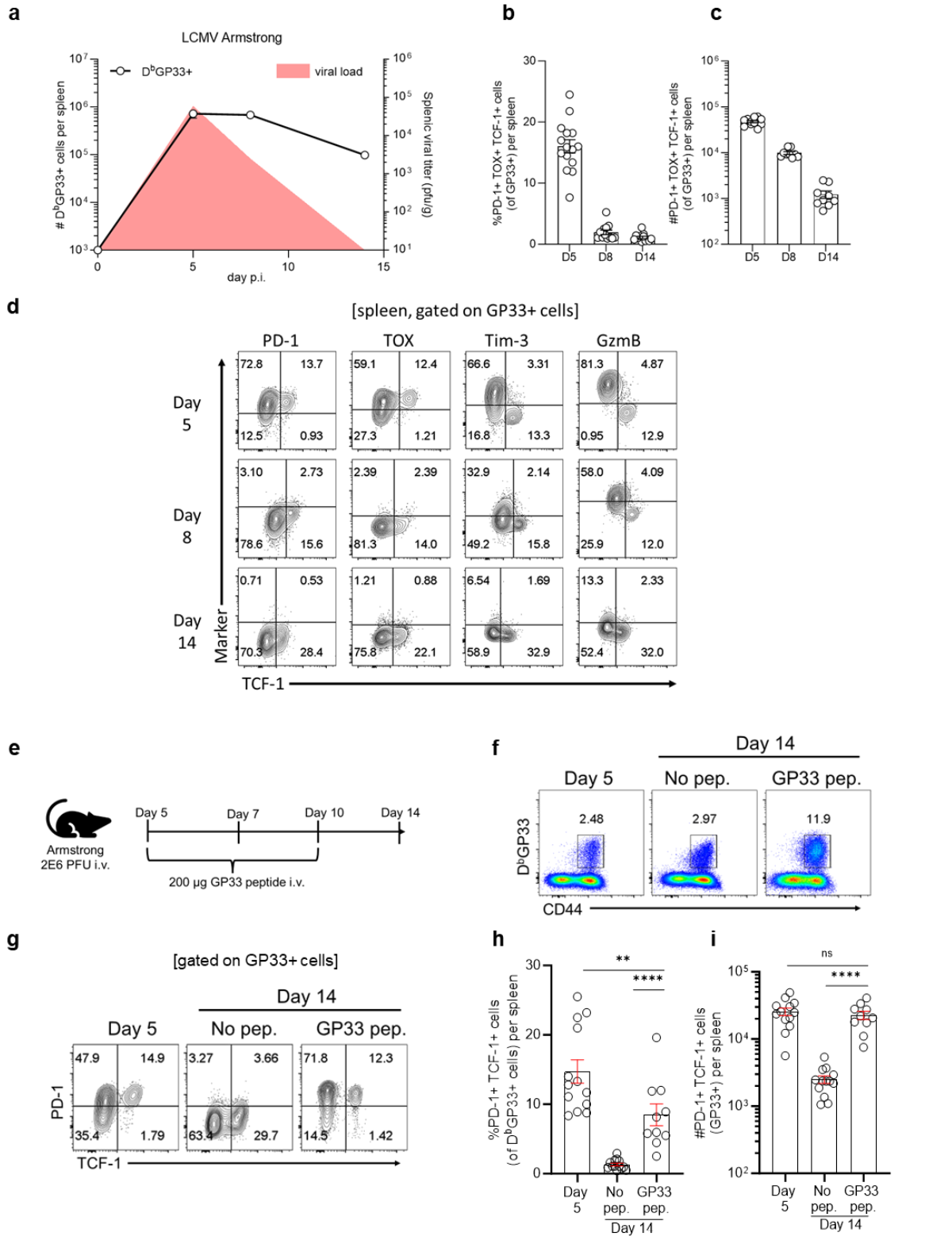
a
LCMV Armstrong
DbGP33+
viral load
DbGP33+ cells per spleen
Splenic viral titer (pfu/g)
day p.i.
b
%PD-1+ TOX+ TCF-1+ cells (of GP33+) per spleen
D5
D8
D14
c
#PD-1+ TOX+ TCF-1+ cells (of GP33+) per spleen
D5
D8
D14
d
[spleen, gated on GP33+ cells]
PD-1
TOX
Tim-3
GzmB
Day 5
Day 8
Day 14
Marker
TCF-1
72.8
13.7
12.5
0.93
59.1
12.4
27.3
1.21
66.6
3.31
16.8
13.3
81.3
4.87
0.95
12.9
3.10
2.73
78.6
15.6
2.39
2.39
81.3
14.0
32.9
2.14
49.2
15.8
58.0
4.09
25.9
12.0
0.71
0.53
70.3
28.4
1.21
0.88
75.8
22.1
6.54
1.69
58.9
32.9
13.3
2.33
52.4
32.0
e
Armstrong
2E6 PFU i.v.
Day 5
Day 7
Day 10
Day 14
200 µg GP33 peptide i.v.
f
Day 14
Day 5
No pep.
GP33 pep.
DbGP33
CD44
2.48
2.97
11.9
g
[gated on GP33+ cells]
Day 14
Day 5
No pep.
GP33 pep.
PD-1
TCF-1
47.9
14.9
35.4
1.79
3.27
3.66
63.4
29.7
71.8
12.3
14.5
1.42
h
%PD-1+ TCF-1+ cells (of DbGP33+ cells) per spleen
**
****
Day 5
No pep.
GP33 pep.
Day 14
i
#PD-1+ TCF-1+ cells (GP33+) per spleen
ns
****
Day 5
No pep.
GP33 pep.
Day 14

Fig. 5| Antigen is required for the maintenance of stem-like CD8+ T cells during acute viral infection. Mice were infected intravenously with $2x10^6$ PFU of LCMV Armstrong (acute). **a,** Viral titer kinetics (red curve) and numbers of LCMV-specific D^bGP33+ CD8+ T cells in the spleen over time. Viral titer data shown are from one independent experiment (n= 3-5 mice per time point) and are consistent with historical data (Matloubian et al.,1993). Curve showing numbers of D^bGP33+ CD8+ T cells is combined data from 3 independent experiments (*n*= 12-15 per time point) with mean and SEM included. **b,c,** Frequency (b) and numbers (c) of GP33+ PD-1+ TOX+ TCF-1+ stem-like CD8+ T cells in the spleen at indicated times post-acute infection. Graphs b and c show mean ± SEM and data are combined from 3 independent experiments (*n*= 12-15 mice per time point). **d,** Expression of indicated markers on GP33+ TCF-1+ CD8+ T cells during course of acute infection. Flow plots are representative of 1 of 3 independent experiments (*n*=3-5 mice per time point per experiment). **e,** On day 5 after acute infection, mice were treated i.v. with 200ug of GP33 peptide on days 5, 7, and 10. After clearance of infection (day 14), the phenotype of D^bGP33+ CD8+ T cells was examined **f,** Frequency of D^bGP33+ CD8+ T cells in the spleen. **g-i,** Frequency and number of D^bGP33+ PD-1+ TCF-1+ CD8+ T cells in the spleen. Flow plots shown are representative of 1 of 3 independent experiments (*n*= 3-5 mice per group). Graphs h and i show mean ± SEM and are combined data from 3 independent experiments (*n*= 10-13 mice per group). P values calculated using Mann-Whitney test. ** and **** indicate p values of less than 0.01, and 0.0001, respectively.

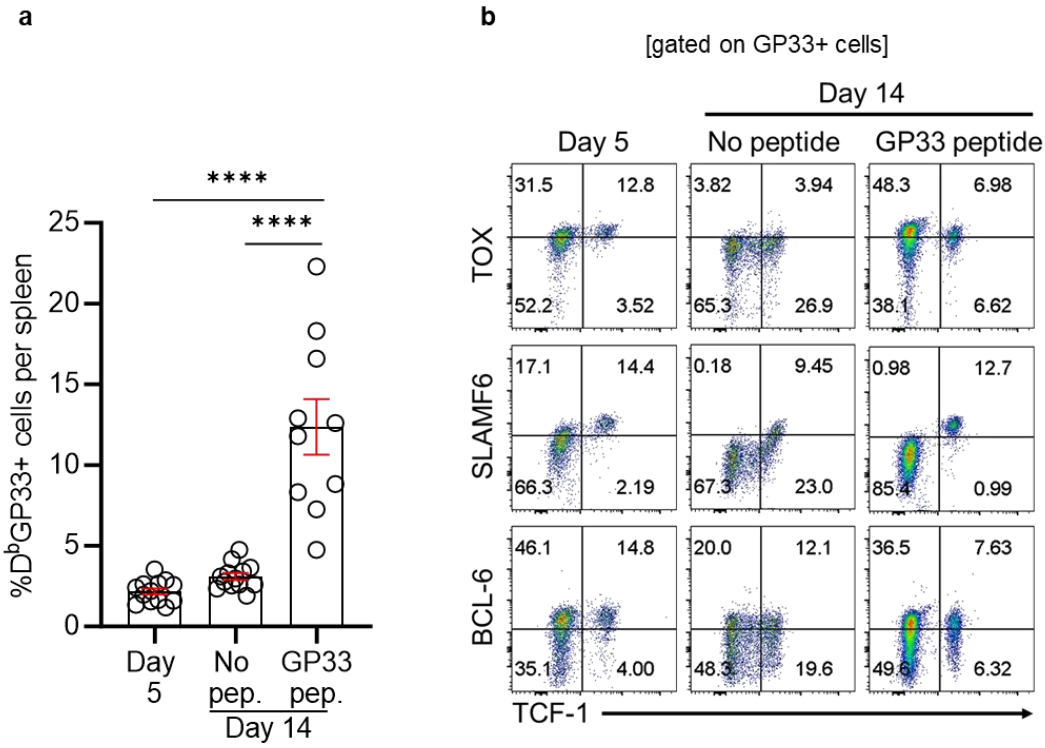

Extended Data Fig. 3| Peptide immunization to assess role of antigen for stem-like CD8 T cells during acute infection. a, Frequencies of splenic LCMV-specific D^bGP33+ CD8+ T cells. **b,** Expression of indicated markers on D^bGP33+ TCF-1+ CD8+ T cells. Graph shows combined data from 3 independent experiments (*n*= 12-15 per time point). Flow plots are representative of 1 of 3 independent experiments. (*n*= 3-5 mice per group). Statistics calculated using Mann-Whitney test. **** indicates a p value of less than 0.0001.

Chapter 5: Fate of stem-like CD8 T cells in acute and chronic viral infection

This chapter is reproduced with edits from:
Early generation of a precursor CD8 T cell that can adapt to acute or chronic viral infection

Daniel T. McManus[1,2,11], Rajesh M. Valanparambil[1,2,11], Christopher B. Medina[1,2], Christopher D. Scharer[2], Donald J. McGuire[1,2], Yinghong Hu[1,2], Ewelina Sobierajska[4], Daniel Y. Chang[9], Andreas Wieland[5], Judong Lee[1,2], Tahseen H. Nasti[1,2], Masao Hashimoto[1,2], James L. Ross[1,2], Nataliya Prokhnevska[6], Maria A. Cardenas[4], Amanda L. Gill[1,2], Elisa C. Clark[8], Kathleen Abadie[8], Arjun Kumar[8], Hao Yuan Kueh[8], Jonathan Kaye[7], Byron B. Au-Yeung[10], Haydn T. Kissick[1,2,3,4], and Rafi Ahmed[1,2,3,*]

[1]Emory Vaccine Center, Emory University School of Medicine, Atlanta, GA, USA
[2]Department of Microbiology and Immunology, Emory University School of Medicine, Atlanta, GA, USA
[3]Winship Cancer Institute of Emory University, Atlanta, GA, USA
[4]Department of Urology, Emory University School of Medicine, Atlanta, GA, USA
[5]Department of Otolaryngology, The Ohio State University College of Medicine, Columbus, OH
[6]The Precision Immunology Institute, Icahn School of Medicine at Mount Sinai, New York, NY, USA
[7]Research Division of Immunology, Department of Biomedical Sciences, Cedars-Sinai Medical Center, Los Angeles, CA, USA
[8]Department of Bioengineering, University of Washington, Seattle, WA, USA
[9]Department of Pathology, Mass General Brigham, Harvard Medical School, Boston, MA, USA
[10]Division of Immunology, Lowance Center for Human Immunology, Department of Medicine, Emory University, Atlanta, GA,
[11]These authors contributed equally
*Corresponding author. Email: rahmed@emory.edu
**Under revisions for Nature*

Abstract

In chapter 4, we found that identical populations of stem-like CD8 T cells are generated early (day 5) after acute and chronic viral infection, indicating that this important fate decision is made blind to infection outcome, and that the immune system is equipped *a priori* for a potential chronic infection. To determine the fate of these early stem-like CD8 T cells in acute versus chronic infection we performed reciprocal adoptive transfer experiments. When transferred from chronically infected to acutely infected mice and examined after viral clearance, early stem-like CD8 T cells downregulated canonical markers of stem-like CD8+ T cells from chronic infection (PD-1 and TOX) and adopted features of central memory CD8+ T cells, like CD127 and CD62L expression. When transferred from acutely to chronically infected mice, early stem-like CD8 T cells took on the role of chronic resource cells, supplying lymphoid and nonlymphoid tissues for over a month with virus-specific CD8 T cells. Using scRNA-seq analysis, we found that the daughter pool of these stem-like donor cells was composed of a similar spectrum of differentiation states/clusters (stem, effector, terminally differentiated, dividing) as seen for endogenous GP33-specific CD8 T cells within the same recipient mice. As chronic infection progressed from the early to the established phases, early stem-like donor cells transitioned from proliferation to quiescence and upregulated gene expression for the inhibitory molecule *Cd200*. PD-L1 blockade resulted in a massive expansion of early stem-like donor CD8 T cells within chronically infected recipients, equaling that seen for endogenous virus-specific CD8 T cells within the same mice. These findings provide insight into the generation and differentiation potential of stem-like CD8+ T cells, highlighting the ability of these cells to adapt to acute or chronic viral infection. Furthermore, they raise new questions on the potential importance of stem-like CD8 T cells for T cell memory and re-emphasize the essential role that these cells play during chronic viral infection.

Introduction

Virtually identical populations of stem-like CD8 T cells are generated early after acute and chronic viral infection and, in both contexts, antigen is required for the maintenance of cells with this phenotype (Chapters 3 and 4). These observations raise several intriguing questions regarding the differentiation potential of these early stem-like CD8 T cells and the importance of infection origin on the fate of these cells.

What happens to stem-like CD8 T cells following clearance of acute infection? One possibility is that elimination of antigen initiates the death of these cells. Indeed, stem-like CD8 T cells are essential for continued CD8 T cell immunity during long-term antigen exposure. Hence, making the survival of stem-like CD8 T cells antigen-dependent could serve to cull or discontinue the CD8 T cell response once the threat has been eliminated. A second possibility is that stem-like CD8 T cells give rise to memory CD8 T cells following antigen clearance. These cells share many phenotypic and functional qualities with memory CD8 T cells. Addressing this question will both expand our understanding of the differentiation potential of early stem-like CD8 T cells and potentially reveal new insights into the cellular origins of CD8 T cell memory.

Is the fate of stem-like CD8 T cells pre-determined by infection origin or can they adapt their differentiation trajectory based on the outcome of infection? That is, if generated in an infection destined for rapid clearance (ie LCMV Armstrong) what will happen to these cells if transferred into mice harboring a chronic viral infection?

To address these questions, we tracked the fate of early stem-like CD8 T cells in contexts of antigen clearance versus persistence using reciprocal adoptive transfer experiments. Specifically, we examine if stem-like CD8 T cells generated in a chronic viral infection can give rise to memory CD8 T cells if transferred into a clearing viral infection. We then transfer stem-like CD8 T cells from acute infection into mice inflicted with a life-long infection to assess the ability of these cells to not only sustain an antigen-specific CD8 T cell response but also reinvigorate it in response to PD-L1 blockade.

Results

Early day 5 virus-specific stem-like CD8+ T cells from LCMV clone 13-infected mice acquire the phenotype of central memory CD8+ T cells after transfer into acutely infected mice

To examine the fate of early stem-like CD8 T cells following viral clearance, we sorted stem-like and effector P14 cells from clone 13-infected mice at day 5 and transferred these sorted P14 CD8+ T cell subsets into congenically distinct mice acutely infected with LCMV Armstrong at day 5. The fate of these adoptively transferred cells was then analyzed on days 8 and 14 post-transfer, time points when the infection has been fully resolved. We used *Tcf7*-YFP reporter P14 cells in this experiment; stem-like cells were sorted as *Tcf7*-YFP+ Tim-3- and the effector cells as *Tcf7*-YFP- Tim-3+ (Fig. 1a and b). Both donor populations were detectable in the spleens of recipient mice after transfer, comparable numbers (Extended Data Fig. 1a and b). The transferred donor stem-like cells retained TCF-1 expression and remained negative for Tim-3 and granzyme B but there were other striking phenotypic changes in these cells; PD-1 and TOX were almost completely downregulated and most interestingly, there was upregulation of CD127 and CD62L. Also of interest is that the donor stem-like cells remained mostly negative for KLRG1 (Fig. 1c and d). Co-staining of the canonical memory T cells markers (CD127, KLRG1, CD62L) showed that the donor stem-like cells from clone 13-infected mice were acquiring markers associated with central memory T cells in the absence of antigen (Extended Data Fig. 1c-e)[52,110–112]. Thus, the virus-specific PD-1+ TCF-1+ CD8+ T cells generated during the early phase of chronic infection can also adapt to an acute infection and contribute to the pool of central memory CD8+ T cells following antigen clearance.

The donor effector cell population from clone 13-infected mice also exhibited several phenotypic changes after transfer into the acutely infected mice (Fig. 1e and f). These cells downregulated PD-1, TOX, granzyme B, and Tim-3 since antigen is needed to sustain expression of these molecules but most interestingly, a subset of donor effector

cells expressed *Tcf7*-YFP and CD127 in the absence of antigen. The co-staining of CD127, KLRG1, CD62L, and *Tcf7*-YFP (Extended Data Fig. 1c-e) shows that the PD-1+ Tim-3+ TOX+ GzmB+, and TCF-1 negative effector CD8+ T cell subset from day 5 clone 13 infection has the capacity to differentiate into the canonical short-lived effector cell (SLEC) subset (KLRG1+ CD127-)[113] and more importantly also give rise to the memory precursor effector cell (MPEC)[113] subset that expresses TCF-1 after clearance of antigen. This is consistent with our previous studies showing de-differentiation of a subset of effector CD8+ T cells after clearance of an acute viral infection[52,110,111,114,115]. A recent paper has further confirmed and extended these findings[116]. These previous studies examined effector CD8+ T cells generated during an acute infection and showed that the major pool of both effector and central memory cells emerges by the process of de-differentiation[117,118]. We now show in this study that some of the effector CD8+ T cells generated during the early phase of a chronic infection also have the capacity to de-differentiate and express TCF-1.

Early day 5 virus-specific stem-like CD8+ T cells from LCMV Armstrong-infected mice act as chronic resource cells after transfer into chronically infected mice

The studies described above showed that early day 5 stem-like CD8+ T cells generated during chronic infection can adapt to an acute infection setting and contribute to the pool of central memory cells (Fig. 1c, d, and Extended Data Fig. 1c-e). We now asked the reciprocal question of whether day 5 stem-like CD8+ T cells generated during an acute infection can act as resource cells in a chronic setting. The experimental design of this acute into chronic transfer is shown in Fig. 2a and b; sorted stem-like and effector P14 CD8+ T cells from LCMV Armstrong-infected mice at day 5 were transferred into mice infected with LCMV clone 13 at day 5. At day 15 post-clone 13 infection, the donor P14 cell populations were analyzed in the spleen, liver, and lung of recipient mice. We observed a significantly higher expansion of the transferred donor cells in all three tissues of mice that received day 5 P14 stem-like cells compared to P14 effectors (Fig. 2c and d). There were also striking changes in the phenotype of the donor stem-like

cells in the spleen 10 days after transfer into chronically infected mice due to the generation of effector CD8+ T cells from the transferred donor stem-like cells (Fig. 2e and f). These progeny effector cells derived from the donor day 5 stem-like cells expressed effector markers such as granzyme B, CX3CR1, Tim-3, and downregulated stem-like markers *Tcf7*-YFP and Slamf6. These progeny effector cells comprised ~90% of the total P14 cells and the remaining ~10% retained the phenotype of the stem-like cells. This is important because it shows that the stem-like cells maintain themselves and differentiate into effector cells. As expected, both the donor stem-like cells and their effector progeny expressed high levels of PD-1 and TOX. Similar results were seen in the liver and lung of mice that received the donor stem-like cells and in these non-lymphoid tissues the frequency of effector cells generated from the donor stem-like cells was even greater (>98%) (Extended Data Fig. 2a-d). Taken together these results show that day 5 P14 stem-like cells isolated from acute infection can function efficiently as a resource cell in the setting of a chronic infection.

In contrast to the efficient expansion and differentiation of the transferred P14 stem-like cells, the P14 effector cells showed significantly less expansion in all three tissues (spleen, liver, and lung) and showed minimal to no changes in their phenotypic markers (Fig. 2c, d, and Extended Data Fig. 3A-D). Even when five times fewer donor stem-like cells were transferred compared to donor effector cells, the stem-like cells gave rise to substantially higher numbers of progeny compared to effector donor cells (Extended Data Fig. 4a and b). Once again, these early (day 5) stem-like cells isolated from acutely infected mice differentiated into a large percentage of effector cells and also maintained their stem-like state to continue functioning as a resource cell under conditions of chronic infection (Extended Data Fig. 4c-f).

Early day 5 virus-specific stem-like CD8+ T cells from acute LCMV sustain CD8 T cell immunity in mice with a life-long viral infection as chronic resource cells

To determine whether day 5 stem-like CD8 T cells from acute LCMV can maintain the virus-specific CD8 T cell response in mice harboring a life-long viral infection, stem-like and effector P14 CD8+ T cells from day 5 LCMV Armstrong-infected mice were

transferred into separate groups of day 5 LCMV clone 13 mice that were transiently depleted of CD4 T cells prior to infection. Donor P14 cells were then analyzed in the spleen, liver, and lungs of recipient mice on days 8, 15, and 35 post-transfer (Fig. 3a, b). As observed before in the CD4 T cell helped chronic LCMV model (Fig. 2c, d), stem-like donor cells underwent a much greater initial expansion (day 8 post-transfer) in the spleens and lungs of recipient mice compared to effector donor cells. Although acute LCMV stem-like donor cells showed a larger expansion in the presence of CD4 T cells (Fig. 2c and d), these data show that the superior expansion capacity of stem-like vs. effector donor cells is not dependent on CD4 T help (Fig. 3c and d). Interestingly, stem-like and effector donor cells initially showed a comparable frequency and number of progeny cells in the liver. This may reflect the preferential trafficking of effector donor cells to the liver, compared to other tissue sites. As chronic LCMV progressed from the early to established phase of infection, effector donor cells were lost from all tissues examined in recipient mice. In contrast, stem-like donor cells were maintained in the spleen, liver, and lungs of recipients throughout chronic LCMV, albeit with a slight contraction by day 35 post-transfer (Fig. 3c and d). As before (Fig. 2e, and f), populations of stem-like (TCF-1+ Tim-3-) and effector (TCF-1- Tim-3+) CD8 T cells could be seen in the spleen, liver, and lungs of stem-like donor recipient mice on day 8 post-transfer. As chronic LCMV progressed to the established phase of infection, stem-like donor cells sustained the spleen, liver, and lungs with effector CD8 T cells but self-maintained a population of stem-like CD8 T cells only in the spleen (Fig. 3e). Interestingly, the presence of small populations of stem-like CD8 T cells in peripheral tissues early on but not late during chronic LCMV infection matches the same dynamics exhibited by the endogenous LCMV-specific CD8 T cell response. Moreover, between the pre-transfer time point (day 5, acute LCMV) and day 35 post-transfer (chronic LCMV), acute LCMV stem-like donor stem progeny (TCF-1+ Tim-3-) and endogenous GP33-specific stem-like CD8 T cells from stem-like donor recipients both gradually lost the expression of the proliferation marker, Ki67 (Fig. 3f). This provides definitive evidence for the notion observed in chapter 3, that stem-like CD8 T cells first emerge as rapidly dividing cells before transitioning to quiescence if the viral infection persists long-term. Together these longitudinal analyses show that early stem-like CD8 T cells from

acute LCMV can sustain CD8 T cell immunity via self-maintenance and effector differentiation following transfer into mice harboring a life-long viral infection.

We next compared the transcriptional signatures of P14 donor cells and endogenous LCMV-specific GP33+ cells from chronic LCMV mice that previously received (day 5 p.i.) stem-like donor CD8 T cells from day 5 acute LCMV mice. Our goal was to more comprehensively understand how the progeny of acute LCMV stem-like CD8 T cells donor cells compare to endogenous LCMV-specific CD8 T cells originating from chronic LCMV infection. On day 15 post-transfer, stem-like donor P14s (GP33+ CD45.2+) were sorted from the spleens of chronic LCMV recipients along with endogenous LCMV-specific (GP33+ CD45.2-) CD8 T cells and analyzed using scRNA-seq (Extended Data Fig. 5a). Interestingly, both acute LCMV stem-like donor and endogenous GP33+ CD8 T cells gave rise to 4 main cell clusters (stem, effector, terminally differentiated (TD), dividing) (Extended Data Fig. 5b and c), which were almost completely overlapping when projected together on a UMAP plot (Extended Data Fig. 5d). As expected for virus-specific cells isolated from an active viral infection, all clusters derived from stem-like donor and endogenous GP33+ CD8 T cells expressed *Pdcd1* and *Tox*. Stem For both stem-like donor and endogenous GP33+ cells, the stem cluster was distinguished from effector, TD, and dividing clusters based on the hallmark gene pattern combining high expression of *Tcf7*, *Id3*, *Xcl1*, *Cxcr5*, and *Slamf6* with the absence of effector marks like *Havcr2, GzmB,* and *Cd244a*. Interestingly, both stem clusters also showed high expression of the inhibitory molecule, *Cd200*, coupled with low expression of the proliferation marker, *Miki67* (Extended Data Fig. 5e-h). This aligns with data in chapter 3 (Fig. 3c-e) and chapter 5 (Fig. 3f) showing that as chronic LCMV infection progresses, stem-like CD8 T cells upregulate inhibitory molecules associated with TGFβ signaling and become quiescent. Effector and TD clusters from stem-like donor and endogenous GP33+ also shared similar gene profiles including high expression of *Havcr2* and *GzmB* but higher and more uniform expression of *Cd244a* in cells from the TD cluster compared to effector (Extended Data Fig. 5e-h). The dividing cluster for both stem-like donor and endogenous GP33+ cells was distinguished from all other clusters based on the high expression of *Mki67* (Extended Data Fig. 5e-h). Together these data show that

early stem-like CD8 T cells from acute LCMV infection can give rise to the full spectrum of transcriptional heterogeneity seen among endogenous virus-specific CD8 T cells during chronic LCMV infection.

Early day 5 virus-specific stem-like CD8+ T cells from acute LCMV provide the proliferative burst following PD-1 blockade

A key feature of stem-like CD8 T cells is that they supply the massive expansion of antigen-specific cells following PD-1 blockade during chronic viral infections and cancers[60]. We next tested the ability of stem-like CD8 T cells from acute LCMV to respond to PD-L1 blockade following transfer into chronic LCMV mice. As in Fig. 3a and b, stem-like CD8 T cells were first sorted from day 5 acute LCMV and transferred into time-matched, chronic LCMV recipients. On day 35 post-transfer, separate groups of stem-like donor recipient mice were either treated with anti-PD-L1 antibody (aPD-L1) or were left untreated (Fig. 4a). Both stem-like donor and endogenous GP33+ cells expanded substantially following PD-L1 blockade. Relative to untreated mice, stem-like donor and endogenous GP33+ cells gave rise to a similar increase in cell frequencies and numbers in the spleen, liver (~2-3 fold), and lungs (~6-10 fold) of aPD-L1 mice (Fig. 4b and c). Thus, infection origin does not impact the ability of stem-like CD8 T cells to respond to PD-L1 blockade during chronic viral infection.

Discussion

Here we address the fate and plasticity of the identical populations of virus-specific stem-like CD8 T cells that are generated early after acute and chronic viral infection using reciprocal adoptive transfer experiments.

In the first experiment we transferred day 5 stem-like CD8+ T cells from chronically infected into acutely infected mice and examined their differentiation after viral clearance. We found that early stem-like CD8+ T cells downregulated canonical markers of the chronic stem-like CD8+ T cells and expressed markers (CD127 and CD62L) associated with central memory CD8+ T cells. This experiment rules out the notion that continuous TCR signaling is necessary for the survival of stem-like CD8 T cells. Rather than being lost after viral clearance, stem-like CD8 T cells swap marks of antigen stimulation (ie PD-1 TOX) for the expression of molecules typical of memory CD8 T cells (ie CD127). Indeed, this experiment clarifies our observation in chapter 4 (Fig. 5 and Extended Data Fig. 3), regarding the antigen-dependent *loss* of the stem-like CD8 T cell phenotype following clearance of acute LCMV infection.

A large part of the memory pool arises via the de-differentiation of a portion of the initial effector pool referred to as memory precursor effector cells (MPECs). These cells were originally identified using the acute LCMV infection model, based on the expression of CD127 and absence of KLRG1. Follow up studies re-emphasized the point that they do indeed derive from an effector origin, showing that they arise from a GzmB+ population of KLRG1- CD25- cells. Our findings that stem-like CD8 T cells can become memory cells suggest that there also exists a non-effector route to the memory pool. This statement cannot be made definitively yet as it is unclear whether stem-like CD8 T cells arise directly from naïve cells or from the early de-differentiation of some effector subset. However, what can be said is that a portion of the memory pool is directly derived from a non-effector subset. This finding revisits decades old questions regarding the origins and development of memory CD8 T cells. For example, what is the quantitative and qualitative contribution of stem-like CD8 T cells to the memory pool? How do these answers change based on infection/antigen dose? To study memory CD8 T cells in the LCMV model, most experiments were performed by infecting mice

intraperitoneally at a dose of $2x10^5$ PFU. These studies provided invaluable insight into the lifestyles of memory CD8 T cells including their origins, development, and protective capacity/anatomical distribution/lineage relationships of different memory subsets. However, we show in chapter 4 (Extended Data Fig. 1b-d) that this infection setup leads to a population of stem-like CD8 T cells comprising a mere 5-10% of LCMV-specific (GP33+) CD8 T cells on day 5 post-infection. The remaining 90-95% consists of GzmB+ TCF-1- effector subsets like MPECs (GzmB+ KLRG1- TCF-1-) and short-lived effector cells (SLECs) (GzmB+ KLRG1+ TCF-1-). This suggests that most of what we know about memory, at least from the LCMV model, is based on studying memory CD8 T cells that come from effector cells, not stem-like CD8 T cells. This is exemplified by our findings in this chapter (Fig 1c and Extended Data Fig. 1c and d) where we surprisingly observed stem donor cells giving rise to between 30 and 75% CD62L+ cells so soon after viral clearance. In previous studies, the percentage of CD62L+ cells is <10% just 1-2 weeks after LCMV Armstrong infection. Whether there are differences in the anatomical distribution, protective capacity, or longevity of effector-vs stem-like cell-derived memory CD8 T cells is not yet clear. However, the function and molecular program of stem-like CD8 T cells during infection- which appears almost designed to support progenitor T cell biology- warrants further investigation into what these cells do after infection.

In the second and third experiments, we transferred day 5 stem-like cells from acutely infected mice into chronically infected mice and found that these early stem-like CD8+ T cells took on all the ‘chronic resource cell’ properties originally defined for stem-like CD8 T cells in the chronic LCMV infection model. Specifically, they underwent a much larger expansion compared to their effector donor cell counter parts populating lymphoid and non-lymphoid tissues with progeny. Despite originating in an acute LCMV infection destined for clearance, early stem-like donor cells gave rise to the entire differentiation (exhaustion) pathway defined for chronic antigen exposure: stem→ effector→ terminally differentiated. They also maintained the CD8 T cell response in the spleen, liver, and lungs of chronically infected animals for over a month after initial transfer. During this time, they acquired a key feature of chronic resource cells, quiescence. This observation provides conclusive evidence that stem-like CD8 T cells

arise early during infection as rapidly dividing cells and progressively stop dividing with time post-antigen exposure.
Importantly, the reduced proliferation of stem-like cells does not represent senescence or the inability to expand upon restimulation (exhaustion) observed for terminally differentiated. These cells retain proliferative potential, as evidenced by the enormous expansion they can undergo following PD-1 blockade. When their chronically infected hosts were treated with PD-L1 blocking antibodies, early stem-like donor cells exited quiescence and underwent a huge proliferative burst equaling that of endogenous GP33+ CD8 T cells within the same mice. This observation further solidifies the notion that early stem-like CD8 T cells become *bona fide* chronic resource cells in the context of antigen persistence.

Altogether, these data demonstrate the ability of early stem-like CD8 T cells to adapt to acute or chronic viral infection. Furthermore, it shows that the differentiation trajectory of early stem-like CD8 T cells is not pre-destined by infection origin. Rather, the development of early stem-like CD8 T cells is gradually shaped by the progression and outcome of infection. Ultimately, stem-like CD8 T cells equip the host with adaptability when challenged; conferring an inherently unforeseeing immune system with the ability to protect against re-challenge (memory, antigen clears) or control the challenge without excessive damage to the host (exhaustion, antigen persists).

Methods

Mice, viral infections, and virus titration

C57BL/6 and CD45.1 B6 mice were purchased from Jackson laboratory. CD45.1/45.1 or CD45.1/45.2 P14 TCR transgenic mice[109] were bred and maintained in house. 6-8 week old mice were used for infections. *Tcf7*-YFP P14 transgenic mice were provided as a gift from the Kueh laboratory at the University of Washington. Chronic viral infections that result in lifelong viremia were performed as follows: mice were transiently depleted of CD4+ T cells via intraperitoneal injection with 300 µg of a rat anti-mouse CD4 antibody (clone GK 1.5 from BioXcell) 2 days before infection and again on the day of infection. Mice were then injected intravenously (i.v.) with $2x10^6$ PFU LCMV clone 13 (Figs. 1, 5, and Extended Data Figs. 1-4, 5). All other figures feature chronic viral infections that eventually clear from most tissues. These were performed by injecting $2x10^6$ PFU LCMV clone 13 i.v. without transient CD4+ T cell depletion. For acute viral infections, mice were injected i.v. with $2x10^6$ PFU of LCMV Armstrong. All mice were used in accordance with the Emory University Institutional Animal Care and Use Committee Guidelines.

Lymphocyte isolation

Lymphocyte isolation from the blood, spleen, liver, and lungs were performed as described previously (Wherry's JV paper). Spleens were dissociated by passing through a 70 uM cell strainer (Corning). Livers were first perfused with cold PBS prior homogenization via mechanical disruption. Lungs chopped prior to shaking at 37C in 1.3 mM EDTA in HBSS for 30 mins. They were then treated with 150 U mL^{-1} of collagenase (Thermo Fisher Scientific) in RPMI 1640 medium containing 5% FBS, 1mM $MgCl_2$ and 1mM $CaCl_2$ for 60 min at 37C with shaking at 200 rpm. Collogenase-treated lungs were then homogenized and filtered through a 70uM cell strainer. A 44-67% Percoll gradient was then used to purify lymphocytes (800g at 20C for 20min).

Reagents and flow cytometry

All antibodies used for flow cytometry were purchased from Biolegend, Thermo Fisher Scientific, Miltenyi Biotec, Cell Signaling Technology, BD Biosciences, and R&D Systems. The following antibody/fluorochrome conjugates were used at the following

dilutions: anti-CD8a PerCp-Cy5.5 (1:200), anti-CD8a BUV395 (1:200), anti-CD8b PerCp-Cy5.5 (1:200), anti-PD-1 Pe-Cy7 (1:200), anti-PD-1 BV785 (1:200), anti-CD44 Alexa Fluor 700 (1:200), anti-CD44 BUV737 (1:200), anti-CD4 BUV805 (1:200), anti-CD19 BUV805 (1:200), anti-B220 BV786 (1:200), anti-TCF-1 FITC (1:50), anti-Tim-3 PE (1:25), anti-Tim-3 FITC (1:25), anti-Granzyme B PE-CF594 (1:100), anti-CD73 APC (1:100), anti-CD73 BV421 (1:100), anti-CD28 PE (1:50), anti-CD28 APC (1:50), anti-Ki67 BV711 (1:25), anti-CD45.1 BV711 (1:200), anti-CD45.1 BUV563 (1:200), CD45.2 FITC (1:200), CD45.2 Pe-Cy7 (1:200), anti-TOX PE (1:50), anti-TOX APC (1:50), anti-BCL6 PE (1:50), anti-BCL6 APC (1:50), anti-SLAMF6 APC (1:100), anti-SLAMF6 Pacific blue (1:100), SLAMF6 BUV496 (1:100), anti-CD226 PE-Texas Red (1:100), anti-CX3CR1 PE-Cy7 (1:100), anti-CX3CR1 APC-Fire 810 (1:100), anti-KLRG1 PE/Dazzle 594 (1:100), anti-KLRG1 BV605 (1:100), anti-KLRG1 BV421 (1:100), anti-CD127 PE (1:50), anti-CD127 BV421 (1:50), anti-CD127 BV711 (1:50), anti-CD25 PE (1:100), anti-CXCR3 PE-Cy7 (1:100), anti-CD27 BV785 (1:100), and anti-CD62L BV605 (1:100). Endogenous LCMV-specific CD8 T cells were detected using the D^bGP33-41 tetramer (1:100), which was prepared in house. Streptavidin-APC was purchased from (Thermo Fisher Scientific). Dead cells were excluded using the Live/Dead Fixable Near-IR (1:250) or Live/Dead Fixable Aqua (1:250) (Thermo Fisher Scientific). For cell surface staining, antibodies were prepared in PBS supplemented with 2% FBS at indicated concentrations before being added to cells on ice for 30mins. Cells were then washed two times. For detecting intracellular proteins (TCF-1, GzmB, TOX, and Bcl6), the FOXP3 staining buffer set (Thermo Fisher Scientific) was used according to the manufacturer's instructions. Samples were acquired on a Canto, LSR II, the FAC Symphony A3 (BD Biosciences) system, or the Cytek Aurora spectral analyzer. Data were analyzed using FlowJo (v.10.7.1, BD Biosciences).

Cell Sorting and adoptive transfers

For adoptive transfers of sorted CD8 T cell subsets into infected, time-matched recipients, 2000-4000 *Tcf7*-YFP P14s (gifted by Hao Yuan Kueh) were first transferred into naïve congenically mismatched recipients prior to infection with $2x10^6$ PFU i.v. of LCMV Armstrong or clone 13. On day 5, stem-like (CD8+ CD45.2+ *TCF7*-YFP+ Tim-3-)

or effector cells (CD8+ CD45.2+ *TCF7*-YFP- Tim-3+) were FACs sorted from the spleens of infected mice and $1x10^6$ (or when indicated, $2.5x10^5$) cells of each were transferred into time-matched (infection indicated) recipients.

PD-L1 therapy *in vivo*

To assess the ability of early stem-like CD8 T cells from acute LCMV to respond to PD-L1 blockade, chronically infected recipient mice (day 35 post-transfer) were either left untreated or treated intraperitoneally with 200 ug, of rat anti-mouse PD-L1 antibody (clone 10F.9G2, prepared in house) every 3 days for 12 days total (4 total injections).

scRNA-seq

scRNA-seq libraries were generated using the Chromium Single cell 5' Library & Gel Bead Kit (10x Genomics) according to the manufacturer. Early (day 5) stem-like CD8 T cell donor P14s were transferred from acutely infected to chronically infected mice. On day 15 post-transfer, stem-like donor P14s (CD45.2+ GP33+), endogenous D^bGP33+ CD8 T cells (CD45.2- GP33+), and naïve CD44lo CD8 T cells were sorted and captured into gel beads-in-emulsion. After being reverse transcribed, gel beads-in-emulsion were disrupted and barcoded cDNA was isolated, pooled, then amplified by PCR for 13 cycles. Amplified cDNA was then fragmented and processed for end repair and A-tailing before undergoing sample index PCR for 16 cycles. Purified libraries were sequenced to a depth of 50,000 reads per cell on the HiSeq3000 (Illumina) systems with 26 cycles for read 1, 8 cycles for index (i7) and 91 cycles for read 2.

Cell Ranger v.3.1 was used to align, filter, and count barcodes as well as unique molecular identifiers. Further data analyses was performed using Seurat (v.3.0) (Satija, Nature biotech 2015). Cells with greater than 8% mitochondrial genes were excluded from analysis. Cells with more than 2,500-5,000 or less than 100-1,000 detected genes were considered outliers and excluded from downstream analyses. Raw unique molecular identifier counts were then normalized to unique molecular identifier counts per million total counts before being log-transformed. Principle component analysis was performed, and the 10 most statistically significant principal components were used for uniform manifold approximation and projection (UMAP) analysis. Clusters were identified using the nearest neighbor algorithm in Seurat and UMAP plots were

generated based on selected PCA dimensions. The Seurat function FindAllMarkers was used to identify marker genes. Log-normalized data are shown. Gene set scoring was performed using the VISION R package v.2.1.0, following the scoring algorithm as described previously (DeTomaso, BMC Bioinformatics 2016). In brief, the expression of signature genes is weighted based on the predicted dropout probability calculated from nearest neighbors, and the normalized expression summed for all genes in the gene set.

Statistical analysis

GraphPad Prism (v.10.0.3) was used for statistical analysis. The difference between experimental groups was assessed using two-tailed unpaired t-tests or two-tailed unpaired Mann-Whitney *U*-tests or one-tailed paired Wilcoxon matched-pairs signed rank test.

Figure 1

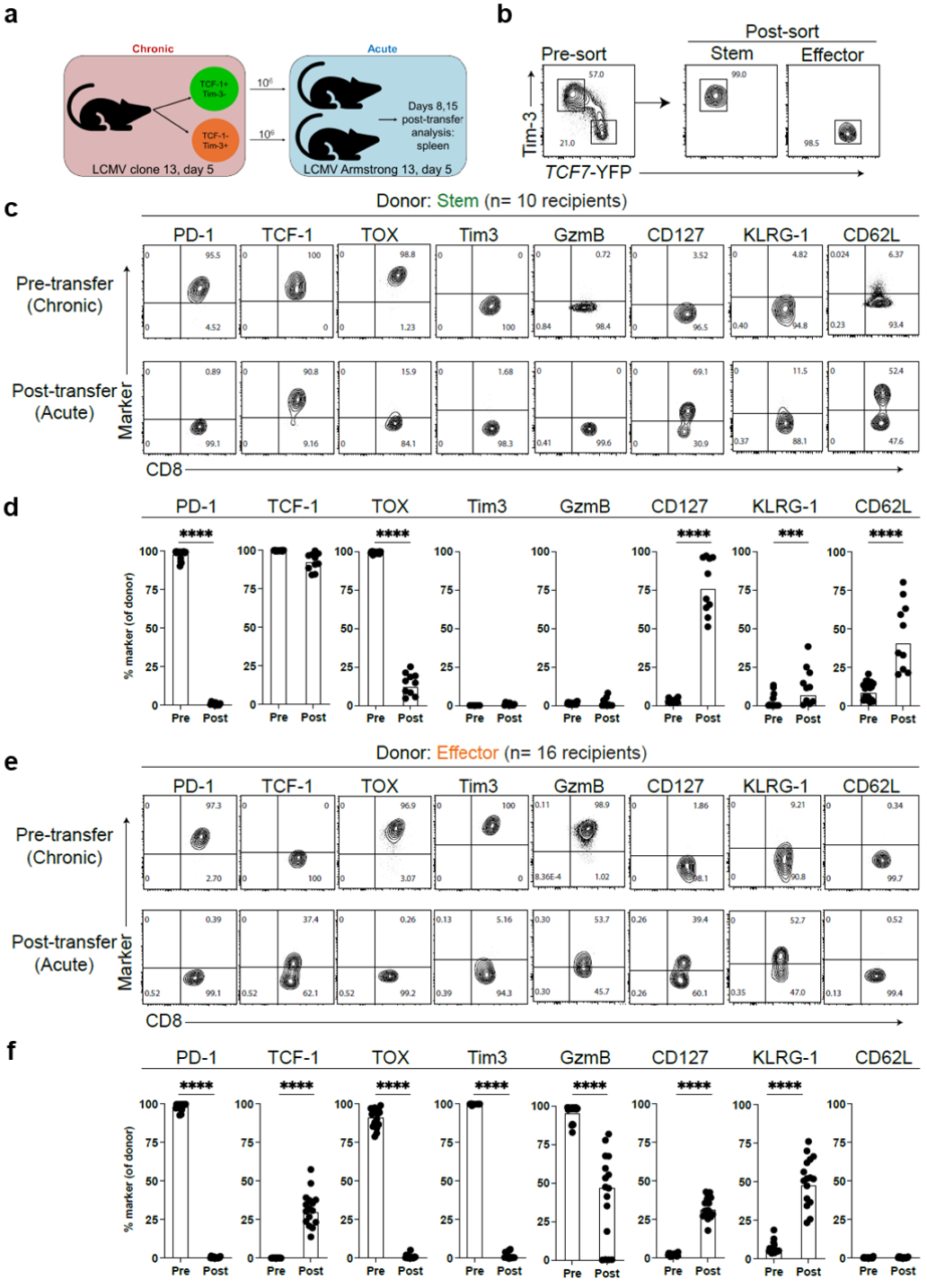
a
Chronic
Acute
TCF-1+ Tim-3-
TCF-1- Tim-3+
10^6
10^6
Days 8,15 post-transfer analysis: spleen
LCMV clone 13, day 5
LCMV Armstrong 13, day 5
b
Pre-sort
Post-sort
Stem
Effector
Tim-3
TCF7-YFP
c
Donor: Stem (n= 10 recipients)
PD-1
TCF-1
TOX
Tim3
GzmB
CD127
KLRG-1
CD62L
Pre-transfer (Chronic)
Post-transfer (Acute)
Marker
CD8
d
% marker (of donor)
Pre
Post
e
Donor: Effector (n= 16 recipients)
f

Fig. 1| Early stem-like CD8+ T cells from chronic viral infection become memory CD8+ T cells after transfer into acutely infected mice. a,b $2x10^3$ *TCF7*-YFP reporter P14 CD8+ T cells were transferred into congenically mismatched naïve mice prior to intravenous infection with $2x10^6$ PFU LCMV clone 13. On day 5 p.i. *TCF7*-YFP+ Tim-3- (stem) and *TCF7*-YFP- Tim-3+ (effect.) P14 CD8+ T cells were isolated from the spleen via FACS and transferred intravenously into separate groups of congenically distinct, day 5 LCMV Armstrong-infected recipiens. On days 8 and 15 after transfer, the phenotype of donor cells was analyzed. **c,** Expression of indicated markers on stem-like donor cells pre- (spleen, day 5 p.i., chronic) and post-transfer (representative of days 8/15 post-transfer, acute) in the spleen. **d,** Frequencies of stem-like donor cells positive for indicated markers pre- and post-transfer. **e,** Expression of indicated markers on effector donor cells pre- and post-transfer in the spleen. **f,** Frequencies of effector donor cells positive for indicated markers pre- and post-transfer. Flow plots are representative of 1 of 3 independent experiments. Graphs show data pooled from 3 independent experiments (pre-transfer n=15, post-transfer n= 10-16). P values calculated using Mann-Whitney test. *** and **** indicate p values of less than 0.001, and 0.0001, respectively.

Extended Data Fig. 1

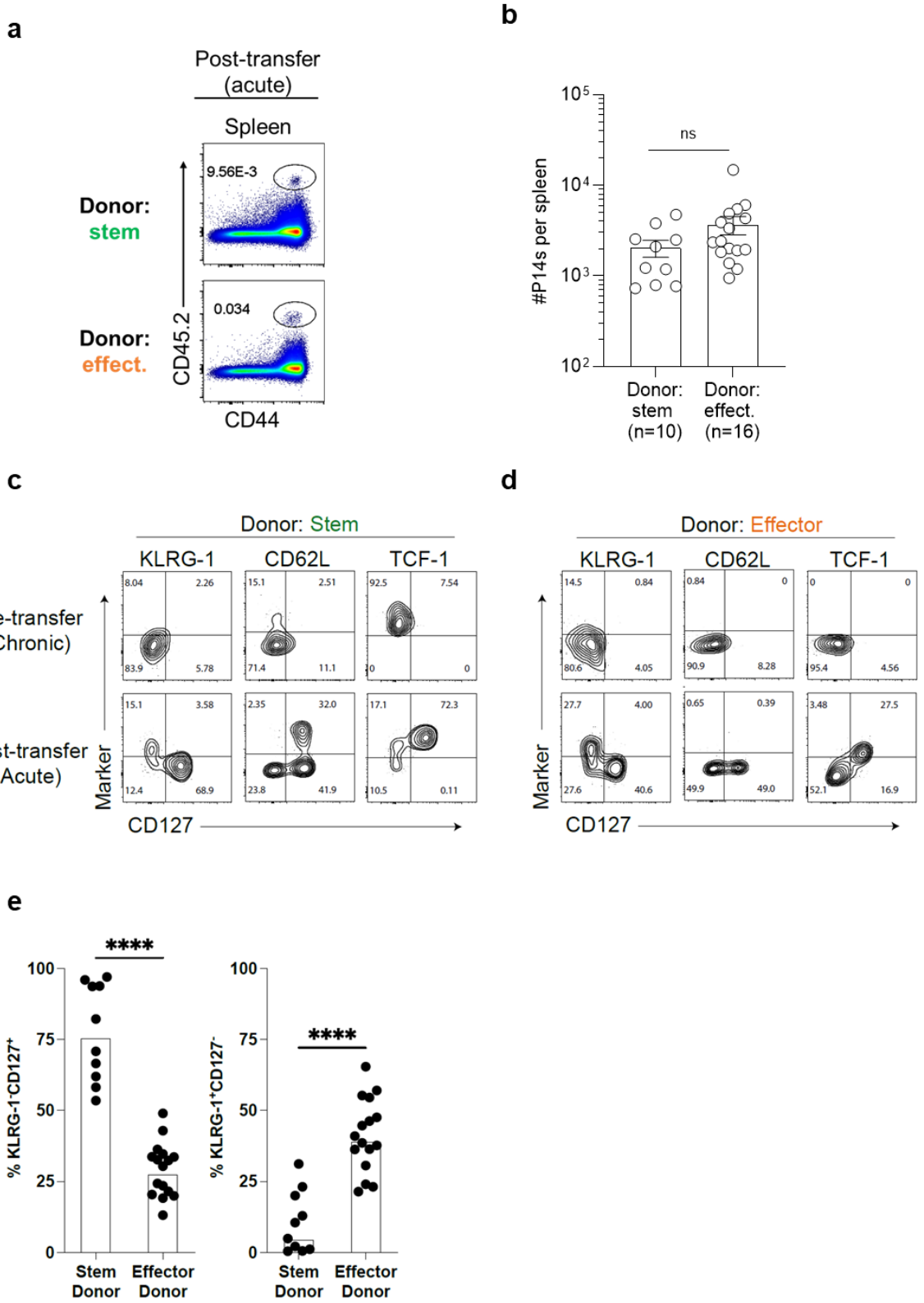

Extended Data Fig. 1| Adoptive transfer of stem-like and effector CD8+ T cells from day 5 LCMV clone 13 (chronic) mice into day 5 LCMV Armstrong (acute) mice. a,b, Frequency (a) and numbers (b) of stem-like and effector donor cells recovered from the spleens of LCMV Armstrong-infected recipients on days 8/15post-transfer. **c,** Expression of CD127, KLRG1, CD62L and *Tcf7*-YFP on stem-like donor cells in the spleen pre- (day 5 p.i.,chronic) and post-transfer (days 8/15 post-transfer, acute). **d,** Expression of CD127, KLRG1, CD62L and *Tcf7*-YFP on effector donor cells in the spleen pre- (day 5 p.i., chronic) and post-transfer (days 8/15 post-transfer, acute). **e,** Frequencies of memory precursors (left, KLRG1- CD127+) and terminal effectors (right, KLRG1+ CD127-) within stem vs effector donor cells post-transfer. Graphs show data pooled from 3 independent experiments (pre-transfer *n*=15, post-transfer *n*= 10-16). P values calculated using Mann-Whitney test. **** indicate p value of less than 0.0001. Flow plots are representative of 1 of 3 independent experiments.

Figure. 2

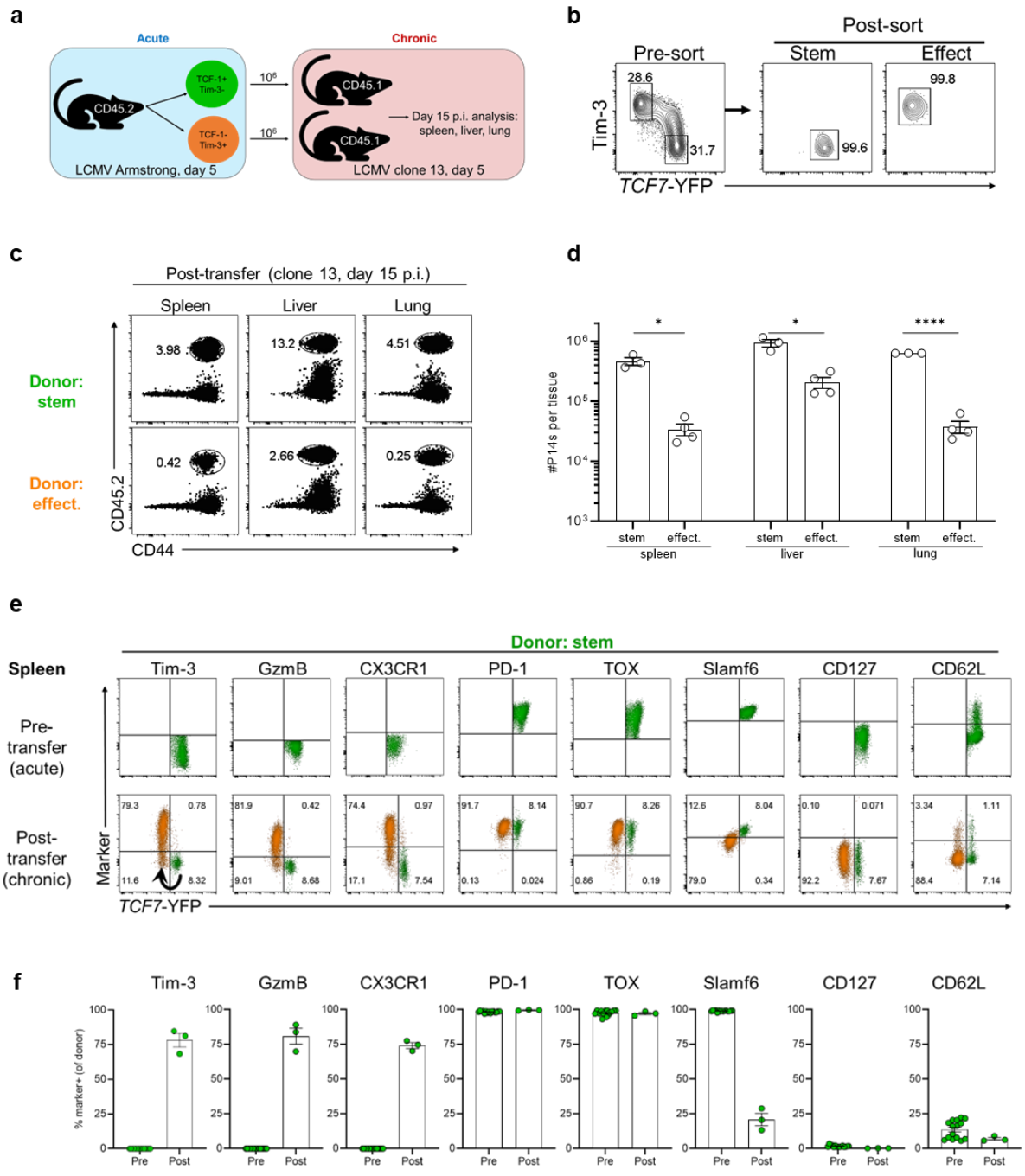
a
Acute
Chronic
CD45.2
TCF-1+ Tim-3-
TCF-1- Tim-3+
10^6
10^6
CD45.1
CD45.1
Day 15 p.i. analysis: spleen, liver, lung
LCMV Armstrong, day 5
LCMV clone 13, day 5
b
Pre-sort
Post-sort
Stem
Effect
28.6
31.7
99.6
99.8
Tim-3
TCF7-YFP
c
Post-transfer (clone 13, day 15 p.i.)
Spleen
Liver
Lung
Donor: stem
Donor: effect.
3.98
13.2
4.51
0.42
2.66
0.25
CD45.2
CD44
d
#P14s per tissue
*
*
****
stem
effect.
spleen
liver
lung
e
Donor: stem
Spleen
Tim-3
GzmB
CX3CR1
PD-1
TOX
Slamf6
CD127
CD62L
Pre-transfer (acute)
Post-transfer (chronic)
Marker
TCF7-YFP
f
% marker+ (of donor)
Pre
Post

Fig. 2| Early stem-like CD8+ T cells from acute viral infection become chronic resource CD8+ T cells after transfer into chronically infected mice. **a,b,** $2x10^3$ *TCF7*-YFP reporter P14 CD8+ T cells were transferred into congenically mismatched naïve mice prior to intravenous infection with $2x10^6$ PFU of LCMV Armstrong (acute). On day 5, *TCF7*-YFP+ Tim-3- (stem) and *TCF7*-YFP- Tim-3+ (effect.) P14 CD8+ T cells were FACS sorted from the spleen and $1x10^6$ of each were transferred intravenously into separate groups of congenically distinct, day 5 LCMV clone 13 (chronic) mice. The recovery and phenotype of donor cells was analyzed 10 days later. **c,d,** Frequencies and numbers of stem-like and effector donor cells recovered from the spleens, livers, and lungs, of chronic LCMV recipient mice post-transfer. **e,** Expression of indicated markers on stem-like donor cells pre- (spleen, day 5 p.i., acute) and post-transfer (spleen, day 15 p.i., chronic). Arrow indicates differentiation trajectory of donor Tim-3- stem-like cells into Tim-3+ effector cells. **f,** Frequency of stem-like donor cells positive for indicated markers pre- and post-transfer in the spleen. Flow plots are representative of 1 independent experiment. Graphs show data from 1 independent experiment (pre-transfer *n*=9, post-transfer *n*= 3). Analysis of D^bGP33+ TCF-1- Tim-3+ stem-like CD8+ T cells from a separate experiment was used to illustrate the pre-transfer expression of CX3CR1.

Extended Data Fig. 2

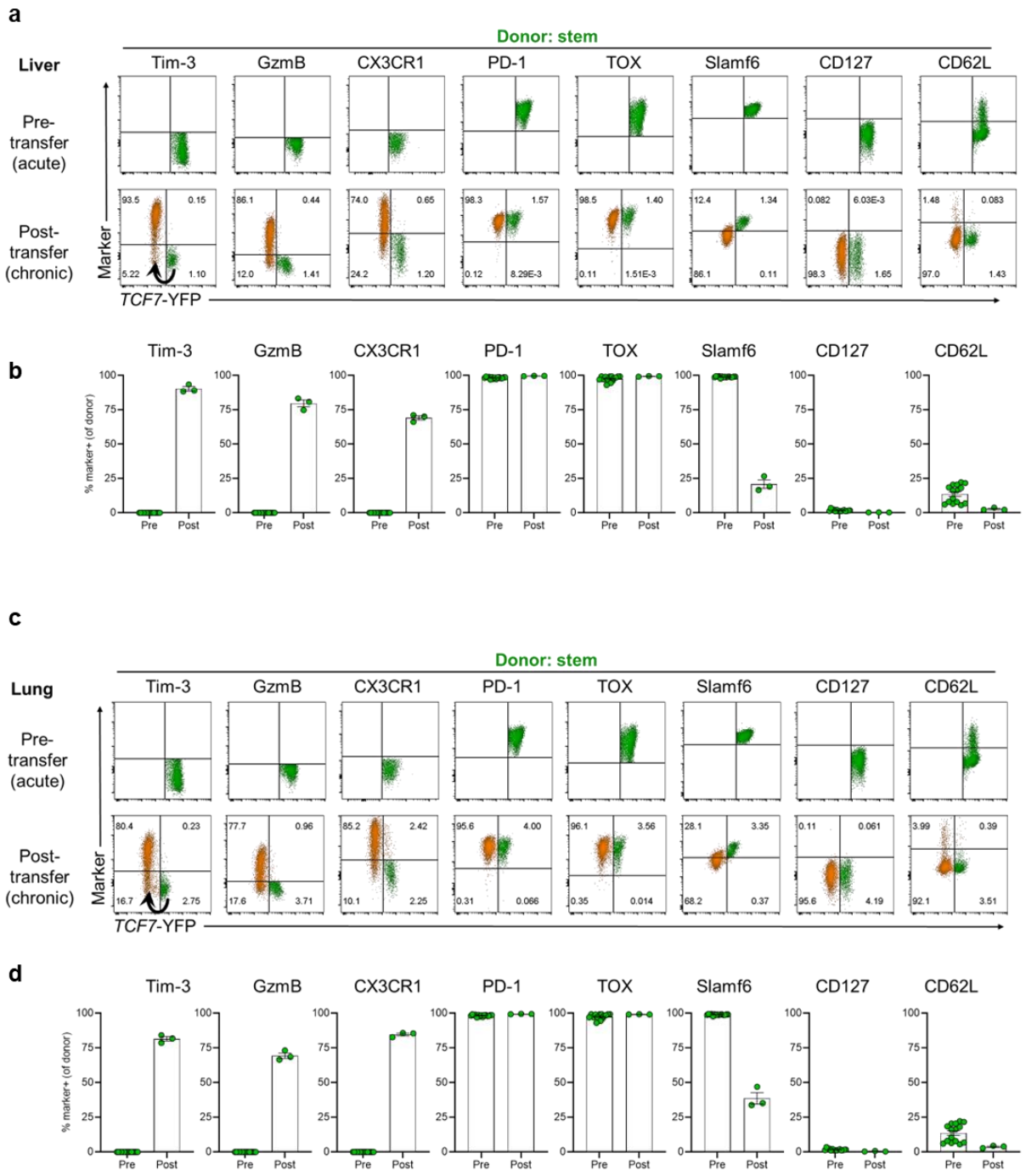

Extended Data Fig. 2| Phenotype of stem-like donor cells in the liver and lung following transfer from day 5 LCMV Armstrong mice into day 5 LCMV clone 13 mice. a, Expression of indicated markers on stem-like donor cells pre- (spleen, day 5 p.i., acute) and post-transfer (liver, day 15 p.i., chronic). Arrow indicates differentiation trajectory of donor Tim-3- stem-like cells into Tim-3+ effector cells. **b,** Frequency of stem-like donor cells positive for indicated markers pre- (spleen) and post-transfer (liver). **c,** Expression of indicated markers on stem-like donor cells pre- (spleen, day 5 p.i., acute) and post-transfer (lung, day 15 p.i., chronic). Arrow indicates differentiation trajectory of donor Tim-3- stem-like cells into Tim-3+ effector cells. **d,** Frequency of stem-like donor cells positive for indicated markers pre- (spleen) and post-transfer (lung). Flow plots are representative of 1 independent experiment. Graphs show data from 1 independent experiment (pre-transfer *n*=9, post-transfer *n*= 3). Analysis of D^bGP33+ TCF-1- Tim-3+ stem-like CD8+ T cells from a separate experiment was used to illustrate the pre-transfer expression of CX3CR1.

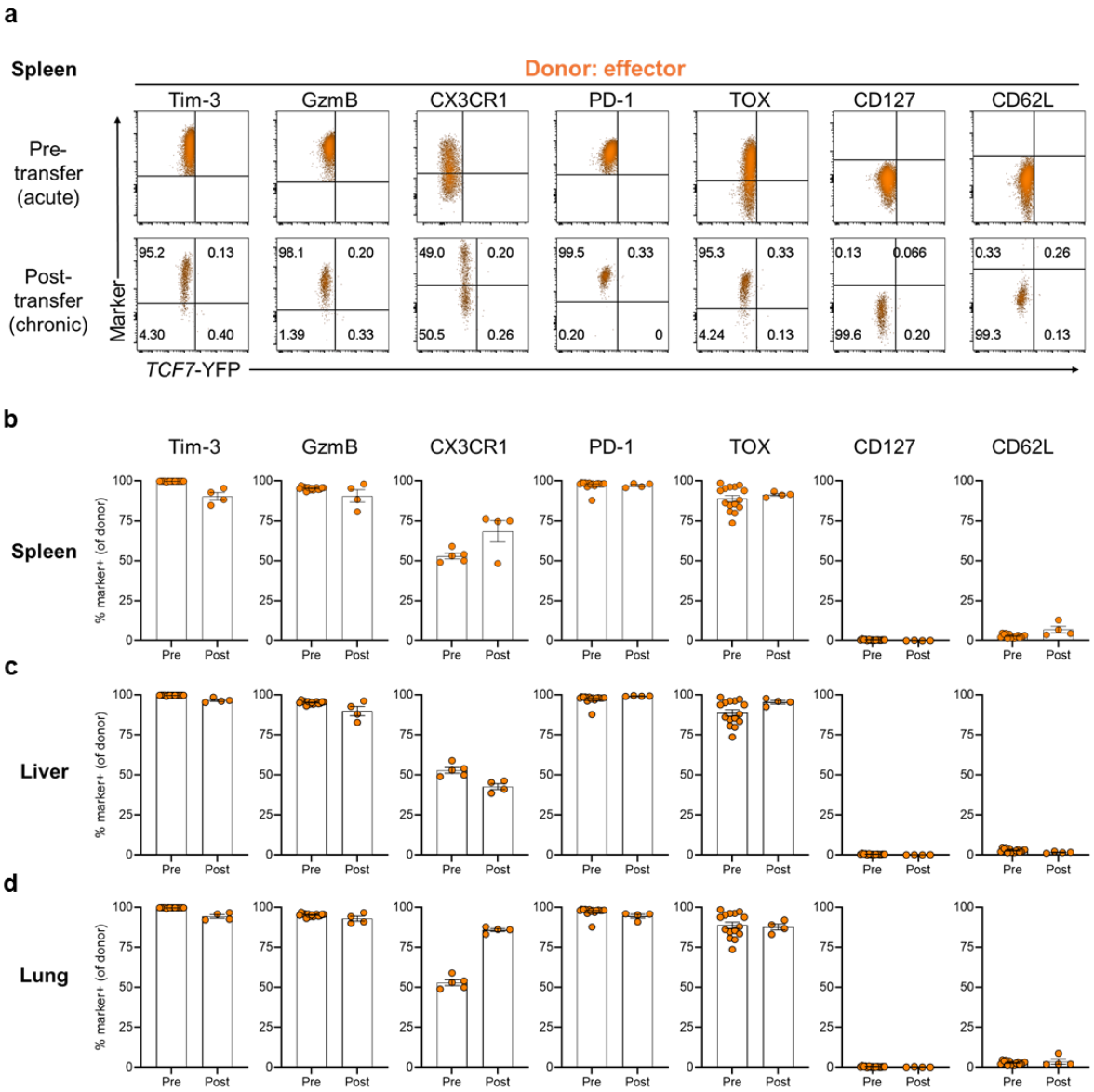

Extended Data Fig. 3| Phenotype of effector donor cells in the spleen, liver, and lung following transfer from day 5 LCMV Armstrong mice into day 5 LCMV clone 13 mice. **a,** Expression of indicated markers on effector donor cells pre- (spleen, day 5 p.i., acute) and post-transfer (spleen, day 15 p.i., chronic). **b,** Frequency of effector donor cells positive for indicated markers pre- (spleen) and post-transfer (spleen). **c,** Frequency of effector donor cells positive for indicated markers pre- (spleen) and post-transfer (liver). **d,** Frequency of effector donor cells positive for indicated markers pre- (spleen) and post-transfer (lung). Flow plots are representative of 1 independent experiment. Graphs show data from 1 independent experiment (pre-transfer *n*=9, post-transfer *n*= 3). Analysis of D^bGP33+ TCF-1- Tim-3+ effector CD8+ T cells from a separate experiment was used to illustrate the pre-transfer expression of CX3CR1.

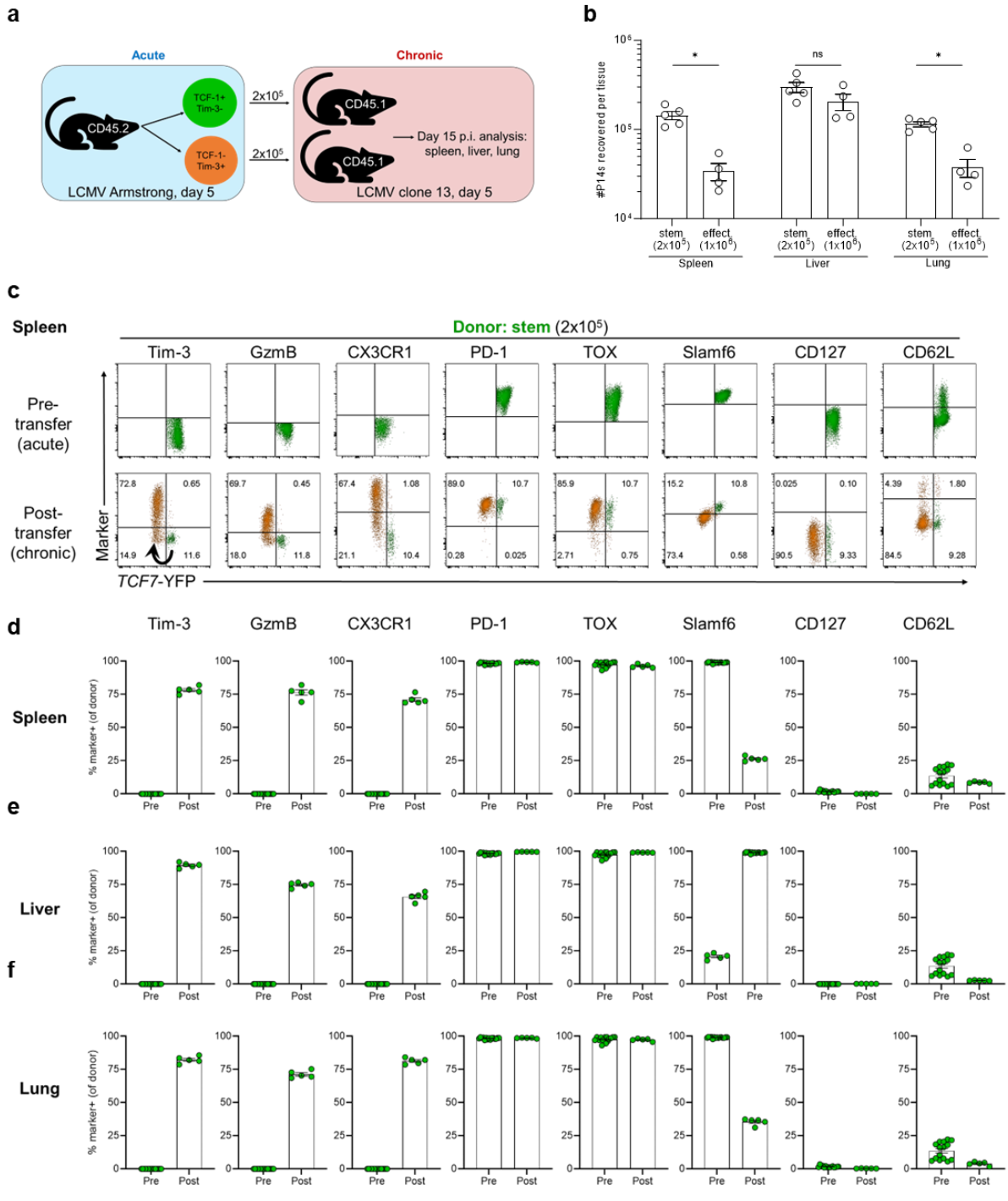
a
Acute
Chronic
CD45.2
TCF-1+ Tim-3-
TCF-1- Tim-3+
2x10^5
2x10^5
CD45.1
CD45.1
Day 15 p.i. analysis: spleen, liver, lung
LCMV Armstrong, day 5
LCMV clone 13, day 5
b
#P14s recovered per tissue
stem (2x10^5)
effect (1x10^6)
Spleen
Liver
Lung
ns
c
Spleen
Donor: stem (2x10^5)
Tim-3
GzmB
CX3CR1
PD-1
TOX
Slamf6
CD127
CD62L
Pre-transfer (acute)
Post-transfer (chronic)
Marker
TCF7-YFP
d
Spleen
e
Liver
f
Lung
% marker+ (of donor)
Pre
Post

Extended Data Fig. 4| Transfer of 2x10^5 stem-like donor cells from day 5 LCMV Armstrong mice into day 5 LCMV clone 13 mice. a, 2x10^3 *TCF7*-YFP reporter P14 CD8+ T cells were transferred into congenically mismatched naïve mice prior to intravenous infection with 2x10^6 PFU of LCMV Armstrong (acute). On day 5, 2x10^5 *TCF7*-YFP+ Tim-3- (stem) and 1x10^6 *TCF7*-YFP- Tim-3+ (effect.) P14 CD8+ T cells were FACS sorted from the spleen and transferred intravenously into separate groups of congenically distinct, day 5 LCMV clone 13 (chronic) mice. The recovery and phenotype of donor cells was analyzed 10 days later. **b,** Numbers of stem-like and effector donor cells recovered from the spleens of chronic LCMV recipient mice post-transfer. **c,** Expression of indicated markers on stem-like donor cells pre- (spleen, day 5 p.i., acute) and post-transfer (spleen, day 15 p.i., chronic). Arrow indicates differentiation trajectory of donor Tim-3- stem-like cells into Tim-3+ effector cells. **d,** Frequency of stem-like donor cells positive for indicated markers pre- and post-transfer in the spleen. **e,** Frequency of stem-like donor cells positive for indicated markers pre- (spleen) and post-transfer (liver). **f,** Frequency of stem-like donor cells positive for indicated markers pre- (spleen) and post-transfer (lung). Graph shows data from 1 independent experiment (pre-transfer *n*=9, post-transfer *n*= 5). Flow plots are representative of 1 independent experiment. Analysis of D^{b}GP33+ TCF-1+ Tim-3- stem-like CD8+ T cells from a separate experiment was used to illustrate the pre-transfer expression of CX3CR1.

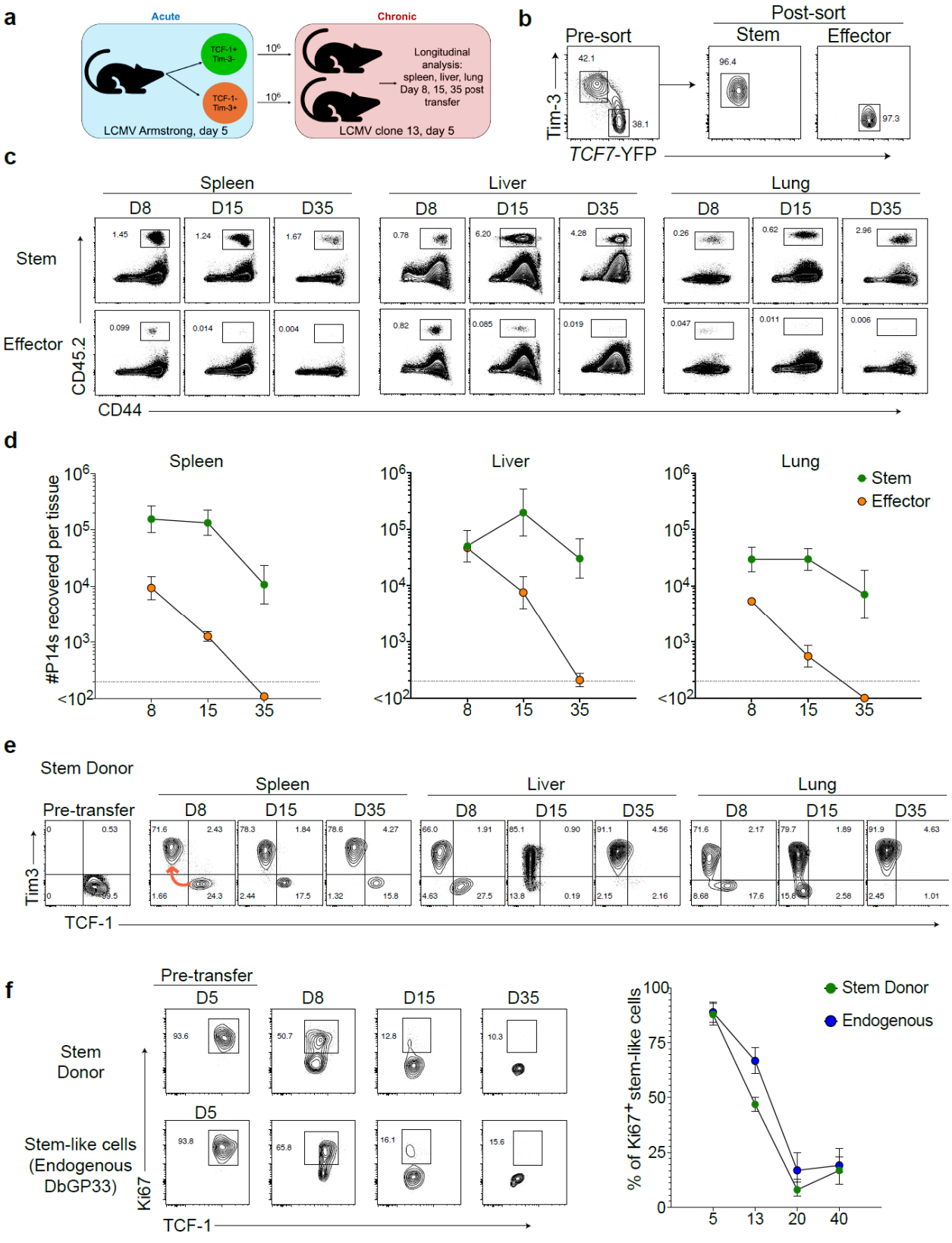
a
Acute
Chronic
TCF-1+ Tim-3-
TCF-1- Tim-3+
10^6
10^6
LCMV Armstrong, day 5
Longitudinal analysis: spleen, liver, lung Day 8, 15, 35 post transfer
LCMV clone 13, day 5
b
Pre-sort
Post-sort
Stem
Effector
Tim-3
TCF7-YFP
42.1
38.1
96.4
97.3
c
Spleen
Liver
Lung
D8
D15
D35
Stem
Effector
CD45.2
CD44
1.45
1.24
1.67
0.78
6.20
4.28
0.26
0.62
2.96
0.099
0.014
0.004
0.82
0.085
0.019
0.047
0.011
0.006
d
Spleen
Liver
Lung
Stem
Effector
#P14s recovered per tissue
10^6
10^5
10^4
10^3
<10^2
8
15
35
e
Stem Donor
Pre-transfer
Spleen
Liver
Lung
D8
D15
D35
Tim3
TCF-1
0
0.53
99.5
71.6
2.43
1.66
24.3
78.3
1.84
2.44
17.5
78.6
4.27
1.32
15.8
66.0
1.91
4.63
27.5
85.1
0.90
13.8
0.19
91.1
4.56
2.15
2.16
71.6
2.17
8.68
17.6
79.7
1.89
15.6
2.58
91.9
4.63
2.45
1.01
f
Pre-transfer
D5
D8
D15
D35
Stem Donor
Stem-like cells (Endogenous DbGP33)
Ki67
TCF-1
93.6
50.7
12.8
10.3
93.8
65.8
16.1
15.6
% of Ki67+ stem-like cells
100
75
50
25
0
5
13
20
40
Stem Donor
Endogenous

Fig. 3| Early stem-like CD8+ T cells from acute viral infection become chronic resource cells when transferred into mice with a life-long viral infection. a,b, $2x10^3$ *TCF7*-YFP reporter P14 CD8+ T cells were transferred into congenically mismatched naïve mice prior to intravenous infection with $2x10^6$ PFU of LCMV Armstrong (acute). On day 5, *TCF7*-YFP+ Tim-3- (stem) and *TCF7*-YFP- Tim-3+ (effect.) P14 CD8+ T cells were FACS sorted from the spleen and $1x10^6$ of each were transferred intravenously into separate groups of congenically distinct, day 5 LCMV clone 13 (chronic) mice that had received transient CD4 depletion prior to infection to induce a life-long, chronic infection. The recovery and phenotype of donor cells was assessed on days 8,15, and 35 post-transfer in the spleen, liver, and lungs. **c,d,** Frequencies and numbers of stem-like and effector donor cells recovered from the spleens, livers, and lungs, of chronic LCMV recipient mice at indicated times post-transfer. **e,** Expression of TCF-1 and Tim-3 on stem-like donor cells pre-transfer (spleen, day 5 p.i., acute) and at indicated times post-transfer in the spleens of chronically infected recipients. Arrow indicates differentiation trajectory of donor Tim-3- stem-like cells into Tim-3+ effector cells. **f,** Expression of TCF-1 and Ki-67 on stem-like CD8 T cells derived from acute stem donor cells (top row) versus endogenous GP33-specific stem-like CD8 T cells (bottom row) in the spleens of chronic LCMV recipient mice at indicated times post-transfer. Summary graph on right shows frequencies of Ki67+ stem-like CD8 T cells derived from stem donor cells (green) or endogenous GP33-specific cells (blue). Pre-transfer phenotype for stem donor cells is from the spleen of a day 5 acute LCMV mouse. Pre-transfer phenotype shown for endogenous GP33-specific stem-like cells is from the spleen of a day 5 chronic LCMV mouse. Flow plots are representative of 1 independent experiment. Graphs show data from 1 independent experiment (n= 3-6 mice per group per time point).

Extended Data Fig. 5

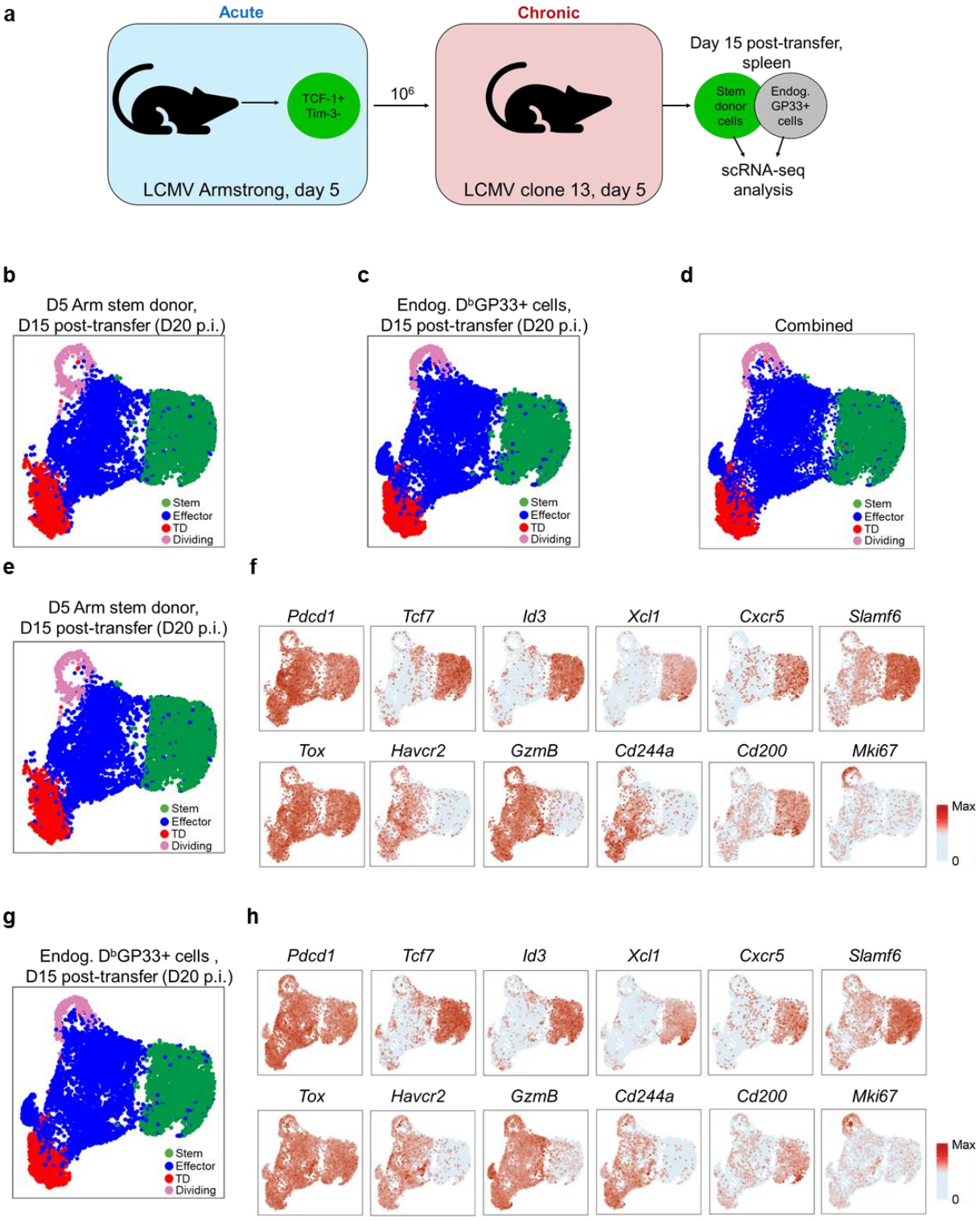

Extended Data Fig. 5| scRNA-sequencing of acute LCMV stem-like CD8 T cell donor cells following transfer into mice with a life-long viral infection. Part of analysis performed for experiment in figure 3. **a,** On day 5, *TCF7*-YFP+ Tim-3- (stem) P14 CD8+ T cells were FACS sorted from the spleens of acute LCMV mice and $1x10^6$ cells were transferred intravenously into congenically distinct, day 5 LCMV clone 13 (chronic) mice that had received transient CD4 depletion prior to infection to induce a life-long viral infection. On day 15 post-transfer, scRNA-seq analysis was performed on stem donor (CD45.2+ CD45.1-) and endogenous GP33-specific (CD45.2- CD45.1+) CD8 T cells both isolated from the spleens of stem recipient mice. **b-d,** Data from stem donor cells (b), endogenous GP33+ cells (c), and both combined (d) projected onto UMAP plots. Stem donor and endogenous GP33+ cells both formed four clusters: stem, effector, terminally differentiated (TD), and dividing. **e,** Same UMAP as in b showing stem donor cell clusters. **f,** Expression of selected genes by stem donor cell clusters. **g,** Same UMAP as in c showing endogenous GP33+ cell clusters. **h,** Expression of selected genes by endogenous GP33+ cell clusters. Max, maximum.

Figure. 4

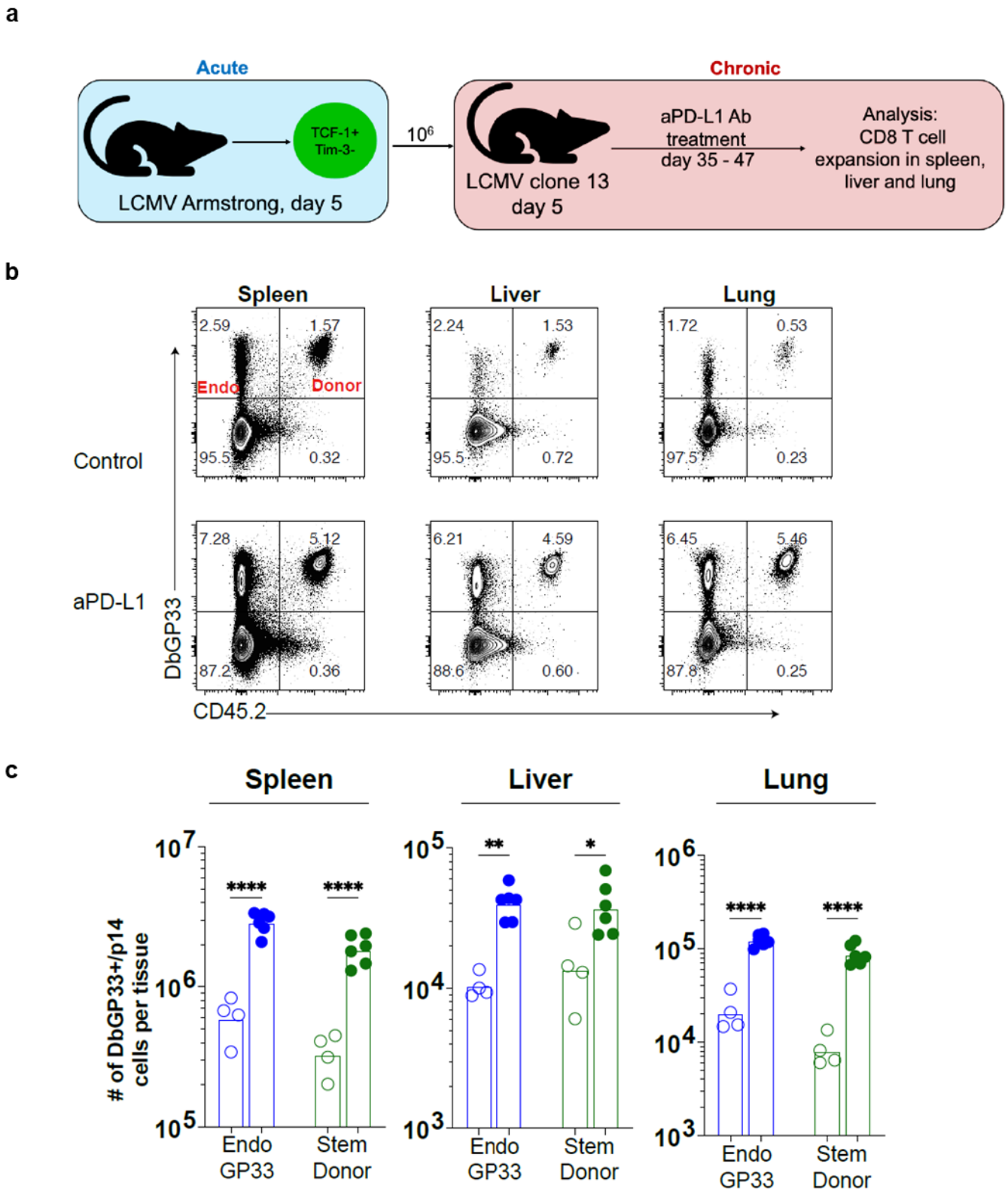
a
Acute
TCF-1+
Tim-3-
LCMV Armstrong, day 5
10^6
Chronic
LCMV clone 13
day 5
aPD-L1 Ab
treatment
day 35 - 47
Analysis:
CD8 T cell
expansion in spleen,
liver and lung
b
Spleen
Liver
Lung
Control
aPD-L1
Endo
Donor
2.59
1.57
95.5
0.32
2.24
1.53
95.5
0.72
1.72
0.53
97.5
0.23
7.28
5.12
87.2
0.36
6.21
4.59
88.6
0.60
6.45
5.46
87.8
0.25
DbGP33
CD45.2
c
Spleen
Liver
Lung
# of DbGP33+/p14
cells per tissue
****
****
**
*
****
****
Endo
GP33
Stem
Donor

Fig. 4| Early stem-like CD8+ T cells from acute viral infection can provide the response to PD-1 blockade in mice with a life-long viral infection. Part of analysis performed for experiment in figure 3. **a,** On day 5, *TCF7*-YFP+ Tim-3- (stem) P14 CD8+ T cells were FACS sorted from the spleens of acute LCMV mice and $1x10^6$ cells were transferred intravenously into congenically distinct, day 5 LCMV clone 13 (chronic) mice that had received transient CD4 depletion prior to infection to induce a life-long viral infection. Beginning on day 35 post-transfer, separate groups of stem recipients were left untreated or given anti-PD-L1 blocking antibody over the course of 12 days (1 Tx/ 3 days). Expansion of stem donor and endogenous GP33+ cells was then assessed in the spleen, liver, and lungs of stem recipient mice. **b,** Representative flow plots from indicated tissues showing frequencies of stem donor (CD45.2+ GP33+) and endogenous GP33+ (CD45.2-) cells in control (top) versus anti-PD-L1 treated (bottom) stem recipient mice. **c,** Summary graphs showing numbers of endogenous GP33+ (blue) and stem donor (green) cells in indicated tissues from control (open circles) and anti-PD-L1 treated (closed circles) mice. Data shown from 1 experiment (n= 4-6 mice per group). P values calculated using Mann-Whitney test. *, **, and **** indicate p values of less than 0.05, 0.01, and 0.0001, respectively.

Chapter 6: Discussion (need to add chapter/figure annotations)

Here we document the generation of stem-like CD8 T cells and examine the plasticity and fate of these cells in acute versus chronic antigen exposure. We found that virus-specific cells with the phenotypic and transcriptional program of stem-like CD8 T cells from an established chronic infection were present just days into chronic infection.

Spatiotemporal dynamics of stem-like CD8 T cells during chronic infection

Location is central to immune cell identity and function. CD8 T cell differentiation during the established phase of chronic LCMV infection is anatomically organized. Stem-like CD8 T cells primarily found in the splenic white pulp whereas their effector/terminally differentiated counterparts are located mainly in the splenic red pulp [60]. Intravascular labeling and imaging revealed that these anatomical commitments are also made early, with stem-like cells showing a bias for the splenic white pulp relative to effector CD8 T cells. The anatomical differences between stem-like and TD cells on day 5 was not owed to the absence of CD4 T cell help as mice with virus-specific CD4 T cells showed similar differences. We also noted populations of stem-like CD8 T cells in the red pulp, blood, and liver early during chronic LCMV infection but the importance of this is unclear. At this stage of infection, the number of virus-infected cells in peripheral tissues is very high and still rising. It's possible that stem-like CD8 T cells are needed in these sites early on to help maintain a numerically relevant effector population while naïve cell-derived effectors are still arriving from lymphoid tissues. There is evidence for a similar phenomenon in certain tumor models where control of the tumor relies on stem-like CD8 T cells migrating into the tumor and locally generating effector cells[72].

As chronic infection progressed, the numbers of stem-like CD8 T cells in the circulation, liver, and red pulp declined dramatically. However, a similar decline was not observed in the white pulp wherein stem-like CD8 T cells remained relatively stable between days 5 and >45. Multiple phenomena could account for these dynamics, including the terminal differentiation of peripheral site stem-like CD8 T cells but preservation of those in lymphoid tissues; or the retrograde migration[119] of stem-like CD8 T cells from peripheral tissues back to their respective induction sites of origin. Related to this, we also do not

know which factors enable stem-like CD8 T cells to access the blood and peripheral tissues early during chronic LCMV.

CD69 is a known retention factor for T cells to lymphoid tissues [86]. Although an imperfect marker for resident memory CD8 T cells[120], CD69 has been shown to promote the retention of these cells in the skin[121]. CD69 is also associated with the residence of stem-like CD8 T cells during the late phase of chronic LCMV infection[80]. Aligning with this, CD69 expression was associated with the anatomical dynamics of stem-like CD8 T cells between the early and late stages of chronic infection in our study and in a previous report[88]. Stem-like CD8 T cells present in the blood, red pulp, and liver early (day 5) during chronic infection were all negative for CD69. As infection progressed to day>45, stem-like CD8 T cells in peripheral compartments, all CD69-, were dramatically reduced whereas those in the white pulp remained relatively stable were nearly all CD69+. Interestingly, there was a small fraction of CD69+ stem-like CD8 T cells located specifically in the white pulp early during infection. Whether these dynamics reflect the preservation of that subset of CD69+ stem-like cells in the white pulp and loss of CD69- cells is unclear. As shown in Beltra et al,. phenotypic and functional heterogeneity can be observed among stem-like CD8 T cells based on CD69 expression. It's possible that CD69 expression predisposes a subset of stem-like CD8 T cells to be lymphoid-resident and those that fail to acquire CD69 become migratory. CXCR5, CCR7, and CXCR3 are other receptors expressed by stem-like CD8 T cells[60] and known regulators of CD8 T cell location[122–128], including stem-like CD8 T cells, that warrant inquiry as potential mediators of stem-like CD8 T cell positioning during chronic infection.

Paradoxical relationship between stem-like CD8 T cells and antigen

How stem-like CD8 T cells resist antigen-induced terminal differentiation amidst virus-infected tissues is one of the most intriguing features of these cells. One possibility is that stem-like CD8 T cells receive less TCR stimulation during chronic infection than their effector counterparts. Based on the expression of *Nur77*-GFP[94–96], TCR signaling did not differ between stem-like and effector CD8 T cells neither early nor late during chronic infection. TCF-1[60,67] and TOX[68–70] are important for the generation of stem-like CD8 T cells while PD-1 regulates the activity of these cells[60,81,129]. Using a mixed

chronic viral infection setup during which antigen exposure for GP33-specific CD8 T cells is gradually lost as the infection progresses [97–100], we found that antigen, but not the chronic infection environment was crucial for sustaining the expression of PD-1 and TOX. Interestingly, TCF-1 expression also decreased on virus-specific cells. Bcl-6, a transcription factor that represses effector differentiation[66,92,93,130], was also lost in the absence of antigen. Together, these data highlight an important and somewhat paradoxical feature of the stem-like CD8 T cell program: active resistance to effector differentiation driven by TCR signaling.

Impact of long-term antigen exposure on stem-like CD8 T cells

Long-term antigen exposure and the chronic infection environment has dramatic effects on the molecular program and function of CD8 T cells[13–15,89]. We used our early and late comparison to understand the development of stem-like CD8 T cells during chronic LCMV infection. Early during infection, stem-like CD8 T cells exhibited hallmark features of rapidly dividing cells: uniform Ki67 expression, large cell size, an enriched mTOR gene signature, and the co-expression of genes involved in glucose and amino acid metabolism. As infection progresses to the late phase, these cells stop dividing and upregulate multiple inhibitory molecules related to TGF-beta signaling[76].

One conceptual takeaway from these observations is that quiescence and elevated inhibitory molecules, though maybe important for the longevity of stem-like CD8 T cells, are not necessarily defining features of these cells. Rather, they are features that these cells can acquire during prolonged antigen exposure and/or in a particular environment. This is an important insight for three main reasons: firstly, it may be useful for inferring time of antigen exposure and/or the cytokine milieu for studies of stem-like CD8 T cells in humans or other difficult to define contexts. Secondly, it dissociates a circumstantial feature of stem-like CD8 T cells from the dysfunction described by exhaustion. Established phase stem-like CD8 T cells retain enormous proliferative potential, as evidenced by PD-1 blockade. Hence, it is more accurate to describe these cells —with respect to proliferative activity— as quiescent, rather than dysfunctional or exhausted[60]. Thirdly, it highlights the importance of using basic models that enable longitudinal

analyses of cells in a disease context for distinguishing between traits that are fundamental to a cell's 'identity' versus circumstantial/contextual.

Stem-like CD8 T cell fate decision is made agnostic to infection outcome

We next show that nearly identical populations of stem-like CD8 T cells are generated early after acute and chronic LCMV infection; these cells differed in gene expression by less than 1%; had zero differences in chromatin accessibility; were equally biased for positioning in the splenic white pulp; and were equally functional. Hence, the generation of stem-like CD8 T cells is not unique to viral infections destined for chronicity. Nor is it the result of a secondary differentiation wave occurring later during chronic infection. These cells arise from one of the earliest differentiation/fate divergence events, irrespective of infection outcome. This is important because it underscores a concept that is axiomatic/bordering on too-foolish-to-mention but is easily forgotten: CD8 T cells are inherently non-prescient. When the host is insulted, the CD8 T cell response (or the immune system, for that matter) can neither know the nature nor the duration of the insult ahead of time. The solution evidently evolved by CD8 T cells for this myopia is to prepare in advance; to generate a precursor cell early on that can sustain the response long-term, lest the insult persists.

Differential impact of infection origin on early stem-like versus effector CD8 T cells

An interesting observation from our comparison of virus-specific cells during acute versus chronic LCMV was that infection origin impacted the function of effector but not stem-like CD8 T cells. Stem-like CD8 T cells from acute and chronic infection were equally capable of cytokine production and expanding in response to clone 13 challenge. Conversely, effector cells from chronic infection were impaired both in terms of polyfunctionality (IFNy and TNFa production) and expansion capacity compared to their counterparts from acute infection. Possible explanations for the different effect of infection origin on stem-like vs effector cells are elaborated on in the discussion section of chapter 4. In short, the impaired polyfunctionality of effector CD8 T cells during chronic infection, compared to stem-like CD8 T cells, may be due to inherent differences in how these two cell types sense and respond to TCR and environmental signals. An additional factor is the location of these subsets and the major difference in initial

antigen exposure that chronic LCMV effector versus stem-like CD8 T cells might have had prior to transfer.

Early stem-like CD8 T cells become chronic resource cells if infection persists

We next examined the fate of early stem-like CD8 T cells in viral clearance vs. persistence, and further examined the impact of infection origin on differentiation potential using reciprocal adoptive transfer experiments.

To determine the fate of early stem-like CD8 T cells in the context of infection persistence, we transferred day 5 stem-like cells from acutely infected mice into chronically infected mice and found that these early stem-like CD8+ T cells took on all the 'chronic resource cell' properties originally defined for stem-like CD8 T cells in the chronic LCMV infection model. Specifically, they underwent a much larger expansion compared to their effector donor cell counter parts populating lymphoid and non-lymphoid tissues with progeny. Despite originating in an acute LCMV infection destined for clearance, early stem-like donor cells gave rise to the entire differentiation (exhaustion) pathway defined for chronic antigen exposure: stem→ effector→ terminally differentiated. They also maintained the CD8 T cell response in the spleen, liver, and lungs of chronically infected animals for over a month after initial transfer. During this time, they acquired a key feature of chronic resource cells, quiescence. This observation provides conclusive evidence that stem-like CD8 T cells arise early during infection as rapidly dividing cells and progressively stop dividing with time post-antigen exposure.

Importantly, the reduced proliferation of stem-like cells does not represent senescence or the inability to expand upon restimulation (exhaustion) observed for terminally differentiated. These cells retain proliferative potential, as evidenced by the enormous expansion they can undergo following PD-1 blockade. When their chronically infected hosts were treated with PD-L1 blocking antibodies, early stem-like donor cells exited quiescence and underwent a huge proliferative burst equaling that of endogenous GP33+ CD8 T cells within the same mice. This observation further solidifies the notion that early stem-like CD8 T cells become *bona fide* chronic resource cells in the context of antigen persistence.

Early stem-like CD8 T cells become memory if infection rapidly clears

To determine the fate of early stem-like CD8 T cells following clearance of acute infection, we transferred day 5 stem-like CD8+ T cells from LCMV clone 13-infected (chronic) into LCMV Armstrong-infected (acute) mice and examined their differentiation after viral clearance. One possible outcome was that viral clearance would trigger the death of early stem-like CD8 T cells (perhaps owing to the cessation of TCR signaling) since a continuous effector pool was no longer needed. A second possibility is that stem-like CD8 T cells convert to memory following viral clearance. Rather than being lost, stem-like CD8 T cells swapped marks of antigen stimulation (ie PD-1 TOX) for the expression of the survival receptor, CD127, and mark of central memory CD8 T cells, CD62L. This rules out the notion that continuous TCR signaling is necessary for the survival of stem-like CD8 T cells and shows that they can become memory CD8 T cells.

Studying the origins of CD8 T cell memory using LCMV Armstrong

The LCMV Armstrong infection model has provided invaluable insight into the origins of memory CD8 T cells. A key takeaway from this work is that memory cells arise from the de-differentiation of specific types of effector cells referred to as memory precursor effector cells (MPECs), which express CD127 but not KLRG1 [52,114,115]. Follow up studies further showed that early during LCMV Armstrong infection when CD127 is not expressed by virus-specific cells, MPECs can be identified as GzmB+ KLRG1- CD25- [110,111].

The presence of stem-like CD8 T cells during LCMV Armstrong infection was overlooked by previous studies. This is likely because infections were performed intraperitoneally using a dose of $2x10^5$ PFU, which results in a virus-specific CD8 T cell population early on that is comprised almost entirely (~90-95%) of TCF-1- GzmB+ effector cells. The remaining ~5-10% of the population are TCF-1+ GzmB- stem-like CD8 T cells, which increase as a proportion of the virus-specific CD8 T cell pool as infection dose increases (Chapter 4, Extended Data Fig. 1b-d). This is important to note because it suggests that most of what we know about memory, at least from the LCMV model, is based on studying memory CD8 T cells that come from effector cells, not

stem-like CD8 T cells.

**Interestingly, the presence of this small population of stem-like CD8 T cells can be inferred in a 2010 Immunity paper from Kalia et al.,*[110]. Figure 3a of this paper shows a panel of histograms depicting the expression of various markers on CD25 hi vs CD25 lo GP33-specific CD8 T cells analyzed on day 3.5 after acute LCMV infection. If one examines the GzmB histogram using a magnifying glass, one will notice a small bump of GzmB- cells among CD25 lo cells, consistent with the stem-like CD8 T cell phenotype.*

Future work: stem-like- vs. effector-derived memory CD8 T cells

Our data showing that stem-like CD8 T cells can become memory cells indicates that there exists both effector- and non-effector differentiation routes to memory. Whether memory CD8 T cells derived from effector versus stem-like cells differ in biologically meaningful ways is unclear. Though, it would be surprising if the distinct anatomical, molecular, and functional characteristics that distinguish stem-like and effector CD8 T cells during viral infection did not carry over to the memory cells they generate once the infection is cleared. Consistent with this, 30-75% of the memory cells that arose from early stem-like CD8 T cells expressed CD62L compared to 0% for effector-derived memory cells. This suggests that the primary sources of central memory and effector memory CD8 T cells may be from different origins.

Future work should focus on determining the quantitative and qualitative contributions of stem-like vs. effector-derived CD8 T cells to the memory pool. Stem-like vs. effector-derived memory cells may confer different properties to the memory CD8 T cell compartment. Owing to pre-existing accessibility at effector gene loci inherited from their parents, effector-derived memory cells may be more capable of rapidly elaborating effector function compared to stem-like cell-derived memory cells. The ability to quickly produce anti-viral cytokines and cytotoxic molecules without having to divide first would be advantageous at barrier sites, like the big toe. The ability of stem-like cell-derived memory cells to continuously produce effector cells while self-renewing might serve as a second wave of protection, say if the pathogen overwhelms effector-derived memories at the big toe and spreads to distant tissues.

Conclusion

Altogether, these data demonstrate the ability of early stem-like CD8 T cells to adapt to acute or chronic viral infection. Furthermore, it shows that the differentiation trajectory of early stem-like CD8 T cells is not pre-destined by infection origin. Rather, the development of early stem-like CD8 T cells is gradually shaped by the progression and outcome of infection. Ultimately, stem-like CD8 T cells equip the host with adaptability when challenged; conferring an inherently unforeseeing immune system with the ability to protect against re-challenge (memory, antigen clears) or control the challenge without excessive damage to the host (exhaustion, antigen persists).

Philosophizing on the design of CD8 T cell differentiation and what CD8 T cell memory and exhaustion really means

Ultimately, it appears that the design of CD8 T cell differentiation for acute versus chronic viral infection is the same. The host is insulted and a clone specific to that insult is selected to expand extensively via signals 1, 2, and 3. The goal of this cell division is to produce two major cell types each of numerically relevant sizes: a stem-like cell and an effector cell. The goal of the stem-like CD8 T cell is to ensure for the host that the selected clone is propagated indefinitely. The goal of the effector CD8 T cell is to quickly rid the host of the insult. Rather than constituting separate lineages, perhaps what we call CD8 T cell memory and exhaustion simply describe what happens to stem-like and effector CD8 T cells when the insult is rapidly cleared versus when it persists. If the insult is cleared, populations of stem-like and effector CD8 T cells live on and continue to carry out their respective goals. If the insult persists, the initial population of effector cells is lost and stem-like CD8 T cells serve as the source of new effector cells.

Figure 1

a

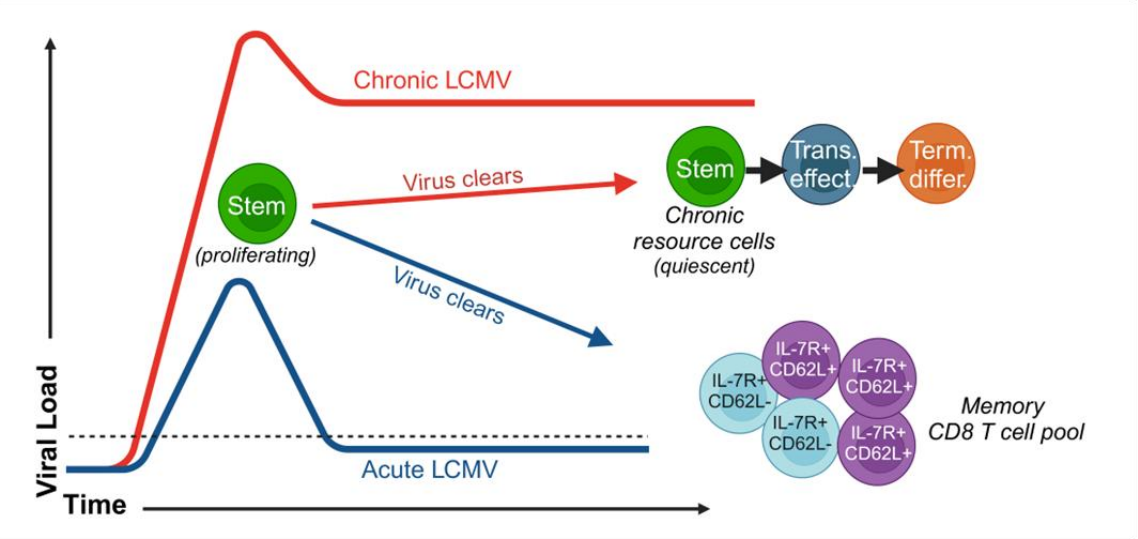

Fig. 1| A precursor CD8 T cell that adapts to acute or chronic viral infection. a, Stem-like CD8 T cells arise early after acute and chronic viral infection. If virus persists, they take on the role of chronic resource cells (top). If virus clears, they become memory CD8 T cells, including CD62L+ cells.

References

1. Hendrix, R. W., Smith, M. C. M., Neil Burns, R., Ford, M. E. & Hatfull, G. F. *Evolutionary Relationships among Diverse Bacteriophages and Prophages: All the World's a Phage*. vol. 96 www.pnas.org. (1999).
2. Mushegian, A. R. Are There 10 31 Virus Particles on Earth, or More, or Fewer? *Proc Natl Acad Sci U S A* **96**, 2192–2197 (1999).
3. Hogquist, K. A. & Jameson, S. C. The self-obsession of T cells: How TCR signaling thresholds affect fate 'decisions' and effector function. *Nat Immunol* **15**, 815–823 (2014).
4. Li, H. M. *et al.* TCRβ repertoire of CD4+ and CD8+ T cells is distinct in richness, distribution, and CDR3 amino acid composition. *J Leukoc Biol* **99**, 505–513 (2016).
5. Weng, N. ping. Numbers and odds: TCR repertoire size and its age changes impacting on T cell functions. *Seminars in Immunology* vol. 69 Preprint at https://doi.org/10.1016/j.smim.2023.101810 (2023).
6. Soerens, A. G. *et al.* Functional T cells are capable of supernumerary cell division and longevity. *Nature* (2023) doi:10.1038/s41586-022-05626-9.
7. Ahmed, R. & Gray, D. Immunological Memory and Protective Immunity: Understanding Their Relation. *Science (1979)* **272**, 54–61 (1996).
8. Gallimore, A. *et al. Induction and Exhaustion of Lymphocytic Choriomeningitis Virus-Specific Cytotoxic T Lymphocytes Visualized Using Soluble Tetrameric Major Histocompatibility Complex Class I-Peptide Complexes*. *J. Exp. Med* vol. 187 http://www.jem.org (1998).
9. Zajac, A. J. *et al.* Viral immune evasion due to persistence of activated T cells without effector function. *Journal of Experimental Medicine* **188**, 2205–2213 (1998).
10. Wherry, E. J., Blattman, J. N., Murali-krishna, K., Most, R. Van Der & Ahmed, R. Viral Persistence Alters CD8 T-Cell Immunodominance and Tissue Distribution and Results in Distinct Stages of Functional Impairment Viral Persistence Alters CD8 T-Cell Immunodominance and Tissue Distribution and Results in Distinct Stages of Functional Im. *J Virol* **77**, 4911–3927 (2003).
11. Wherry, E. J. *et al.* Molecular Signature of CD8+ T Cell Exhaustion during Chronic Viral Infection. *Immunity* **27**, 670–684 (2007).
12. Kaech, S. M., Hemby, S., Kersh, E. & Ahmed, R. *Molecular and Functional Profiling of Memory CD8 T Cell Differentiation*. *Cell* vol. 111 http://www.cell.com/cgi/content/full/111/6/837/DC1. (2002).

13. Henning, A. N., Roychoudhuri, R. & Restifo, N. P. Epigenetic control of CD8+ T'cell differentiation. *Nat Rev Immunol* **18**, 340–356 (2018).

14. Sen, D. R. *et al.* The epigenetic landscape of T cell exhaustion. *Science* **354**, 1165–1169 (2016).

15. Henning, A. N., Roychoudhuri, R. & Restifo, N. P. Epigenetic control of CD8+ T cell differentiation. *Nat Rev Immunol* (2018) doi:10.1038/nri.2017.146.

16. Abdel-hakeem, M. S. *et al.* Epigenetic scarring of exhausted T cells hinders memory differentiation upon eliminating chronic antigenic stimulation. *Nat Immunol* **22**, (2021).

17. Giles, J. R. *et al. Shared and Distinct Biological Circuits in Effector, Memory and Exhausted CD8+ T Cells Revealed by Temporal Single-Cell Transcriptomics and Epigenetics*. *Nature Immunology* (Nature Immunology, 2022). doi:10.1038/s41590-022-01338-4.

18. Kristen E. Pauken & E. John Wherry. Epigenetic Stability of exhausted T cells limits durability of reinvigoration by PD-1 blockade. *Science (1979)* **354**, 1156–1160 (2016).

19. Jadhav, R. R. *et al.* Epigenetic signature of PD-1+ TCF1+ CD8 T cells that act as resource cells during chronic viral infection and respond to PD-1 blockade. *Proc Natl Acad Sci U S A* **116**, 14113–14118 (2019).

20. Armstrong, C. & Lillie, R. D. Experimental Lymphocytic Choriomeningitis of Monkeys and Mice Produced by a Virus Encountered in Studies of the 1933 St. Louis Encephalitis Epidemic. *Public Health Reports (1896-1970)* **49**, 1019 (1934).

21. Traub, E. *AN EPIDEMIC IN A MOUSE COLONY DUE TO THE VIRUS OF ACUTE LYMPHOCYTIC CHORIOMENINGITIS*. http://rupress.org/jem/article-pdf/63/4/533/1180665/533.pdf.

22. Rivers, T. & McNair Scott, T. F. Meningitis in man caused by a filterable virus. *Journal of Experimental Medicine* (1935).

23. Oldstone, M. B. A. & Campbell, K. P. Decoding arenavirus pathogenesis: Essential roles for alpha-dystroglycan-virus interactions and the immune response. (2011) doi:10.1016/j.virol.2010.11.023.

24. Singh, M. K., Fuller-Pace, F. V, Buchmeier, M. J. & Southern, P. J. Analysis of the genomic L RNA segment from lymphocytic choriomeningitis virus. *Virology* **161**, 448–56 (1987).

25. Burns, J. W. & Buchmeier, M. J. Protein-protein interactions in lymphocytic choriomeningitis virus. *Virology* **183**, 620–9 (1991).

26. Cao, W. *et al.* Identification of alpha-dystroglycan as a receptor for lymphocytic choriomeningitis virus and Lassa fever virus. *Science* **282**, 2079–81 (1998).

27. RAFI AHMED, AIMO SALMI, LARRY D. BUTLER, JACQUES M. CHILLER, A. M. B. A. O. SELECTION OF GENETIC VARIANTS OF LYMPHOCYTIC CHORIOMENINGITIS VIRUS IN SPLEENS OF PERSISTENTLY INFECTED MICE Role in Suppression of Cytotoxic T Lymphocyte Response and Viral Persistence. **60**, 521–540 (1984).

28. Kunz, S., Sevilla, N., McGavern, D. B., Campbell, K. P. & Oldstone, M. B. Molecular analysis of the interaction of LCMV with its cellular receptor [alpha]-dystroglycan. *J Cell Biol* **155**, 301–10 (2001).

29. Matloubian, M., Kolhekar, S. R., Somasundaram, T. & Ahmed, R. Molecular determinants of macrophage tropism and viral persistence: importance of single amino acid changes in the polymerase and glycoprotein of lymphocytic choriomeningitis virus. *J Virol* **67**, 7340–9 (1993).

30. Matloubian, B. M., Somasundaram, T., Kolhekar, S. R., Selvakumar, R. & Ahmed, R. Genetic Basis of Viral Persistence: Single Amino Acid Change in the Viral Glycoprotein Affects Ability of Lymphocytic Choriomeningitis Virus to Persist in Adult Mice. *October* **172**, (1990).

31. Ahmed, R. *et al.* Molecular basis of organ-specific selection of viral variants during chronic infection. *J Virol* **65**, 4242–7 (1991).

32. Matloubian, M., Concepcion, R. J. & Ahmed, R. CD4+ T cells are required to sustain CD8+ cytotoxic T-cell responses during chronic viral infection. *J Virol* **68**, 8056–63 (1994).

33. Zhou, X., Ramachandran, S., Mann, M. & Popkin, D. L. Role of lymphocytic choriomeningitis virus (LCMV) in understanding viral immunology: Past, present and future. *Viruses* vol. 4 2650–2669 Preprint at https://doi.org/10.3390/v4112650 (2012).

34. VOLKERT, M. & LARSEN, J. H. Studies on Immunological Tolerance To Lcm Virus. 5. the Induction of. *Acta Pathol Microbiol Scand* **63**, 161–171 (1965).

35. Giles, J. R., Globig, A. M., Kaech, S. M. & Wherry, E. J. CD8+ T cells in the cancer-immunity cycle. *Immunity* vol. 56 2231–2253 Preprint at https://doi.org/10.1016/j.immuni.2023.09.005 (2023).

36. McLane, L. M., Abdel-Hakeem, M. S. & Wherry, E. J. CD8 T Cell Exhaustion During Chronic Viral Infection and Cancer. *Annu Rev Immunol* **37**, 457–495 (2019).

37. Givan, A. L., Fisher, J. L., Waugh, M., Ernstoff, M. S. & Wallace, P. K. A flow cytometric method to estimate the precursor frequencies of cells proliferating in response to specific antigens. *J Immunol Methods* **230**, 99–112 (1999).

38. Jenkins, M. K. & Moon, J. J. The role of naive T cell precursor frequency and recruitment in dictating immune response magnitude. *J Immunol* **188**, 4135–40 (2012).

39. Blattman, J. N. *et al.* Estimating the Precursor Frequency of Naive Antigen-specific CD8 T Cells. *J. Exp. Med.* *The* **195**, 657–664 (2002).

40. Beura, L. K. *et al.* T Cells in Nonlymphoid Tissues Give Rise to Lymph-Node-Resident Memory T Cells. *Immunity* **48**, 327-338.e5 (2018).

41. Curtsinger, J. M. & Mescher, M. F. Inflammatory cytokines as a third signal for T cell activation. *Curr Opin Immunol* **22**, 333–40 (2010).

42. Jung, J., Zeng, H. & Horng, T. Metabolism as a guiding force for immunity. *Nat Cell Biol* **21**, 85–93 (2019).

43. Franco, F., Jaccard, A., Romero, P., Yu, Y.-R. & Ho, P.-C. Metabolic and epigenetic regulation of T-cell exhaustion. *Nat Metab* **2**, 1001–1012 (2020).

44. Murali-Krishna, K. *et al. Counting Antigen-Specific CD8 T Cells: A Reevaluation of Bystander Activation during Viral Infection*. *Immunity* vol. 8 https://ac.els-cdn.com/S1074761300804707/1-s2.0-S1074761300804707-main.pdf?_tid=65f7508a-3a3a-4500-bdb7-f25beece0aae&acdnat=1548365055_7d0c3fb6948986b14ab2828230b3e579 (1998).

45. Tough, D. F. & Sprent, J. Viruses and T cell turnover: evidence for bystander proliferation. *Immunol Rev* **150**, 129–42 (1996).

46. Tough, D. F., Borrow, P. & Sprent, J. Induction of bystander T cell proliferation by viruses and type I interferon in vivo. *Science* **272**, 1947–50 (1996).

47. Altman, J. D. *et al.* Phenotypic analysis of antigen-specific T lymphocytes. *Science* **274**, 94–6 (1996).

48. Kaech, S. M., Wherry, E. J. & Ahmed, R. Effector and memory T-cell differentiation: Implications for vaccine development. *Nature Reviews Immunology* vol. 2 251–262 Preprint at https://doi.org/10.1038/nri778 (2002).

49. Kaech, S. M. & Ahmed, R. Memory CD8+ T cell differentiation: Initial antigen encounter triggers a developmental program in naïve cells. *Nat Immunol* **2**, 415–422 (2001).

50. Lau, L. L., Jamieson, B. D., Somasundaram, T. & Ahmed, R. Cytotoxic T-cell memory without antigen. *Nature* **369**, 648–652 (1994).

51. Jamieson, B. D. & Ahmed, R. T CELL MEMORY Long-term Persistence of Virus-specific Cytotoxic T Cells. (1989) doi:10.1084/jem.169.6.1993.

52. Kaech, S. M. *et al.* Selective expression of the interleukin 7 receptor identifies effector CD8 T cells that give rise to long-lived memory cells. *Nat Immunol* **4**, 1191–1198 (2003).

53. Schluns, K. S., Kieper, W. C., Jameson, S. C. & Lefrançois, L. Interleukin-7 mediates the homeostasis of naïve and memory CD8 T cells in vivo. *Nat Immunol* **1**, 426–32 (2000).

54. Goldrath, A. W. *et al.* Cytokine requirements for acute and Basal homeostatic proliferation of naive and memory CD8+ T cells. *J Exp Med* **195**, 1515–22 (2002).

55. Becker, T. C. *et al.* Interleukin 15 is required for proliferative renewal of virus-specific memory CD8 T cells. *J Exp Med* **195**, 1541–8 (2002).

56. Wherry, E. J. *et al.* Homeostatic proliferation but not the generation of virus specific memory CD8 T cells is impaired in the absence of IL-15 or IL-15Ralpha. *Adv Exp Med Biol* **512**, 165–75 (2002).

57. Barber, D. L. *et al.* Restoring function in exhausted CD8 T cells during chronic viral infection. *Nature* **439**, 682–687 (2006).

58. Blackburn, S. D., Shin, H., Freeman, G. J. & Wherry, E. J. *Selective Expansion of a Subset of Exhausted CD8 T Cells by PD-L1 Blockade*. www.pnas.org/cgi/content/full/ (2008).

59. Paley, M. A. *et al.* Progenitor and terminal subsets of CD8+ T cells cooperate to contain chronic viral infection. *Science* **338**, 1220–5 (2012).

60. Im, S. J. *et al.* Defining CD8+T cells that provide the proliferative burst after PD-1 therapy. *Nature* **537**, 417–421 (2016).

61. Utzschneider, D. T. *et al.* T Cell Factor 1-Expressing Memory-like CD8+ T Cells Sustain the Immune Response to Chronic Viral Infections. *Immunity* **45**, 415–427 (2016).

62. He, R. *et al.* Follicular CXCR5-expressing CD8+ T cells curtail chronic viral infection. *Nature* **537**, 412–416 (2016).

63. Hudson, W. H. *et al.* Proliferating Transitory T Cells with an Effector-like Transcriptional Signature Emerge from PD-1 + Stem- Article Proliferating Transitory T Cells with an Effector-like Transcriptional Signature Emerge from PD-1 + Stem-like CD8 + T Cells during Chronic In. *Immunity* 1–16 (2019) doi:10.1016/j.immuni.2019.11.002.

64. Zander Ryan, Schauder David, Xin Gang, Nguyen Christine, Wu Xiaopeng, Zajac Alla, C. W. CD4 help is required for the formation of a transcriptionally distinct

cytolytic CD8 T cell subset that protects against chronic infection and cancer. *Immunity* **Accepted**, 1–15 (2019).

65. Leong, Y. A. *et al.* CXCR5+ follicular cytotoxic T cells control viral infection in B cell follicles. *Nat Immunol* **17**, 1187–1196 (2016).

66. Wu, T. *et al.* The TCF1-Bcl6 axis counteracts type I interferon to repress exhaustion and maintain T cell stemness. *Sci Immunol* **1**, 1–13 (2016).

67. Gomes Silva, J. *et al. Emergence and Fate of Stem Cell-like Tcf7 + CD8 + T Cells during a Primary Immune Response to Viral Infection*. https://www.science.org (2023).

68. Khan, O. *et al.* TOX transcriptionally and epigenetically programs CD8+ T cell exhaustion. *Nature* **571**, 211–218 (2019).

69. Alfei, F. *et al.* TOX reinforces the phenotype and longevity of exhausted T cells in chronic viral infection. *Nature* (2019) doi:10.1038/s41586-019-1326-9.

70. Yao, C. *et al.* Single-cell RNA-seq reveals TOX as a key regulator of CD8+ T cell persistence in chronic infection. *Nat Immunol* **20**, 890–901 (2019).

71. Jansen, C. S. *et al.* An intra-tumoral niche maintains and differentiates stem-like CD8 T cells. (2019).

72. Prokhnevska, N. *et al.* CD8+ T cell activation in cancer comprises an initial activation phase in lymph nodes followed by effector differentiation within the tumor. *Immunity* (2022) doi:10.1016/j.immuni.2022.12.002.

73. Miller, B. C. *et al.* Subsets of exhausted CD8+ T cells differentially mediate tumor control and respond to checkpoint blockade. *Nat Immunol* **20**, 326–336 (2019).

74. Eberhardt, C. S., Kissick, H. T., Patel, M. R. & Cardenas, M. A. Functional HPV-specific PD-1 + stem-like CD8 T cells in head and neck cancer. *Nature* (2021) doi:10.1038/s41586-021-03862-z.

75. Sanchez-rivera, J. *et al. An Autoimmune Stem-like CD8 T Cell Population Drives Type 1 Diabetes*. (2021). doi:10.1038/s41586-021-04248-x.

76. Hu, Y. *et al.* TGF- β regulates the stem-like state of PD-1 + TCF-1 + virus-specific CD8 T cells during chronic infection. **219**, (2022).

77. Humblin, E. *et al. Sustained CD28 Costimulation Is Required for Self-Renewal and Differentiation of TCF-1 + PD-1 + CD8 T Cells*. https://www.science.org (2023).

78. Lee, J. *et al.* IL-15 promotes self-renewal of progenitor exhausted CD8 T cells during persistent antigenic stimulation. *Front Immunol* **14**, (2023).

79. Kasmani, M. Y. *et al.* Clonal lineage tracing reveals mechanisms skewing CD8+ T cell fate decisions in chronic infection. *Journal of Experimental Medicine* **220**, (2023).

80. Im, S. J., Konieczny, B. T., Hudson, W. H., Masopust, D. & Ahmed, R. PD-1+ stemlike CD8 T cells are resident in lymphoid tissues during persistent LCMV infection. *Proceedings of the National Academy of Sciences* 201917298 (2020) doi:10.1073/pnas.1917298117.

81. Gill, A. L. *et al. PD-1 Blockade Increases the Self-Renewal of Stem-like CD8 T Cells to Compensate for Their Accelerated Differentiation into Effectors*. https://www.science.org (2023).

82. Utzschneider, D. T. *et al.* Early precursor T cells establish and propagate T cell exhaustion in chronic infection. *Nat Immunol* doi:10.1038/s41590-020-0760-z.

83. Ahn, E. *et al.* Role of PD-1 during effector CD8 T cell differentiation. *Proceedings of the National Academy of Sciences* 201718217 (2018) doi:10.1073/pnas.1718217115.

84. Im, S. J. *et al.* Characteristics and anatomic location of PD-1+TCF1+ stem-like CD8 T cells in chronic viral infection and cancer. *Proc Natl Acad Sci U S A* **120**, (2023).

85. Galkina, E. *et al.* Preferential migration of effector CD8+ T cells into the interstitium of the normal lung. *Journal of Clinical Investigation* **115**, 3473–3483 (2005).

86. Anderson, K. G. *et al.* Intravascular staining for discrimination of vascular and tissue leukocytes. *Nat Protoc* **9**, 209–222 (2014).

87. Shiow, L. R. *et al.* CD69 acts downstream of interferon-α/β to inhibit S1P1 and lymphocyte egress from lymphoid organs. *Nature* **440**, 540–544 (2006).

88. Beltra, J. C. *et al.* Developmental Relationships of Four Exhausted CD8+ T Cell Subsets Reveals Underlying Transcriptional and Epigenetic Landscape Control Mechanisms. *Immunity* **52**, 825-841.e8 (2020).

89. Wherry, E. J. *et al.* Molecular signature of CD8+ T cell exhaustion during chronic viral infection. *Immunity* **27**, 670–84 (2007).

90. Pauken, K. E. *et al.* Epigenetic stability of exhausted T cells limits durability of reinvigoration by PD-1 blockade. *Science* **354**, 1160–1165 (2016).

91. Menner, A. J. *et al.* Id3 Controls Cell Death of 2B4+ Virus-Specific CD8+ T Cells in Chronic Viral Infection. *J Immunol* **195**, 2103–14 (2015).

92. Xia, Y. *et al.* BCL6-dependent TCF-1+ progenitor cells maintain effector and helper CD4+ T cell responses to persistent antigen. *Immunity* 1–16 (2022) doi:10.1016/j.immuni.2022.05.003.

93. Sun, Q. *et al.* BCL6 promotes a stem-like CD8+ T cell program in cancer via antagonizing BLIMP1. *Sci Immunol* **8**, eadh1306 (2023).

94. Moran, A. E. *et al.* T cell receptor signal strength in Treg and iNKT cell development demonstrated by a novel fluorescent reporter mouse. *Journal of Experimental Medicine* **208**, 1279–1289 (2011).

95. Au-Yeung, B. B. *et al.* IL-2 Modulates the TCR Signaling Threshold for CD8 but Not CD4 T Cell Proliferation on a Single-Cell Level. *The Journal of Immunology* **198**, 2445–2456 (2017).

96. Zikherman, J., Parameswaran, R. & Weiss, A. Endogenous antigen tunes the responsiveness of naive B cells but not T cells. *Nature* **489**, 160–164 (2012).

97. Moskophidis, D. & Zinkernagel, R. M. *Immunobiology of Cytotoxic T-Cell Escape Mutants of Lymphocytic Choriomeningitis Virus*. *JOURNAL OF VIROLOGY* vol. 69 https://journals.asm.org/journal/jvi (1995).

98. Puglielli, M. T. *et al.* In Vivo Selection of a Lymphocytic Choriomeningitis Virus Variant That Affects Recognition of the GP33-43 Epitope by H-2D b but Not H-2K b . *J Virol* **75**, 5099–5107 (2001).

99. Johnson, S. *et al.* Protective Efficacy of Individual CD8+ T Cell Specificities in Chronic Viral Infection. *The Journal of Immunology* **194**, 1755–1762 (2015).

100. Utzschneider, D. T. *et al.* High antigen levels induce an exhausted phenotype in a chronic infection without impairing T cell expansion and survival. *Journal of Experimental Medicine* **213**, 1819–1834 (2016).

101. Kamphorst, A. O. *et al.* Rescue of exhausted CD8 T cells by PD-1 – targeted therapies is CD28-dependent. *Science (1979)* **355**, 1423–1427 (2017).

102. Fenwick, C. *et al.* T-cell exhaustion in HIV infection. **1**, 149–163 (2019).

103. Hashimoto, M. *et al.* CD8 T Cell Exhaustion in Chronic Infection and Cancer: Opportunities for Interventions. doi:10.1146/annurev-med-012017.

104. Araki, K. *et al.* mTOR regulates memory CD8 T cell differentiation HHS Public Access. *Nature* **460**, 108–112 (2009).

105. Ando, S. *et al.* mTOR regulates T cell exhaustion and PD-1 targeted immunotherapy response during chronic viral infection. *Journal of Clinical Investigation* (2022) doi:10.1172/JCI160025.

106. Gabriel, S. S. *et al.* Transforming growth factor- b -regulated mTOR activity preserves cellular metabolism to maintain long-term T cell responses in chronic

infection Article Transforming growth factor- b -regulated mTOR activity preserves cellular metabolism to maintain long-. 1–17 (2021) doi:10.1016/j.immuni.2021.06.007.

107. Ma, C. *et al.* TGF-β promotes stem-like T cells via enforcing their lymphoid tissue retention. *J Exp Med* **219**, (2022).

108. Aliahmad, P. & Kaye, J. Development of all CD4 T lineages requires nuclear factor TOX. *Journal of Experimental Medicine* **205**, 245–256 (2008).

109. Pircher, H. *et al.* Molecular analysis of the antigen receptor of virus-specific cytotoxic T cells and identification of a new V alpha family. *Eur J Immunol* **17**, 1843–6 (1987).

110. Kalia, V. *et al.* Prolonged Interleukin-2Rα Expression on Virus-Specific CD8+ T Cells Favors Terminal-Effector Differentiation In Vivo. *Immunity* **32**, 91–103 (2010).

111. Sarkar, S. *et al.* Functional and genomic profiling of effector CD8 T cell subsets with distinct memory fates. *J Exp Med* **205**, 625–640 (2008).

112. Sallusto, F., Lenig, D., Förster, R., Lipp, M. & Lanzavecchia, A. Two subsets of memory T lymphocytes with distinct homing potential and effector functions. *Nature* **401**, 708–712 (1999).

113. Joshi, N. S. *et al.* Inflammation Directs Memory Precursor and Short-Lived Effector CD8+ T Cell Fates via the Graded Expression of T-bet Transcription Factor. *Immunity* **27**, 281–295 (2007).

114. Akondy, R. S. *et al.* Origin and differentiation of human memory CD8 T cells after vaccination. *Nature* **552**, 362–367 (2017).

115. Youngblood, B. *et al.* Effector CD8 T cells dedifferentiate into long-lived memory cells. *Nature* **552**, 404–409 (2017).

116. Abadie, K. *et al.* Reversible, tunable epigenetic silencing of TCF1 generates flexibility in the T cell memory decision. *Immunity* (2024) doi:10.1016/j.immuni.2023.12.006.

117. Wherry, E. J. *et al.* Lineage relationship and protective immunity of memory CD8T cell subsets. *Nat Immunol* **4**, 225–234 (2003).

118. Marzo, A. L. *et al.* Initial T cell frequency dictates memory CD8+ T cell lineage commitment. *Nat Immunol* **6**, 793–799 (2005).

119. Stolley, J. M. *et al.* Retrograde migration supplies resident memory t cells to lung-draining ln after influenza infection. *Journal of Experimental Medicine* **217**, (2020).

120. Steinert, E. M. *et al.* Quantifying memory CD8 T cells reveals regionalization of immunosurveillance. *Cell* **161**, 737–749 (2015).

121. Mackay, L. K. *et al.* Cutting edge: CD69 interference with sphingosine-1-phosphate receptor function regulates peripheral T cell retention. *J Immunol* **194**, 2059–63 (2015).

122. Sharma, N., Benechet, A. P., Lefrançois, L. & Khanna, K. M. CD8 T Cells Enter the Splenic T Cell Zones Independently of CCR7, but the Subsequent Expansion and Trafficking Patterns of Effector T Cells after Infection Are Dysregulated in the Absence of CCR7 Migratory Cues. *The Journal of Immunology* **195**, 5227–5236 (2015).

123. Bromley, S. K., Thomas, S. Y. & Luster, A. D. Chemokine receptor CCR7 guides T cell exit from peripheral tissues and entry into afferent lymphatics. (2005) doi:10.1038/ni1240.

124. Hickman, H. D. *et al.* CXCR3 chemokine receptor enables local CD8+ T cell migration for the destruction of virus-infected cells. *Immunity* **42**, 524–537 (2015).

125. Kurachi, M. *et al.* Chemokine receptor CXCR3 facilitates CD8+ T cell differentiation into short-lived effector cells leading to memory degeneration. *Journal of Experimental Medicine* **208**, 1605–1620 (2011).

126. Duckworth, B. C. *et al.* Effector and stem-like memory cell fates are imprinted in distinct lymph node niches directed by CXCR3 ligands. *Nat Immunol* **22**, 434–448 (2021).

127. Bangs, D. J. *et al.* CXCR3 regulates stem and proliferative CD8+ T cells during chronic infection by promoting interactions with DCs in splenic bridging channels. *Cell Rep* **38**, (2022).

128. Hu, J. K., Kagari, T., Clingan, J. M. & Matloubian, M. Expression of chemokine receptor CXCR3 on T cells affects the balance between effector and memory CD8 T-cell generation. *Proc Natl Acad Sci U S A* **108**, (2011).

129. Cd, E. *et al.* TCF-1-Centered Transcriptional Network Drives an Article TCF-1-Centered Transcriptional Network Drives an Effector versus Exhausted CD8 T Cell-Fate Decision. *Immunity* 1–16 (2019) doi:10.1016/j.immuni.2019.09.013.

130. Choi, J. *et al.* Bcl-6 is the nexus transcription factor of T follicular helper cells via repressor-of-repressor circuits. doi:10.1038/s41590-020-0706-5.

131. Sarkar, S. *et al.* Strength of Stimulus and Clonal Competition Impact the Rate of Memory CD8 T Cell Differentiation. *The Journal of Immunology* **179**, 6704–6714 (2007).